

2005

High Performance Liquid Chromatography Diastereomeric Separation for Chiral Analysis and Kinetic Analysis

Li Li

Seton Hall University

Follow this and additional works at: <https://scholarship.shu.edu/dissertations>



Part of the [Analytical Chemistry Commons](#)

Recommended Citation

Li, Li, "High Performance Liquid Chromatography Diastereomeric Separation for Chiral Analysis and Kinetic Analysis" (2005). *Seton Hall University Dissertations and Theses (ETDs)*. 446.
<https://scholarship.shu.edu/dissertations/446>

**HIGH PERFORMANCE LIQUID CHROMATOGRAPHY
DIASTEREOMERIC SEPARATION FOR CHIRAL ANALYSIS AND
KINETIC ANALYSIS**

**BY
LI LI**

DISSERTATION

A thesis submitted in partial fulfillment of the requirements for the degree of

Doctoral of Philosophy

In the Department of Chemistry and Biochemistry

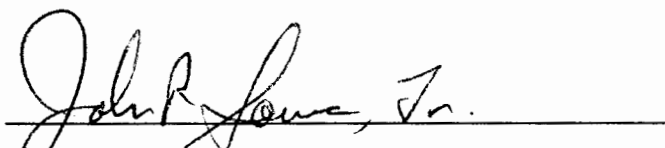
Seton Hall University

South Orange, New Jersey

May, 2005


We certify that we have read this thesis and that in our opinion it is sufficient in scientific scope and quality for a dissertation for the degree of Doctoral of Philosophy.

APPROVED



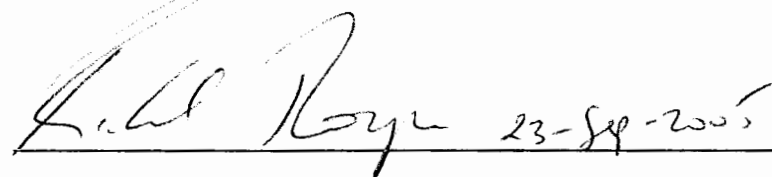
John R. Sowa, Jr., Ph.D.

Research Adviser



Yuri Kazakevich, Ph.D.

Member of Dissertation Committee



Richard A. Thompson, Ph.D.

Member of Dissertation Committee



Nicholas H. Snow, Ph.D.

Chair, Department of Chemistry and Biochemistry

This work is dedicated

To my parents:

Qinghe Li and Luo Mingzhu

To my husband:

Lushi Tan

To my children:

Elmer and Jelisa Tan

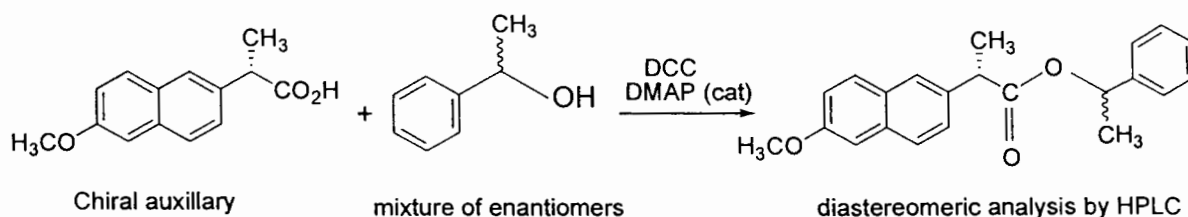
HPLC Diastereomeric Separation for Chiral Analysis and Kinetic Analysis

Abstract

Part (I)

A New Way to Cure Chiral Purity Analysis Headaches

Chiral alcohols and amines are widely used intermediates and pharmaceutically active ingredients. Methods for establishing the chiral purity of these compounds are of great interest to chemists. While state-of-art analysis is focused on direct analysis of these chiral molecules by chiral GC, HPLC and spectroscopic techniques, it is still interesting to develop chiral auxiliaries for traditional diastereomeric analyses. The over-the-counter, non-steroidal anti-inflammatory agent Naproxen is a readily available, inexpensive, enantiomerically pure carboxylic acid.



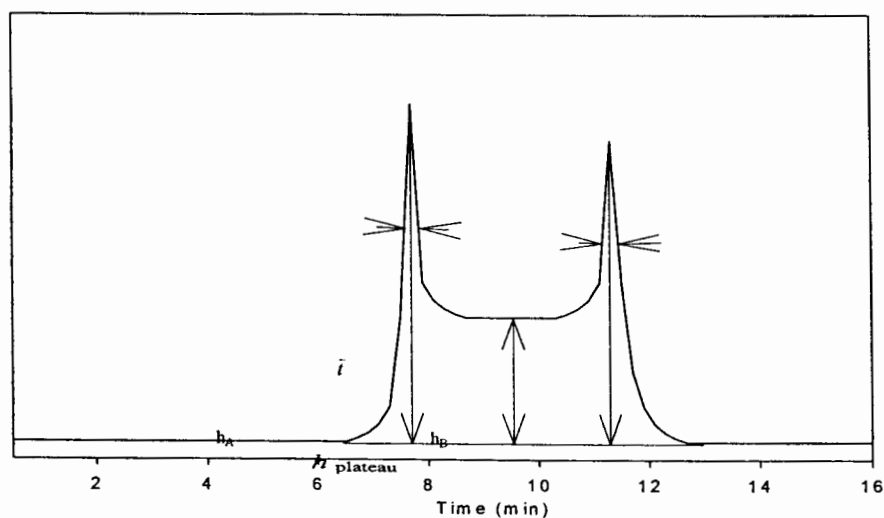
We have developed this compound as an alternative to the more expensive Mosher's acid for chiral analysis. In this study, the use of (S)-Naproxen as a chiral auxiliary (See above reaction scheme) for the analysis of chiral alcohols will be reported. We proved that the S,S diastereomeric product forms at a faster rate (ca. 4 times faster) than the S,R diastereomeric product. Initial attempts at quantitative analysis of enantiomeric mixtures of sec-phenethanol were unsuccessful due to these kinetic differences. However, we show that flooding the reaction with a large excess of (S)-Naproxen results in reproducible analysis of enantiomeric mixtures of sec-phenethanol by HPLC. Also, the diastereomeric separation of S-Naproxen esters by HPLC was thoroughly studied. The NMR measurements of S-Naproxen ester provided a complimentary method for the chiral analysis of chiral alcohols.

Part (II)

Kinetic Studies FOR ON-COLUMN ISOMERIZATION INTERCONVERSION

Investigations into dynamic molecular processes and determination of their kinetic parameters are frequently performed through the utilization of dynamic spectroscopic techniques (NMR, ESR, IR). These kinetic parameters can also be determined chromatographically, specifically for two species that can interconvert on a chromatographic time scale and can be separated chromatographically. This chemical interconversion can occur during sample preparation or on-column and may be influenced by the mobile phase or the stationary phase. Peak distortion might be observed when the conversion occurs during the chromatographic process.

The epimerization of trityloxymethyl butyrolactol has been investigated using dynamic chromatography and an approximation function introduced by Trapp and Schurig that is based on stochastic and theoretical plate models. The epimerization rate constants and Gibbs activation energies of epimerization are directly calculated from chromatographic peak parameters, i.e., retention times of the inter-converting species, peak width at half height and the relative plateau height by using the approximation function. The relationships between peak shape and chromatographic conditions, such as flow-rate, temperature and pH are investigated.



$$\begin{aligned}
 k_1^{approx} = & -\frac{1}{t_R^A} \ln \left[\frac{(c_A^0 + c_B^0)}{(t_R^A - t_R^B)} \left(1 - \frac{h_{plateau}}{100} \left(0.5 + \frac{1}{\sqrt{2\pi N}} \right) \right) \right] \\
 & + \frac{1}{t_R^A} \ln \left[\frac{(c_A^0 + c_B^0)}{(t_R^A - t_R^B)} \left(1 - \frac{h_{plateau}}{100} \left(0.5 + \frac{1}{\sqrt{2\pi N}} \right) \right) \right] + c_A^0 \frac{0.01 h_{plateau} - e^{-\frac{(t_R^B - t_R^A)^2}{8\sigma_A^2}}}{\sigma_A \sqrt{2\pi}} \\
 & + c_B^0 \frac{0.01 h_{plateau} - e^{-\frac{(t_R^A - t_R^B)^2}{8\sigma_B^2}}}{\sigma_B \sqrt{2\pi}}
 \end{aligned}$$

Acknowledgment

Thanks to my mentor Prof. John Sowa, for his scientific advice and guidance through my entire Ph.D. study at Seton Hall University. His continuous encouragement, guidance and patience had provided me invaluable support through my studies at Seton Hall University.

To Dr. Richard Thompson, his scientific guidance and discussion were a big help for the research projects. His scientific literacy has been a strong source of support on where to find references for our research.

To my husband Dr. Lushi Tan, his suggestions on the synthesis of my precursors were always a big help to the project. He spent a lot of time with our kids, while I was doing my research in the lab. Without his constant encouragement and assistant, I'm sure my Ph.D. study would have been impossible.

Table of Contents

Title page.....	1
Approval page.....	2
Dedication.....	3
Abstract.....	4
Acknowledgments.....	6
Table of contents	7
List of figures.....	8
List of Tables.....	11
Part I title page.....	12
Chapter 1. Introduction.....	13
Chapter 2. Accuracy of the Derivatization Methods: Chiral Alcohols/(S)-naproxen.....	41
Chapter 3. Optimization of reaction condition.....	69
Chapter 4. Diastereomeric separation of S-naproxen esters.....	82
Chapter 5. NMR Measurements for S-naproxen Ester.....	106
Part II title page.....	117
Chapter 1: Introduction.....	118
Chapter 2 Theoretical Aspects.....	124
Chapter 3 Approximate Function for the Calculation of Rate Constants.....	134
Chapter 4 Determination of Reaction Rate Constant and the Arrhenius Constant.....	140
Chapter 5 Peak Shape Studies for the for the Inter-conversion Reactions.....	157
Appendix.....	176

List of Figures

Figure 1. Derivatization of analyte X with a pure chiral derivatization reagent.....	14
Figure 2. Typical derivatization reactions for chiral alcohols	18
Figure 3. Structures of derivatization reagents	22
Figure 4. Chromatographic separation of (\pm)-warfarin-(R)-MTPA	27
Figure 5. Chromatographic separation of (\pm)-4-chloroamphetamine-(R)-MTPA amide	28
Figure 6. Chromatographic separation of (DL)-phenylalanine methyl ester-(R)-MTPA amide	29
Figure 7 Linearity studies for esterification reaction of <i>sec</i> -phenyl ethanol and S-naproxen	47
Figure 8 Percent of SR <i>sec</i> -phenyl ethyl alcohol naproxen ester during the process of derivatization reaction.....	56
Figure 9. Kinetic plot for pseudo first order reaction of <i>sec</i> -phenyl ethyl alcohol with S-Naproxen, first measurement of reaction rate constant for R- <i>sec</i> -phenyl ethyl alcohol.....	58
Figure 10. Kinetic plot for pseudo first order reaction of <i>sec</i> -phenyl ethyl alcohol with S-Naproxen, second measurement of reaction rate constant for R- <i>sec</i> -phenyl ethyl alcohol.	59
Figure 11 Kinetic plot for pseudo first order reaction of <i>sec</i> -phenyl ethyl alcohol with S-Naproxen, Third measurement of reaction rate constant for R- <i>sec</i> -phenyl ethyl alcohol.	60
Figure 12. Kinetic plot for pseudo first order reaction of <i>sec</i> -phenyl ethyl alcohol with S-naproxen. Fourth measurement of reaction rate constant for R- <i>sec</i> -phenyl ethyl alcohol.....	61
Figure 13. Kinetic plot for pseudo first order reaction of <i>sec</i> -phenyl ethyl alcohol with S-naproxen. Fifth measurement of reaction rate constant for R- <i>sec</i> -phenyl ethyl alcohol	62
Figure 14. Kinetic plot for pseudo first order reaction of <i>sec</i> -phenyl ethyl alcohol with S-naproxen. First measurement of reaction rate constant for S- <i>sec</i> -phenyl ethyl	

alcohol	63
Figure 15 Kinetic plot for pseudo first order reaction of <i>sec</i> -phenyl ethyl alcohol with S-naproxen. First measurement of reaction rate constant for S- <i>sec</i> -phenyl ethyl alcohol.....	64
Figure 16 Kinetic plot for pseudo first order reaction of <i>sec</i> -phenyl ethyl alcohol with S-naproxen. First measurement of reaction rate constant for S- <i>sec</i> -phenyl ethyl alcohol.....	65
Figure 17. The effective amount of DCC on the reaction linearity	75
Figure 18. The effect of the amount of S-naproxen on the reaction linearity	76
Figure 19. The HPLC separation of R,S-butanol S-naproxen ester	89
Figure 20. The HPLC separation of R,S-pentanol S-naproxen ester	90
Figure 21. The HPLC separation of R,S-hexanol S-naproxen ester	91
Figure 22. The HPLC separation of R,S-heptanol S-naproxen ester	92
Figure 23. The HPLC separation of R,S-octanol S-naproxen ester	93
Figure 24. The HPLC separation of R,S-trifluoro methyl benzyl alcohol S-naproxen ester ..	94
Figure 25. The HPLC separation of R,S-trifluoro octanol-2 S-naproxen ester	95
Figure 26. The HPLC separation 3-methyl-2-cyclohexene-1-ol S-naproxen ester	96
Figure 27. The HPLC separation 20phenyl-butanol-1 S-naproxen ester	97
Figure 28. Isomeric selectivity of (2, 4)-, (2, 5)-, (2, 6)- and (3, 4)- difluorobenzyl amine in Zirchrom-PBD column.....	101
Figure 29. Example of an elution profile of an interconverting species with the experimental parameters needed for calculation of rate constants and the Arrhenius constant	121
Figure 30. Epimerization of Butyrolactol.....	123
Figure 31. Equilibria in a theoretical plate.....	126

Figure 32. Definition for S	131
Figure 33. Typical chromatogram for trityloxymethyl Butyrolactol.....	141
Figure 34. Measurement of peak heights for trityloxymethyl butylrolactol	146
Figure 35. The Arrhenius plot for trityloxymethyl butyrolactol	156
Figure 36. The flow-rate effect on the peak shape of cis-trans proline inter-conversion	159
Figure 37. The flow-rate effect on the peak shape of enalapril inter-conversion.....	160
Figure 38. Effect of flow-rate on the peak shape of trityloxymethyl Butyrolactol	162
Figure 39. The temperature effect on the peak shape of L-analyt-L-proline.....	164
Figure 40. Effect of column temperature on the peak shape and retention of enalapril.....	165
Figure 41. Effect of temperature on the peak shape of trityloxymethyl butyrolactol	166
Figure 42. The reaction mechanism for the acid catalyzed epimerization reaction of lactols	170
Figure 43. The reaction mechanism for the base catalyzed epimerization reaction of lactols	171
Figure 44. Reaction rate constant for some hydroxyl benzaldehydal.....	172
Figure 45. Effect of pH on the peak shape of trityloxymethyl butyrolactol.....	174

List of Tables

Table 1	Reagents used for the chiral derivatization of hydroxyl group.....	20
Table 2	Chromatographic parameter and data of S-naproxen ester of some β -adrenoceptor antagonists and antiarrhythmic agents	35
Table 3.	Reaction rate constants for the reaction of R- <i>sec</i> -phenethanol and S- <i>sec</i> -phenethanol with S-naproxen	65
Table 4	Linearity study under optimized reactant ratio for the reaction of <i>sec</i> -phenyl ethyl alcohol and S-naproxen	78
Table 5	Linearity study under optimized reactant ratio for the reaction of 1-phenyl propyl alcohol and S-naproxen	79
Table 6	Resolution data for diastereomeric separations of S-naproxen esters.....	87
Table 7	Isomer selectivities for Zirchrom-PBD, C8 and C18 columns	99
Table 8	Isomeric separation data for both C18 and Zirchrom-PBD	102
Table 9	Chemical shift differences for S-naproxen alkyl alcohol esters	113
Table 10	Comparison of LC analysis results with NMR analysis results	114
Table 11	The chromatographic data for 5°C	147
Table 12	The chromatographic data for 10°C	148
Table 13	The chromatographic data for 15°C	149
Table 14.	The chromatographic data for 20°C	150
Table 15.	The chromatographic data for 25°C	151
Table 16.	The calculated k_1^{approx} value	152
Table 17.	Literature reported interconversion reaction rate constants for Carbohydrates	153

Part I

Enantiomeric Analysis of Chiral

Alcohol by the Derivatization Reaction

with (S)-Naproxen

Chapter 1 Introduction

It is well known that enantiomers can exhibit different physicochemical properties in chiral environments such as biological systems¹. The different responses of enantiomers in biological systems have led to intensive research in pesticide, food, flavor, and especially, in pharmaceutical industries, where very selective and specific biological responses can be utilized and developed commercially. Regulatory agencies require determination of the relative rates of metabolism and dissipation of the individual enantiomers in biological or environment systems, and also determination of enantiomeric purity^{2, 3}. Enantiomeric purity is commonly determined through chromatographic means. There are two general ways to achieve the separation of enantiomers by chromatographic techniques: 'indirect' or 'direct' methods¹. In a direct method, either a chiral stationary phase (CSP) with an achiral mobile phase is employed or an achiral stationary phase with a chiral additive in the mobile phases is utilized to achieve the separation goal. Indirect methods involve derivatization. The enantiomers are converted to diastereomers by reaction with an optically pure reagent. The products are subsequently separated on achiral chromatographic phases. Practically, the two methods are used complementarily. Although the direct separation method is very convenient, no universal phase is available. Therefore, there is no guarantee that it can be used to separate every chiral compound. On the other hand, indirect method requires no chiral phase (stationary phase or mobile phase). It is usually cheaper and very effective. It is also the choice for the separation of enantiomers low chromophores, since a functional group with a strong chromophore can be attached during the derivatization. Then, the

1. Karl Blau and John M. Halket, "*Handbook of Derivatives for Chromatography*", Chapter Ten

2. Parker, D. *Chem. Rev.*, **1991**, *91*, 1441

3. Vinson, S. C. *Chem. Eng. News*, **1993**, *73*, 38

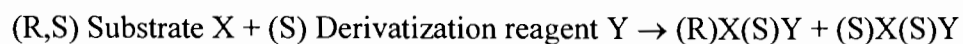
widely used UV detection can be utilized. In this research, the chiral analysis of alcohols by the means of derivatization with S-naproxen is thoroughly studied.

General rules for the selection of chiral derivatizing reagents

With the indirect method, the target analyte is derivatized with an optically pure reagent (derivatizing reagent) to produce two diastereomers that possess small differences in physicochemical properties and can thus be separated in an achiral environment. The choice of the derivatizing reagent has significant effect on the degree of separation, detectability of the resulting diastereomer and accuracy of the analysis method. Therefore, the following criteria are important to follow for choosing the derivatization reagent¹:

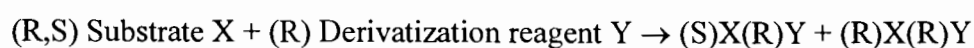
- 1) The derivatization reagent should have very high optical purity (preferably 100%). If the derivatization reagent purity is less than 100%, the enantiomeric impurity will also react with the reagent to form another pair of diastereomers. For example, if an “S” derivatization reagent is contaminated with R enantiomer, this impurity will be reflected in the analysis as discussed in Figure 1.

If “S” Y is the desired derivatization reagent, the reaction will get two products as follow:



I II

The existence of (R)Y can also react with substrate and generate two un-wanted diastereomers, as follow:



III IV

Note that **I + III** and **II + IV** are pairs of enantiomers and cannot be separated in a non-chiral environment.

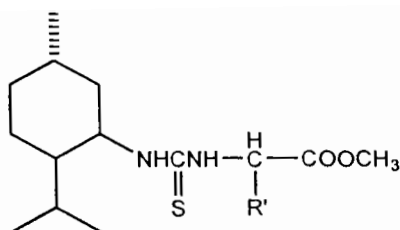
Figure 1. Derivatization of analyte X with a pure chiral derivatization reagent. In non-chiral environment, compounds I and III, II and IV will co-elute. Therefore, the accuracy of the method will be greatly reduced by the impure derivatization reagent.

- 2) The chemical properties of the derivatization reagents and the reaction conditions should ensure a complete derivatization reaction and minimize the chances of racemization or degradation of the analyte. The derivatization reagent should also be a stable compound. In addition, reaction with other functional groups of the analyte is undesirable.
- 3) The nature of the derivatization reagent should be amenable to the chosen chromatographic technique; e.g. for gas chromatography, volatile derivatives can decrease the requirement for high column temperatures and for liquid chromatography, a UV-chromophore in the derivatization reagent's structure can increase detection sensitivity.

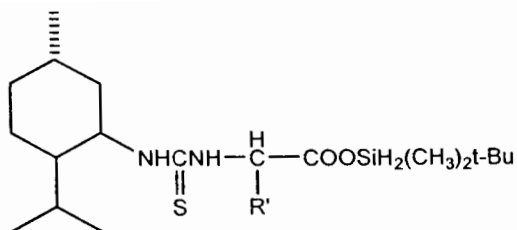
Diastereomers have similar physical, chemical, and consequently chromatographic retention properties. The chromatographic separation of diastereomers can be very challenging. Some of the structural features of the derivatization reagent can enhance the chromatographic separation of the resulting diastereomers:

- a) The conformational rigidity of the resulting diastereomers can maximize their spatial differences and enhance separation. It was reported that the resolution of *t*-butyldimethylsilyl ester is larger than the methylester⁴ (see below for structures).

4. Nambara, T.; Ikegawa, S.; Hasegawa, M. and Goto, J.; *Anal. Chim. Acta*, **1978**, *101*, 111



Methylester



Butyldimethylsilyl ester

- b) In general, a large size difference between the groups attached to the chiral center of the derivatization reagent can improved the separation ⁵
- c) The distance between the asymmetric centers of the derivatization reagent and the analyte should be minimal. The ideal distance is less than three bonds⁶.
- d) The existence of polar or polarizable groups close to the chiral centers of the derivatization reagent and the analyte can promote hydrogen bonding or π - π interactions with the stationary phase to enhance the chromatographic resolution.

All of the above factors are not required but indicate structural features that can be used to identify the correct derivatization reagent for the analyte. It is the responsibility of the analytical chemist to find a suitable derivatization reagent such that the resulting diastereomer can be separated by HPLC and also be easily detected.

5. Rose, H. C.; Stern, R. L. and Karger, B. L.; *Anal. Chem.*; **1966**, *38*, 469

6. Halpern, B.; *Derivatives for Chromatography*, Blau, K and King, G. S. edit; pp457-499

Chiral acids, isocyanates and chloroformates are common reagents used for the derivatization of alcohols and amines¹. Common derivatization reactions and their products are depicted in Figure 2. Among these reactions, esterification is the most popular derivatization reaction when utilizing LC for the subsequent diastereomeric separations. However, the esterification reaction does not easily go to completion. Usually, diastereomeric esters can be prepared from the target alcohol and an activated chiral carboxylic acid in the forms of chloride, anhydride and imidazole. Acid chlorides are most reactive and are especially useful for sterically hindered compounds. However, care should be taken with those reagents containing a proton attached to the chiral center, since racemization could occur under extreme acidic or basic conditions or at an elevated temperature. Also, the stability of these reagents should be evaluated in order to optimize the derivatization reaction. An alternative approach for the synthesis of diastereomeric esters is to use a carbodiimide compound as the coupling reagent. With coupling reagents, the esterification between acids and alcohols can go to completion. Derivatization reagents used for hydroxyl groups are listed in Table 1 and the structures of these derivatization reagents are shown in Figure 3.

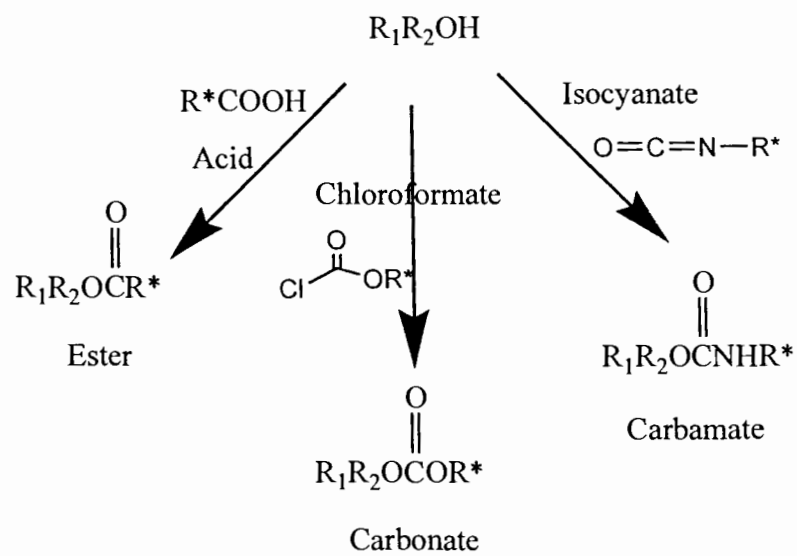


Figure 2 Typical derivatization reactions for chiral alcohols.

Table 1 Reagents used for the chiral derivatization of hydroxyl group. Data are from reference 1. Mosher's reagent is not included in this table, since it will be discussed in detail later.

Chiral Reagent	Chromatographic method	Reference
3 β -acetoxy- δ -etienic acid (1)	GC	7
R(+)-trans-chrysanthemic acid (2)	GC	8, 9, 10
Drimanoic acid (3)	GC	8
(-)-methenyoxyacetic acid (4)	HPLC	11, 12, 13,14
(R) (+)-2-phenylselenopropionic acid (5)	GC	15 ¹⁵
(S)-acetoxypionic acid (6)	GC	16,17,18,19

7. Anders, M. W. and Cooper, M. J.; *Anal. Chem.*, **1971**, *43*, 1093
8. Brooks, C. J.; Gilbert, M. T. and Gilbert J. D.; *Anal. Chem.*, **1972**, *45*, 898
9. Burden, R. S., Deas, A. H. B. and Clarke, T. J. *Chromatogr.*, **1987**, *391*, 273
10. Attygalle, A. B., Morgan, E. D., Evershed, R. P. and Rowland, S. J.; *J. Chromatogr.*, **1983**, *260*, 411,
11. Duke, C. C. and Holder, G. M.; *J. Chromatogr.*, **1988**, *430*, 53
- 12 Harvey, R. G. and Cho, H; *Anal. Biochem.*, **1977**, *80*, 540
13. Yagi, H. and Jerina; *J. Am. Chem.. Soc.*, **1982**, *104*, 4062
14. Lee, H and Harvey, R. G., *J. Org. Chem.*, **1984**, *49*, 1114
15. Michelsen, P. and Odham, G., *J. Chromatogr.*, **1985**, *331*, 295
16. Gil-Av, E.; Charles-Sigler, R.; Fischer, G. and Nurok, D., *J. Gas Chromatogr.*, **1966**, *4*, 51
17. Charles, R.; Fischer, G. and Gil-Av, E.; *Isr. J. Chem.*; **1963**, *1*, 234
18. Mosandl, A.; Gessner, M.; Gunther, C.; Deger W. and Singer G.; *J. High Resolut. Chromatogr. Chromatogr. Commun.*, **1987**, *10*, 67
19. Gil-Av, E.; and Nurok, D., *Proc. Chem. Soc.*, **1962**, 146

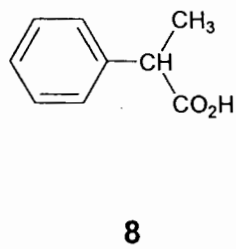
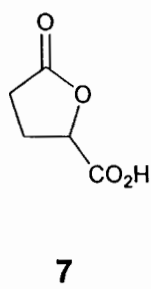
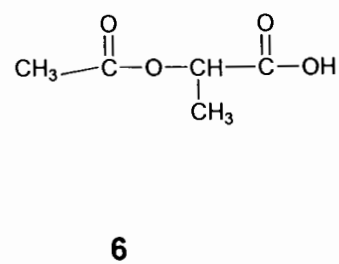
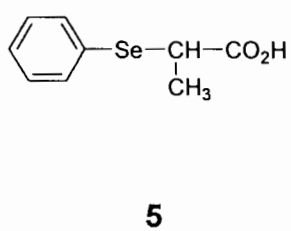
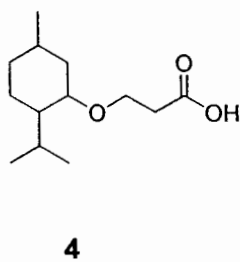
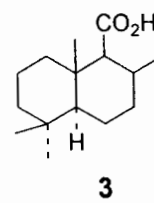
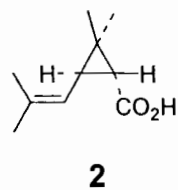
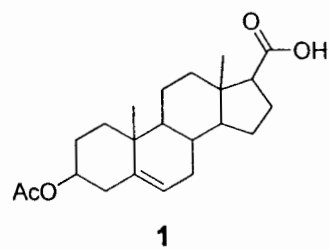
(S)-tetrahydro-5-oxo-2-furancarboxylic acid (7)	GC/HPLC	20
(S)-(+)-phenylpropionic acid (8)	GC	21
D(-)/L(+)-Mandelic acid (9)	GC	22
(S)-(-)-N-(trifluoroacetyl)proline (10)	GC	10
Carbobenzyloxy-L-proline (11)	HPLC	23
(+)-Glucuronic acid (12)	HPLC	24
Acetobromo- α -D-glucose (13)	GC	25, 26
R(+)/S(-)-1-phenylethyl isocyanate (14)	GC	27, 28, 29
R(+)/S(-)-1-(1-Naphthyl)ethyl isocyanate (15)	GC	28, 30, 31

-
20. Doolittle, R. E. and Heath, R. R.; *J. Org. Chem.*; **1984**, 49, 5041
21. Hammarstrom, S. and Hamberg, M.; *Anal. Biochem.*, **1973**, 52, 169
22. Cross J. M.; Putney, B. F. and Bernstein, J. *J. Chromatogr. Sci.*; **1970**, 8, 679
23. Banfield, C. and Rowland M.; *J. Pharm. Sci.*; **1984**, 73, 1292
24. Gerding, T. K.; Drenth, B. F. H. and de Zeeuw, R. A.; *J. High Resolut. Chromatogr. Chromatogr. Commun.*, **1987**, 10, 523
25. Sakata, I. and Iwamura, H.; *Agric. Biol. Chem.*; **1979**, 43, 307
26. Sakata, I. and Koshimizu, K.; *Agric. Biol. Chem.*; **1979**, 43, 411
27. Pereira, W.; Bacon, V. A.; Patton, W. and Halpern, B.; *Anal. Lett.*; **1970**, 3, 23
28. Sonnet, P. E.; Piotrowski, E. G. and Boswell, R. T.; *J. Chromatogr.*, **1988**, 436, 205
29. Gaydou, E. M. and Randriamiharisoa, R. P.; *J. Chromatogr.*, **1987**, 396, 378
30. Pirkle, W. H. and Boeder, C. W.; *J. Org. Chem.*; **1986**, 43, 1950
31. Yamazaki, Y. and Maeda, H.; *Agric. Biol. Chem.*; **1986**, 50, 79

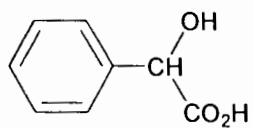
(-)-menthyl chloroformate (16)	GC, HLC	32 33 ,
(1R,4R,5S)-4-hydroxy-6,6-dimethyl-3-oxabicyclo[3.1.0]hexan-2-one (17)	LC	34
(-)/(+)-2-methyl-1, 1'-binaphthalene-2'-carbonyl cyanides (18)	LC/Fluorencence	35
N-(p-toluenesulfonyl)prolyl isocyanate (19)	LC	36
α -Cyano- α -fluorophenylacetic acid (20)	NMR	37
(4R,5R)-dicarbalkoxy-2-chloro-1, 3,2-dioxaphospholanes (21)	^{31}P NMR	38
Phosphoric acid chloride (22)	^{31}P NMR	39
4-(N,N-Dimethylaminosulfonyl)-7-(2-chloroformylpyrrolidin-1-yl)-2,1,3-benzoxadiazole (23)	LC/fluorescence	40
(R)-lactic acid (24)	^1H NMR	41
(S)-trolox methyl ether (25)	GC/SFC	42 43 ,

32. Westley, J. W. and Halpern, B.; *J. Org. Chem.*; **1968**, 33, 3978
33. Jeyaraf, G. L. and Portor, W. R.; *J. Chromatogr.*, **1984**, 315, 378
34. Martel, J. J.; Demoute, J. P.; Teche, A. P. and Tessier, J. R.; *Pestic. Sci.*; **1980**, 11, 188
35. Goto, J.; Goto, N.; Shao, G.; Ito, M.; Hongo, A.; Nakamura, S. and Nambara, T.; *Anal. Sci.*; **1990**, 6(20), 261
36. Zhou, Y.; Sun, Z. and Lin, D J. *Liq. Chromtogr.*; **1990**, 13(5), 875
37. Takeuchi, Y.; Toh, N.; Note, H.; Koizumi, T and Yamaguchi, K.; *J. Am. Chem. Soc.*; **1991**, 113(16), 6318
38. Brunel, J. M.; Pardigon, O.; Maffei, M. and Buono, G. *Tetrahedron: Asymmetry*, **1992**, 3(10), 1243
39. Hulst, R.; Zijlstra, R. W. J.; Feringa, Ben.; Koen de Vries, N.; Ten Hoeve, W. and Wynberg, H.; *Tetrahedron Lett.*; **1993**, 34(8), 1339
40. Toyo'oka, T.; Ishibashi, M.; Terao, T. and Imai, K.; *Analyst*, **1993**, 118(7), 759
41. Tottie, L.; Moberg, C. and Heumann, A.; *Acta Chemica Scandinavica*; **1993**, 47(5), 492
42. Walther, W.; Vetter, W. and Netscher, T.; *J. of Microcolumn Seprtn.*; **1992**, 4(1), 45

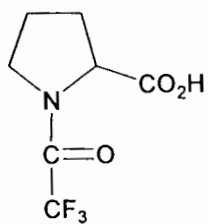
Figure 3 Structures of derivatization reagents listed in Table 1.



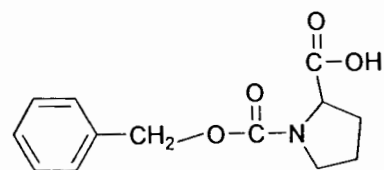
Structure cont.



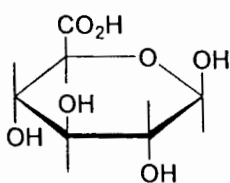
9



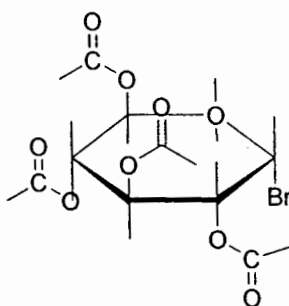
10



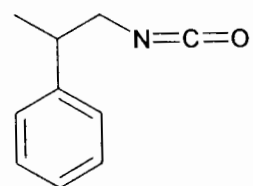
11



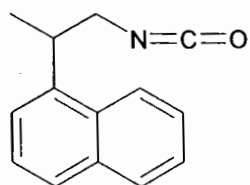
12



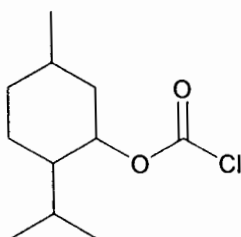
13



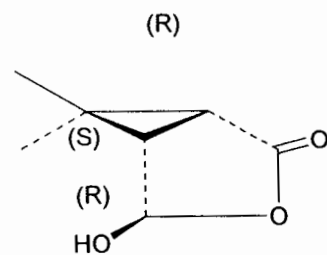
14



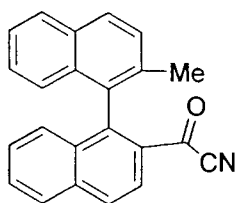
15



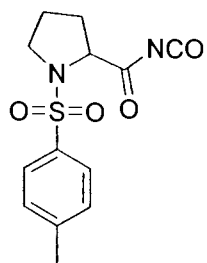
16



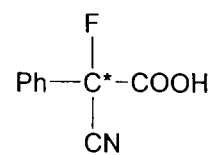
17



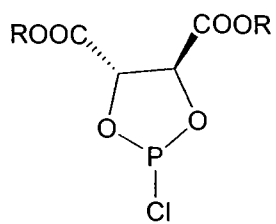
18



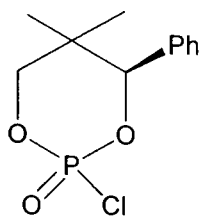
19



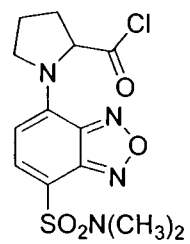
20



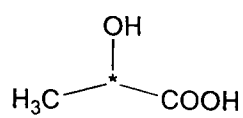
21



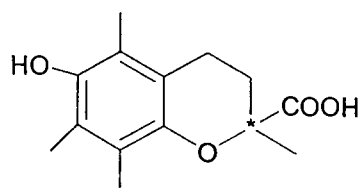
22



23

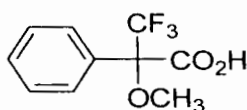


24



25

The most widely used derivatization reagent for alcohols and amines is a compound known as *Mosher's reagent* (MTPA, 26). One reason that the compound is particularly useful is that the aromatic ring induces markedly different chemical shifts in the two diastereomeric



Mosher's acid
26

products (esters or amides) that are formed. This effect provides one of the most convenient ways of detecting and quantitating the two diastereomeric products - using ^1H and ^{19}F NMR spectroscopy^{44, 45, 46}. There are some reports about using MTPA as a chiral auxiliary for both HPLC [47-53]^{47, 48, 49, 50, 51, 52, 53} and GC^{5, 54} separations of chiral alcohols and amines.

44. Dale, J. A.; Dull, D. L.; Mosher, H. S.; *J. Org. Chem.*; **1969**, *34*, 2543

45. Dale, J. A.; Mosher, H. S.; *J. Am. Chem. Soc.*; **1973**, *95*, 512

46. Sullivan, G. R.; Dale, J. A.; Mosher, H. S.; *J. Org. Chem.*; **1973**, *38*, 2143

47. Paul T. Jackson; Tae-Young Kim; and Peter W. Carr, *Anal. Chem.*, **1997**, *69*, 5011

48. Duke, C. C. and Holder, G. M.; *J. Chromatogr.*; **1988**, *430*, 53

49. van Bladeren, P. J.; Sayer, J. M.; Ryan, D. E.; Thomas, P. E.; Levin, W.; Jerina, D. M.; *J. Biol. Chem.*, **1985**, *260*, 10226

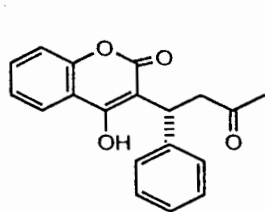
50. Balani, S. K.; van Bladeren, P. J.; Cassidy, E. S.; Boyd, D. R.; Jerina, D. M.; *J. Org. Chem.*, **1987**, *52*, 137

51. Armstrong, R. N.; Kedzierski, R.; Levin, W.; Jerina, D. M.; *J. Biol. Chem.*; **1981**, *256*, 4726

52. Sedman, A. J.; Gal, I.; *J. Chromatogr.*; **1984**, *306*, 155

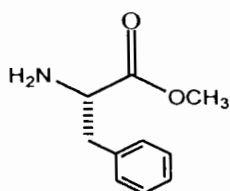
53. Miller, K. J.; Ames, M. M.; *J. Chromatogr.*; **1984**, *307*, 335

In their paper⁴⁷, Carr and *et al.* reported excellent HPLC resolution (see Figure 4, 5, 6 for chromatograms) of warfarin (27) **MTPA** ester, phenylalanine methyl ester (28) **MTPA** amide, and 4-chloroamphetamine (29) **MTPA** amide by a Zirconia-based carbon column. However, the **MTPA** diastereomeric esters of small alkyl alcohols exhibited poor separation with only octanol **MTPA** ester demonstrating partial separation in their study.



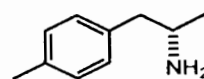
Warfarin

27



Phenylalanine methyl ester

28



4-Chloroamphetamine

29

This factor is one of the particular disadvantages for the use of Mosher's esters for HPLC separation of the diastereomeric products. According to previous reports, a large size difference between the groups attached to the chiral center of the derivatization reagent can improve the separation. For Mosher's reagent, the groups attached to the chiral center are rather small. If the groups attached to analyte chiral center are also small, the separation will be difficult to attain. This size factor is the reason why for some small alcohols, such as

54. Karl Blau and John M. Halket, "*Handbook of Derivatives for Chromatography*", 1977, chapter one

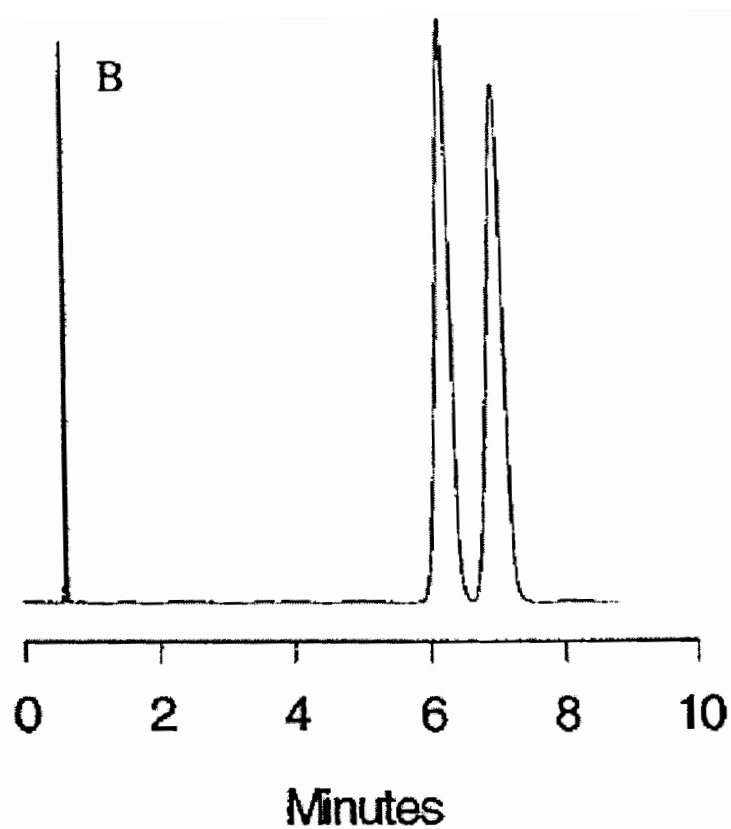


Figure 4 Chromatographic separation of (±)-warfarin-(R)-MTPA.
Re-produced from reference [38]. Chromatographic condition:
column: Hp-C/ZrO₂, 50 mm x 4.6 mm x 2.5 μm, flow rate: 1 ml/min;
mobile phase: 40:60/tetrahydrofuran: water, temperature: 30°C,
wavelength: 254 nm

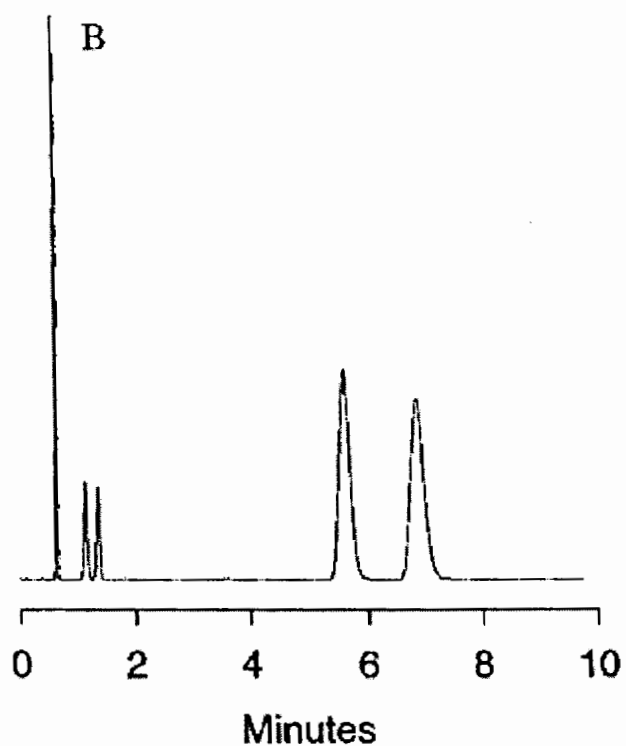


Figure 5 Chromatographic separation of (±)-4-chloroamphetamine-(R)-MTPA amide. Re-produced from reference [38].
Chromatographic condition: column: Hp-C/ZrO₂, 50 mm x 4.6 mm x 2.5 μm, flow rate: 1 ml/min; mobile phase composition: 45:55/tetrahydrofuran: water, temperature: 30°C, wavelength: 254 nm

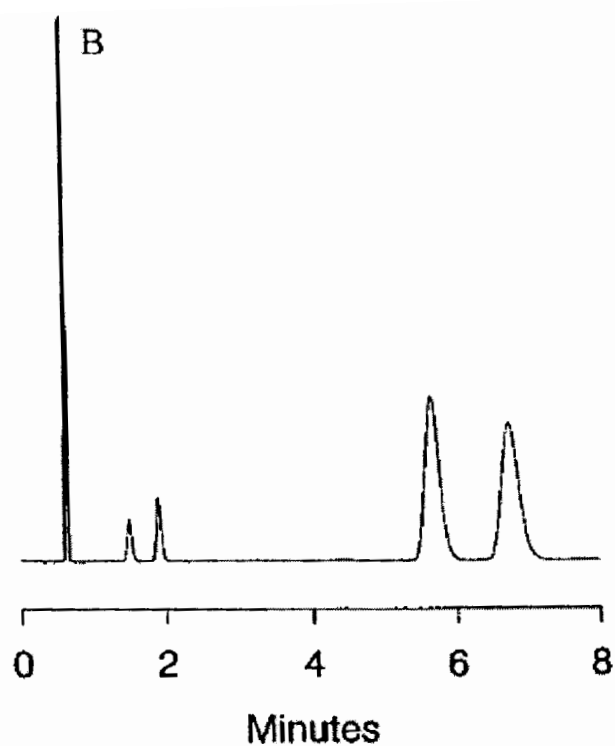
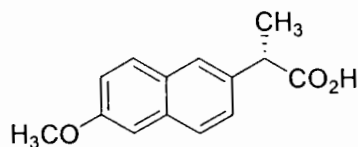


Figure 6 Chromatographic separation of (DL)-phenylalanine methyl ester-(R)-MTPA amide. Re-produced from reference [38]. Chromatographic condition: column: Hp-C/ZrO₂, 50 mm x 4.6 mm x 2.5 μ m, flow rate: 1 ml/min; mobile phase: 45:55/tetrahydrofuran: water, temperature: 30°C, wavelength: 254 nm

butanol, pentanol and heptanol, the co-elution of the resulting Mosher's diastereomeric esters are observed. The other disadvantage of Mosher's reagent is that Mosher's acid and acid chloride are prepared in quite a few steps. Such lengthy synthesis renders Mosher's reagents to be pretty expensive - currently available commercially at about \$230 per gram. A cheaper optically pure derivatization reagent is desirable.

(S)-(+)-6-methoxy- α -methyl-2-naphthaleneacetic acid (S-naproxen, see below for structure) is an anti inflammatory, non steroidal over-the-count medicine for pain.



S-naproxen

30

This compound is commercially available in large quantities with high optical purity. The price is rather cheap, about \$3 / gram. Structurally, the large, highly conjugated naphthyl ring attached to the chiral center provides some unique opportunities for chromatographic separation of the derivatization products. Its high UV absorbance (its molar absorptivity is about $100,000 \text{ cm}^{-1} \times \text{mol}^{-1} \times \text{L}^{55}$) will allow for highly accurate quantitation at low concentrations. The hydrophobic property of the naphthyl ring may also facilitate the achievement of excellent retention and separation. There are several published reports utilizing both chloride and acid forms of Naproxen as a derivatizing agent^{55, 56, 57, 58}.

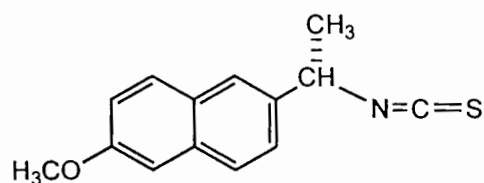
55. Spahn, H., *J. Chromatogr.*, **1988**, 427, 131

56. Büschges, R.; Linde, H.; Mutschler, E.; Spahn-Langguth, H.; *J. Chrom A.*, **1996**, 725, 323

57. Wang, C. P.; Howell, S. R.; Scatina, J.; Sisenwine, S.; *Chirality*, **1992**, 4(2), 84

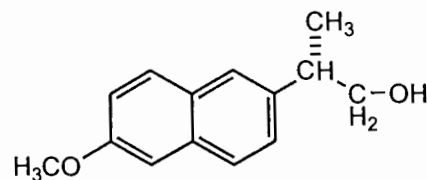
58. Büyüktimkin, N; Büyüktimkin, S.; Grunow, D.; ElZ, S. *Chromatographia*, **1988**, 25, 925

In their paper⁵⁶, Büschges and *et al.*, converted S-naproxen acid to its chloroformate, isothiocyanate and alcohol forms (see below for structures) and used them as derivatization reagents to accomplish chiral analysis through diastereomeric separation of S-naproxen derivative esters, carbonates and carbamates, respectively, for some β -adrenoceptor antagonists and antiarrhythmic agents.



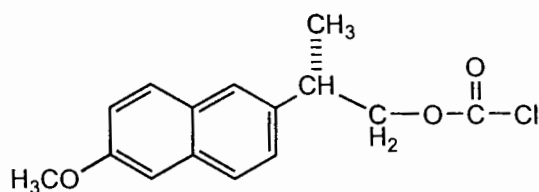
Naproxenisothiocyanate

31



Naproxen alcohol

32



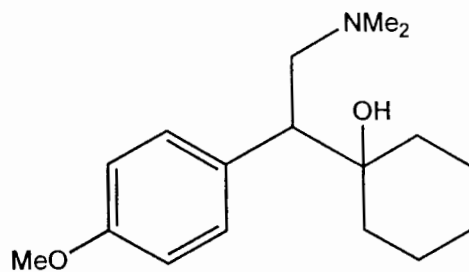
Naproxen chloroformate

33

The chromatographic parameters and resolution data are listed in Table 2. From the resolution data, we can conclude that esters, carbonates and carbamates of S-naproxen can be easily separated by reverse phase LC for these drug substances.

It was also reported that S-naproxen was used to derivatize Venlafaxine (see below for structure) to achieve the purpose of chiral analysis for this compound in the plasma of dog, rat and human⁵⁷. Naproxen exhibits fluorescence⁵⁵ and therefore is suitable for

biological samples to reduce the background noise in comparison to UV detection. In the paper⁵⁵, Spahn used naproxen chloride to derivatize the analytes in biological fluids and tissues to form a chiral marker. HPLC chiral analysis was also achieved in this study.



Venlafaxine

34

Table 2 Chromatographic parameters and data for the S-naproxen esters of some β -adrenoceptor antagonists and antiarrhythmic agents. This is re-produced from reference [56].

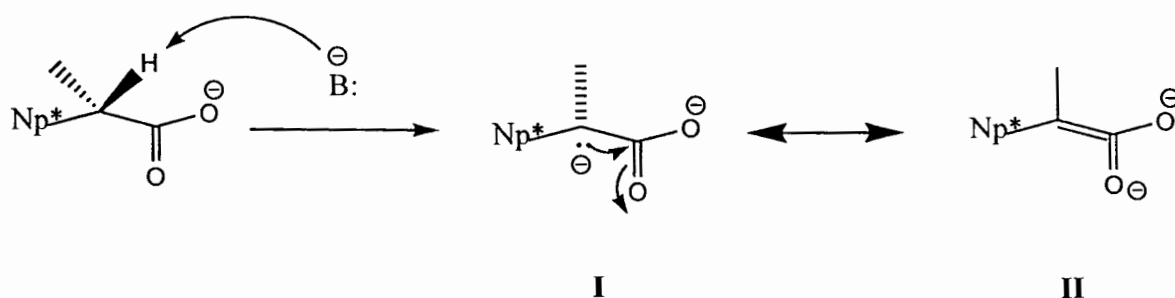
Compound	Mobile phase ^a	k'_1 ^b	k'_2 ^b	α ^b	R ^b	First-eluting enantiomer
Atenolol	A	5.2	6.1	1.17	2.4	(S)-(-)
Diacetolol	A	6.7	8.0	1.19	2.9	(S)-(-)
Metoprolol	B	20.4	25.4	1.25	3.9	(S)-(-)
Carvedilol	C	7.1	8.0	1.13	4.2	(S)-(-)
Propranolol	D	8.7	10.7	1.23	3.9	(S)-(-)
Alprenolol	D	9.4	11.8	1.25	4.1	(S)-(-)
Propafenone	C	9.5	10.2	1.07	1.3	(R)-(-)
Flecainide	C	12.3	12.3	1.00	0.0	-
Tocainide	E	10.1	11.1	1.10	1.1	(S)-(+)

Column, 250 × 4 mm I.D.; packing material, Zorbax ODS, 5 μ m (Bischoff).

^a Mobile phase: acetonitrile-water (v/v): A, 50:50, 1.0 ml/min; B, 55:45, 1.0 ml/min; C, 70:30, 1.0 ml/min; D, 70:30, 0.8 ml/min; E, methanol-water 70:30 (v/v), 0.8 ml/min.

^b k' = capacity factor; α = separation factor; R = resolution factor.

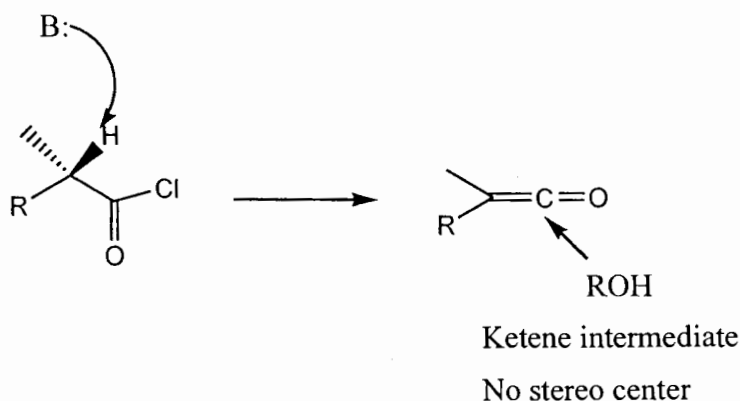
All of the above studies provided useful information on chiral analysis using derivatization with S-naproxen. Compared to the popular Mosher's reagent, S-naproxen has an α -hydrogen atom attached to its chiral center and thus the possibility of racemization exists (see scheme A below for the possible mechanism). From scheme A, the resonance structure **II** indicates a planar ionic intermediate which is the source of racemization. No report has discussed this racemization in detail. Therefore, a more detailed study for these types of reaction and HPLC separation conditions is desired.



Scheme A

The functional group of naproxen is the carboxylic acid moiety. However, the esterification reaction between an acid and alcohol is very difficult to carry out to 100 percent conversion. We either have to use a coupling reagent, such as dicyclohexylcarbodiimide (DCC), or use an activated form, such as the acid chloride of naproxen to completely convert the chiral alcohol. Since there is a hydrogen atom (α hydrogen) attached to the chiral center, extreme basic and acid reaction conditions may cause racemization of naproxen acid chloride. Formation of a ketene intermediate has been

proposed under basic conditions (see Scheme B). Thus, the accuracy of the method will potentially be greatly reduced under basic conditions.



Scheme B

Additionally the preparation of the acid chloride entails an extra step to perform the derivatization process. Therefore, the use of naproxen acid form directly appears to be a better choice. According to previous work^{59, 60}, alcohols can be esterified completely by using DCC as the coupling reagent and base as catalyst. It was reported that optically pure menthol can be esterified by some acids by using diisopropylcarbodiimide as coupling reagent and the distereomeric esters were separated by capillary GC to achieve the purpose of chiral analysis of acids⁵⁵.

In this thesis, S-naproxen acid is used as the chiral auxiliary reagent for chiral analysis of chiral alcohols. The reaction mechanism will be discussed. The reaction kinetics was thoroughly studied for the first time as this was identified as the primary factor for the initial

59. Hassner, A.; Alexanian, V.; *Tetrahedron Lett.*, **1978**, *19*, 4475

60. Neises, B. and Steglich, W.; *Angew. Chem. Int. Engl.* **1978**, *17*, 522

inaccurate results for the chiral analysis. The optimization of synthetic conditions of naproxen esters was the most important issue to ensure the accuracy of this analytical chiral analysis method. The HPLC conditions for the separation of S-naproxen diastereomeric esters were also thoroughly studied in this research.

The Zirconia based polybutadiene column is a new type of commercially available polymer-based reversed phase column. Unlike conventional silica based chromatographic columns, this column offers excellent acid, base and thermal stabilities. Our results have shown that this column exhibits better separation power than conventional C18 and C8 phases, in some cases, for the separation of positional isomers, structurally related isomers and *trans/cis* isomers. This thesis will be the first report of diastereomeric separations on the Zirchrom-PBD column.

For reversed-phase HPLC, the separation power is primarily dependent on the hydrophobic interactions occurring between the solutes and the stationary phase. Thus, the hydrophobic selectivity is a very important parameter for the comparison of separation powers between columns. It is well known that the capacity factor of a homologous series of solutes follows the below relationship⁶¹ over a moderate mobile phase composition range:

$$\ln k' = a + bn_{CH_2} + c\phi + dn_{CH_2}\phi \quad (1)$$

where n_{CH_2} is the number of methylene groups, ϕ is the volume fraction of organic modifier in the mobile phase, and a , b , c and d are empirical fitting coefficients. We can derive eq.2 from eq.1 as follows:

61. Karger, B.; Gant, J. R.; Hartkopf, A.; Weiner, P. H.; *J. Chromatogr.* **1976**, *128*, 65-78

$$\begin{aligned}\ln k' &= (a + c\phi) + (b + d\phi)n_{CH_2} \\ &= A + Bn_{CH_2}\end{aligned}\quad (2)$$

A is the absolute retention and the slope B is the hydrophobic selectivity^{61, 62}. Hydrophobic selectivity *B* consequently can be determined by measurement of the capacity factors for a homologous series. It was found that Zirconia based polybutadiene column has better hydrophobic selectivity than conventional C18 and C8 columns [63, 64]^{63, 64}. The polarity of Zirconia based polybutadiene columns is usually higher than that of silica based C18/C8 columns. For the same solute, 15% to 25% lower acetonitrile is needed to maintain the same retention capacity factor for Zirconia based polybutadiene columns as compared to silica based C18/C8 column. This effect might be the reason for the higher hydrophobic selectivity for Zirconia based polybutadiene columns, since there is less acetonitrile to compete for the hydrophobic sites on the stationary phase.

Zirconia based polybutyldiene columns have exhibited very good selectivities for our S-naproxen esters. This is one of the primary columns we used for separation of S-naproxen esters. Other silica based C18 columns can also separate some of the S-naproxen esters. We have shown that ODS-AM column produced by YMC Inc. and supplied by Waters Inc. also provide excellent resolution for S-naproxen esters.

62. Vigh, G.; Varga-Puchony, Z.; *J. Chromatogr.*; **1980**, *196*, 1-9

63. Jianwei Li and Peter W. Carr, *Analytica Chimica Acta* **1996**, *334*, 239-250

64. Jianwei Li and Peter W. Carr, *Anal. Chem.*, **1996**, *68*, 2857-2868

Chapter 2 Accuracy of the Derivatization Methods:

Chiral Alcohols/(S)-naproxen

§ 2.1 Introduction

The accuracy of the derivatization methods is always a major concern for analytical chemists, since the enantiomeric excess (*ee* ratio) is indirectly determined by the resulting diastereomeric ratio (*de* ratio). There are three key factors which can affect the accuracy for the derivatization methods. The completion of the derivatizing reaction is one of the key factors when the kinetic resolution of the reaction is such that the R enantiomer reacts faster or slower with the derivatizing reagent than does the S enantiomer⁶⁵. A second key factor is racemization of the analyte and/or the chiral derivatizing reagent¹. It has been pointed out that acid chlorides containing a proton attached to chiral carbon (α hydrogen) can racemize under extreme pH conditions or at elevated temperatures¹. S-naproxen acid has an α hydrogen. In this study very mild reaction conditions were utilized to minimize the possibility of racemization. The third factor that can affect analysis accuracy is the lack of base line separation of the resulting diastereomers. In this chapter, the accuracy of our method will to be discussed and the reasons that cause inaccurate results will be analyzed.

65. Morris Zief and Laura J. Crane (editor), *Chromatographic Chiral Separation*, chapter 4

As an indirect method for chiral analysis, the validation of this analytical method is critical. Generally, the purpose of a validation study is to evaluate the accuracy and precision of the analytical method. The accuracy of this derivatization method will be determined by direct comparison of the *ee* ratio of the starting alcohol enantiomer with the *de* ratio of the resulting diastereomeric ester over a broad range. Such direct comparison will give us a very clear indication of the quality of the method.

§ 2.2 Experimental Section

2.1. Reagents

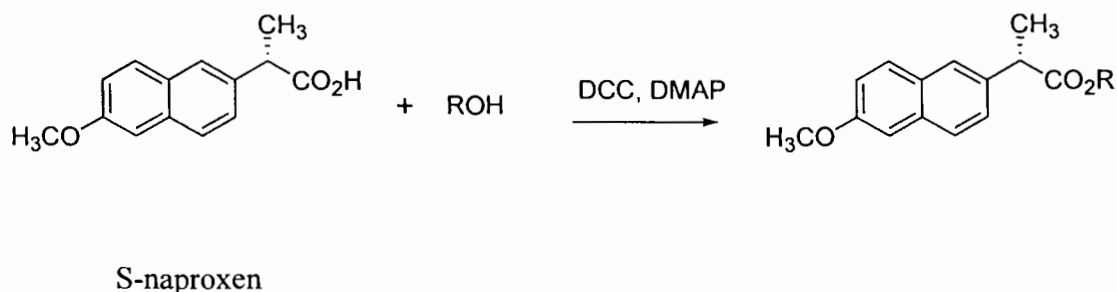
The following chemicals are purchased from Aldrich: S-naproxen acid ((S)-(+)- 6-methoxy- α -methyl-2-naphthaleneacetic acid) with greater than 99% purity and enantiomeric excess ratio; 1,3-dicyclohexylcarbodiimide and 4-dimethylaminopyridine in reagent grade form; (S)-(-)-1-phenylethanol, (R)-(+)-1- phenylethanol, (S)-(-)-1- phenylpropanol and (R)-(+)-1- phenylpropanol were purchased from Fluka in greater than 99% purity and 99% *ee* as ChiralSelect grade.

2.2. Chromatographic conditions

All chromatographic studies were performed on a Hewlett Packard 1100 HPLC system equipped with a photo diode array UV detector. Data acquisition and treatment was performed with a Perkin Elmer Turbochrom system. The reported chromatographic data is the average of triplicate determinations. The void volume was determined as the time of the first disturbance peak. The mobile phase was a mixture of HPLC grade acetonitrile and HPLC grade water. HPLC grade acetonitrile was purchased from EM Science and HPLC grade water was obtained from a Pico water purifying system. The percent of diastereomeric ester was calculated based on the peak area ratio of SS- and SR- form of S-naproxen esters. It is assumed that the molar absorbances are the same. This is confirmed by the analysis of the peak area when the racemic alcohol is used.

2.3. Derivatization reaction procedure

The reaction for the coupling of S-naproxen with a chiral alcohol is based on the work of Hassner and Alexanian⁵⁹, Neises and Steglich⁶⁰, Ballard, Eller and Knapp⁶⁶ and Kovach⁶⁷ with some modification.



10 ml anhydrous ether was added to one equivalent of chiral alcohol, then three equivalents of S-naproxen, three equivalents of dicyclohexylcarbodiimide (DCC) and 0.1 equivalents of 4-dimethylaminopyridine(DMAP) were added to the reaction solution. The reaction was stirred for four hours at room temperature. The white precipitate of urea derivative appeared as one of the major side products. HPLC can be used to check the reaction progress. Generally, the reaction takes four hours to complete. At the end of reaction, the reaction mixture was filtered. Then, the reaction solution was washed with dilute HCl solution, saturated sodium bicarbonate solution and HPLC grade water. With proper dilution, this solution was ready for diastereomeric analysis by HPLC. For the S-naproxen esters made for

66. Ballard, K. D.; Eller, T. D. and Knapp, D. R.; *J. Chromatogr.*; **1983**, 275, 161

67. Kovach, T. F.; *Master degree thesis, the Department of Chemistry and Biochemistry, Seton Hall University, year 2000*

this study, a preparative TLC technique was used to purify the reaction mixtures. A silica plate was used as the stationary phase and 10% ethyl acetate /90% hexanes were used as mobile phase for the TLC. NMR measurements were made of the purified products to confirm their structures.

In this accuracy studies, *sec*-phenyl ethyl alcohol was the target chiral species. Enantiomerically pure R- *sec*-phenyl ethyl alcohol and S- *sec*-phenyl ethyl alcohol were mixed in different ratios as the starting material. After derivatization, the reaction mixture was analyzed by the means of HPLC and the *de* ratio of the resulting S-naproxen esters was compared to the *ee* ratio of the starting mixture.

§ 2.3 Results and discussion

In order to determine if derivatization followed by HPLC separation is feasible for chiral analysis, validation for this reaction is required. In the early stage of this investigation, *sec*-phenethanol was used as a primary probe for the purpose of validation with the ratio of alcohol:S-naproxen:DCC = 1: 3: 3, (the reaction condition described by the reference⁶⁷). It was observed that the accuracy of this derivatization method was influenced by the *ee* ratio of the *sec*-phenyl ethyl alcohol enantiomer starting material. When the percent of R- *sec*-phenyl ethyl alcohol is close to 50%, the discrepancy between the *ee* ratio of the *sec*-phenyl ethyl alcohol enantiomer and the *de* ratio of resulting S-naproxen ester is rather small. However, when the difference between the amount of R and S *sec*-phenyl ethyl alcohol is large, the discrepancy between the *ee* ratio of the *sec*-phenyl ethyl alcohol enantiomer and the *de* ratio of resulting S-naproxen ester is greater (see Figure 7), particularly when the percent of R enantiomer is much lower than that of the S enantiomer. The difference between the *ee* ratio of the *sec*-phenyl ethyl alcohol enantiomer and the *de* ratio of the resulting S-naproxen ester differed by as much as 10%. The error of this derivatization method exceeds the expected requirements of such an analytical method. Typically, the relative standard deviation should be less than 1% for an LC analytical method. The analytical error for this derivatization method could be due to incompleteness of the derivatization reaction with S-naproxen acid. Also, it could be due to racemization occurring during the derivatization reaction. Further studies were needed to confirm which of the two hypotheses were responsible for the observed discrepancies.

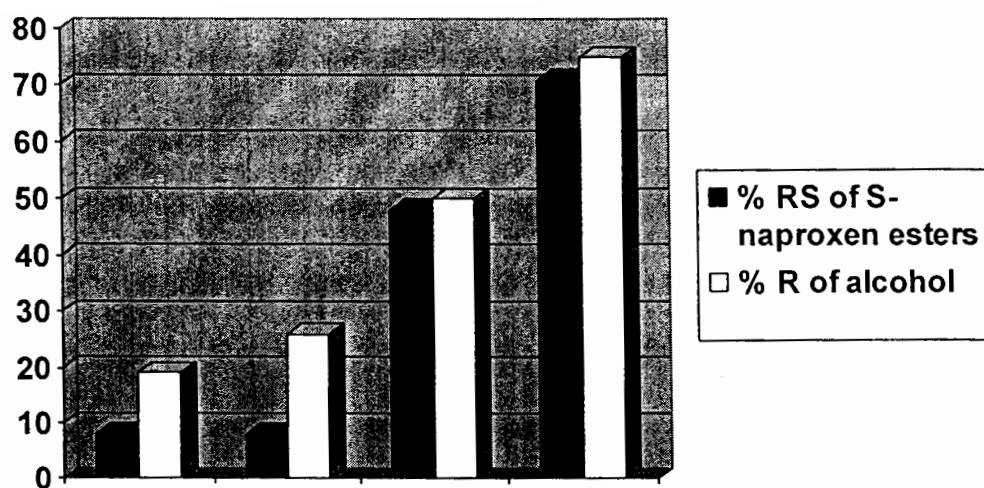
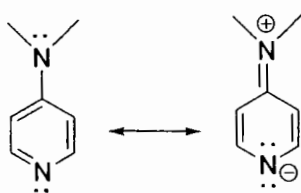


Figure 7 Linearity studies for esterification reaction of *sec*-phenyl ethanol and S-naproxen.
 □: is the percent of R in *sec*-phenyl ethanol starting material and
 ■: is the percent of RS in S-naproxen *sec*-phenyl ethanol ester product.

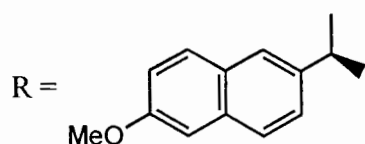
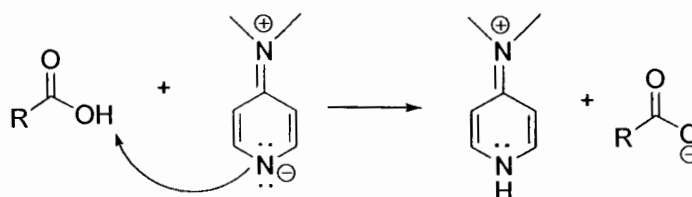
§ 2.4 The possible mechanism of derivatization of chiral alcohol with S-naproxen acid

As discussed in the previous chapter, there is an α hydrogen atom attached to naproxen's chiral center. The existence of this α hydrogen atom could cause racemization for the derivatization reaction. The possible reaction mechanism of this derivatization reaction depicts this clearly. The reaction mechanism can be divided into the following steps:

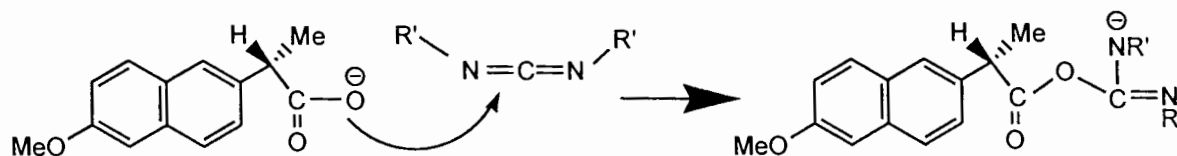
1) resonance structure of 4-dimethylaminopyridine:



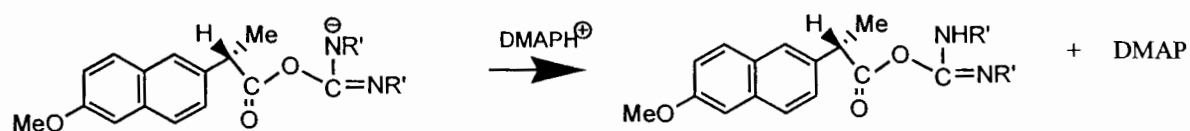
2) Deprotonation of the carboxylic acid occurs:



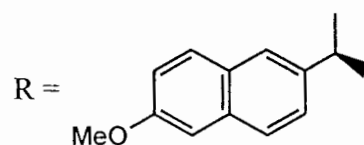
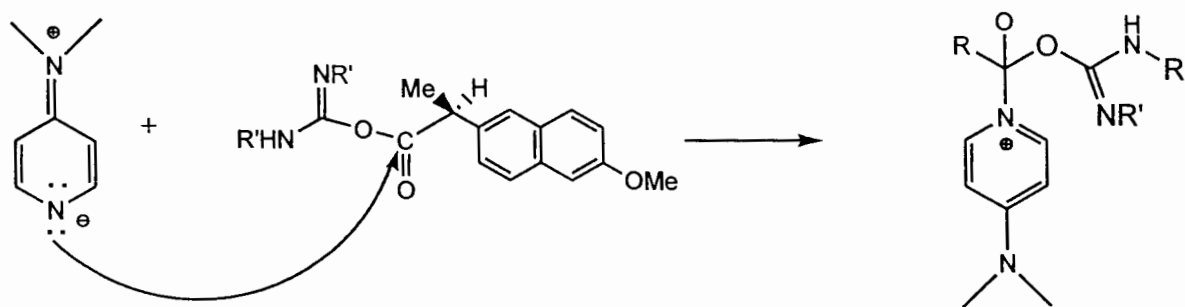
3) Nucleophilic attack on the carbodiimide follows:

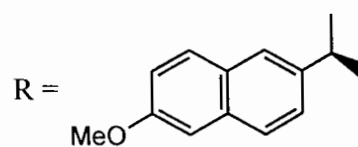
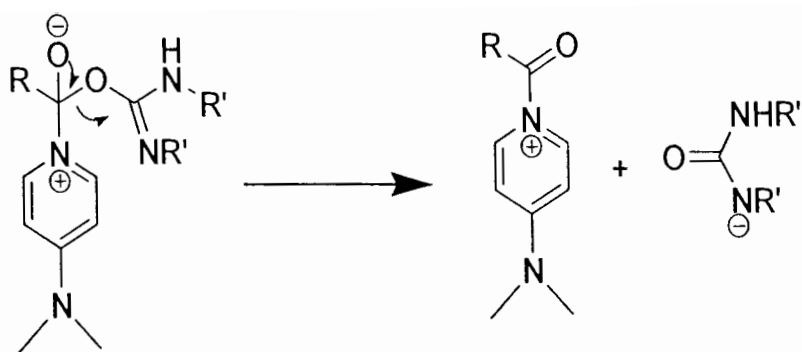


4) Protonation of carbimide adduct:

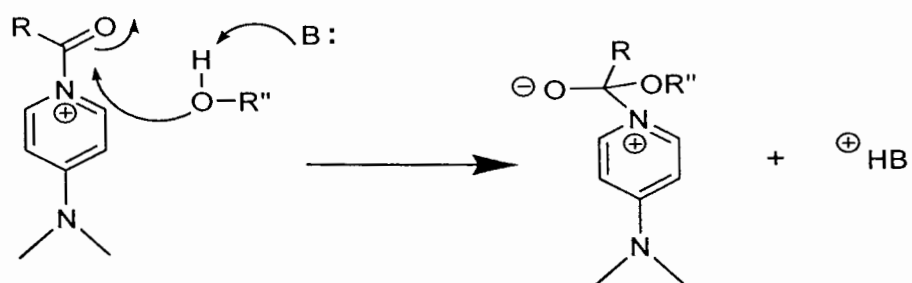


5) Nucleophilic attack on the carbodiimide adduct and generation of acyl-DMAP intermediate:



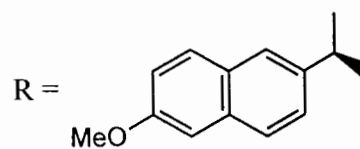


6) Nucleophilic attack of alcohol on the DMAP adduct:

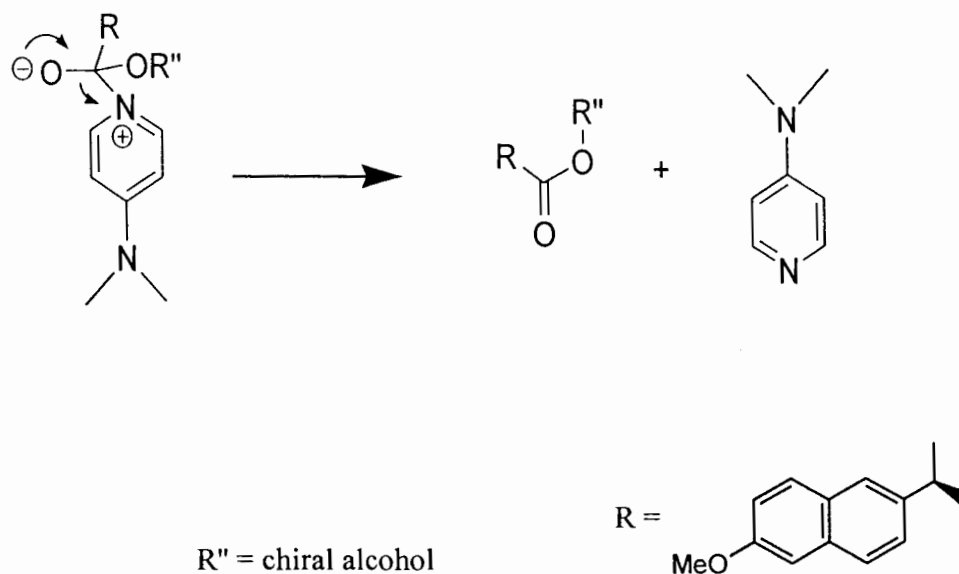


R'' = chiral alcohol

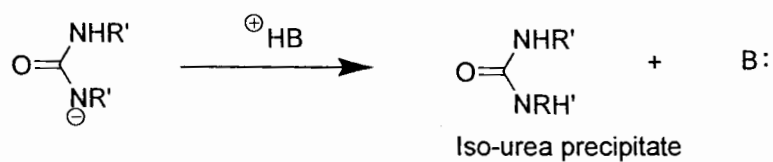
B: = DMAP



7) Formation of S-naproxen chiral alcohol ester:

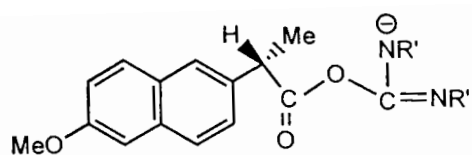


8) Iso-urea precipitates from the ether solution:

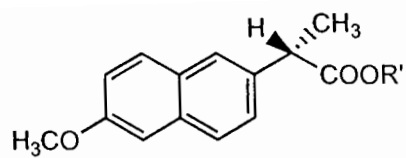


$B: = \text{DMAP}$

This proposed mechanism shows several possible intermediates (see below) where α -hydrogen deprotonation may occur. Strong base can de-protonate the α hydrogen and re-protonation of this hydrogen could occur in both directions of the plane of the molecule.

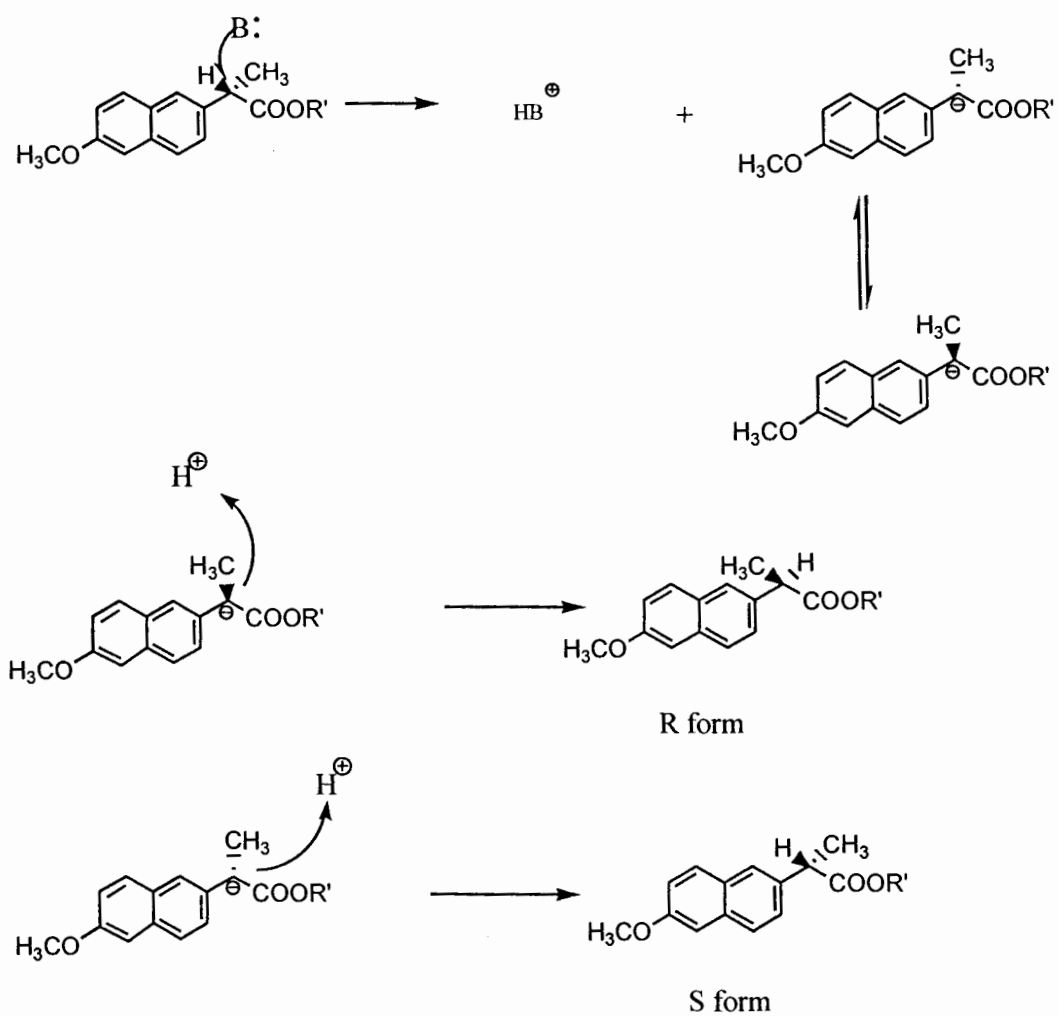


intermediate



S-naproxen ester

Therefore the chiral center could lose its original orientation, as shown below:



However, the pKa of the α hydrogen in this case is about 20 to 25, similar to typical α hydrogen of ketones. It needs a very strong base for deprotonation. The base used in this derivatization reaction is DMAP and its pKa is about 9.7 (data is from Merck Index). Theoretically, it is not strong enough to deprotonate this α hydrogen. Especially, given that DMAP is present at a catalytic amount (0.1 mole ratio). Consequently, we can conclude that the racemization of the S-naproxen ester or possible reaction intermediates is not the primary cause of the observed inaccuracy associated with this derivatization method.

§ 2.5 Kinetic resolution of the derivatization reaction of chiral alcohols with S-naproxen acid

It is possible that one enantiomer may react with a derivatization reagent faster than the other enantiomer. Burden *et al.*⁹ observed some enantioselectivity for incomplete reactions of acid chloride with alcohols, when either 4-dimethylaminopyridine or N-methylimidazole was added as the catalyst. Since one form is not completely derivatized, the *de* ratio of resulting diastereomers is not going to reflect the *ee* ratio of the starting material of the analyte enantiomers. Therefore, the accuracy of the derivatization method is reduced.

The reaction rate difference between the two enantiomers can be easily detected by monitoring the reaction closely. In our studies, aliquots were taken and quenched with 50:50/saturated NaHCO₃ solution : acetonitrile and the quenched solution was analyzed by HPLC. If no kinetic resolution exists, the *de* ratio of the resulting diastereomers constant is not going to change throughout the entire reaction process. However, if the *de* ratio of the resulting diastereomers changes during the reaction, then kinetic resolution is occurring. The kinetics favors the enantiomer whose percentage is decreasing during the reaction. The derivatization reaction of chiral alcohols with S-naproxen acid was monitored by using (±)*sec*-phenyl ethyl alcohol as the model. The data is shown in Figure 8.

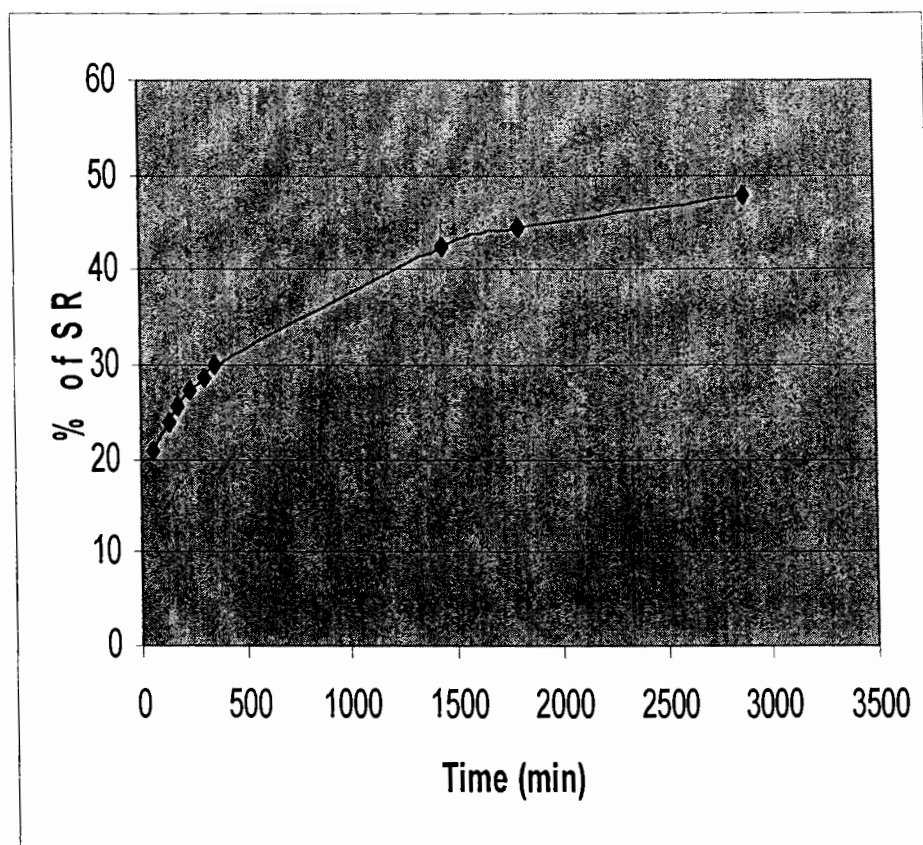


Figure 8 Percent of SR *sec*-phenyl ethyl alcohol naproxen ester during the derivatization reaction.

From Figure 8, we can see that the percentage of the RS form of *sec*-phenyl ethyl alcohol S-naproxen ester is increasing as the reaction proceeds. The percent of SS form of *sec*-phenyl ethyl alcohol S-naproxen ester is always higher than that of the RS form. The reaction clearly favors the formation of SS form of *sec*-phenyl ethyl alcohol S-naproxen ester.

The relative reaction rates constants are measured for the reaction of both enantiomers with S-naproxen acid to confirm the above observation. Ten mLs of anhydrous ether was added to 0.1mmol of pure enantiomeric form of *sec*-phenyl ethyl alcohol, then ten equivalents of S-naproxen, eight equivalents of dicyclohexylcarbodiimide (DCC) and 0.1 equivalents of 4-dimethylaminopyridine(DMAP) was added to the reaction solution. The reaction for *sec*-phenyl ethyl alcohol can be considered as pseudo first reaction, since the S-naproxen acid and dicyclohexylcarbodiimide are present in excess. The concentration of *sec*-phenyl ethyl alcohol is measured by HPLC method. By plotting the logarithmic concentration of *sec*-phenyl ethyl alcohol vs. the time, a straight line is obtained and the reaction rate constant is obtained from the slope of the line. Four measurements for R- *sec*-phenyl ethyl alcohol were made and three measurements for S *sec*-phenyl ethyl alcohol were made. Figure 9 to Figure 16 are the plots for the rate constants and Table 3 is the summary of the whole set of data.

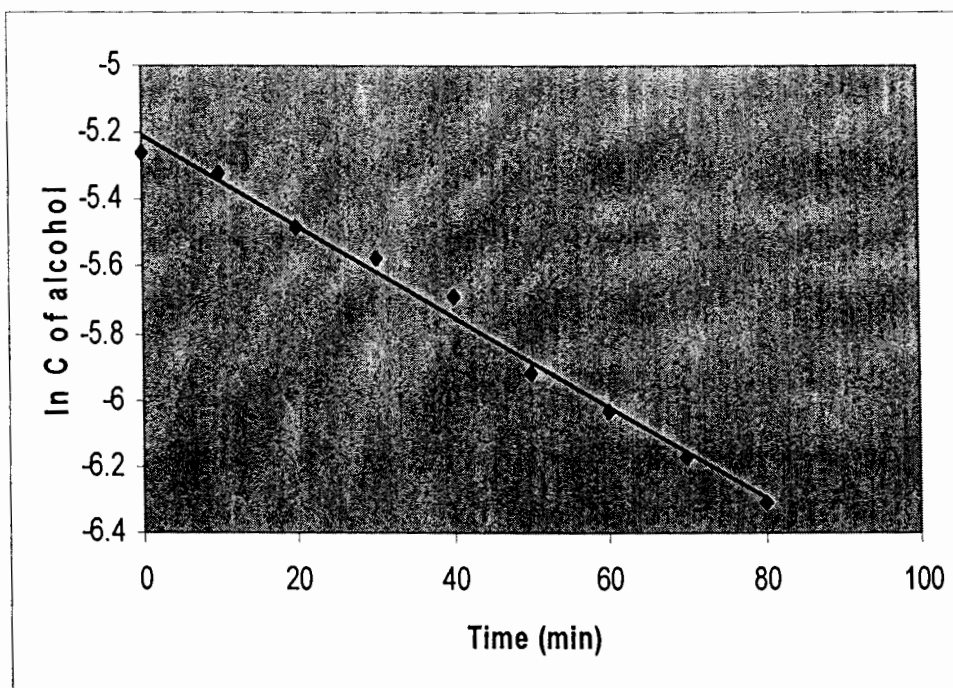


Figure 9 Kinetic plot for pseudo first order reaction of *sec*-phenyl ethyl alcohol with S-naproxen. First measurement of reaction rate constant for R- *sec*- phenyl ethyl alcohol. correlation coefficient $R^2 = 0.99$, reaction rate constant = slope = 0.0136

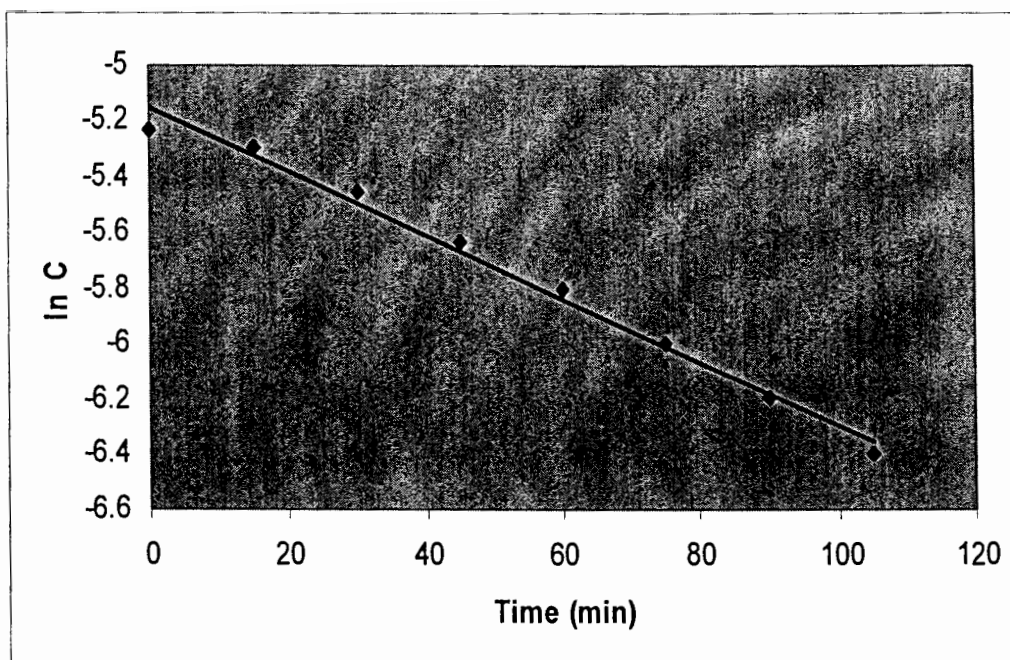


Figure 10 Kinetic plot for pseudo first order reaction of *sec*-phenyl ethyl alcohol with S-naproxen. Second measurement of reaction rate constant for R- *sec*-phenyl ethyl alcohol. correlation coefficient $R^2 = 0.99$, reaction rate constant = slope = 0.0114

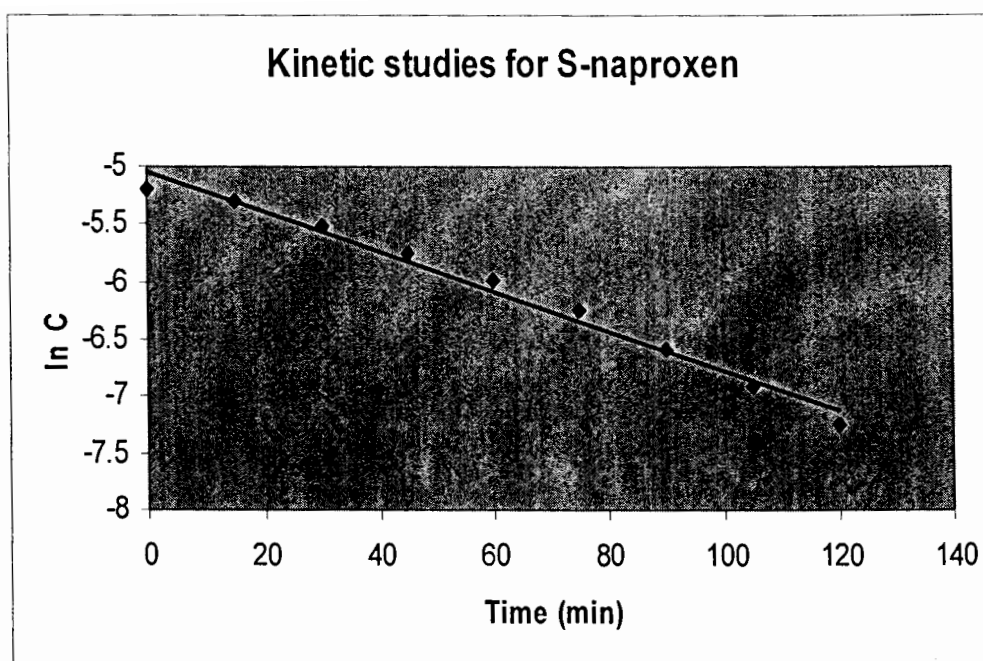


Figure 11 Kinetic plot for pseudo first order reaction of *sec*-phenyl ethyl alcohol with S-naproxen. Third measurement of reaction rate constant for R- *sec*-phenyl ethyl alcohol. correlation coefficient $R^2 = 0.99$, reaction rate constant = slope = 0.0174; This data is rejected according to Q-test.

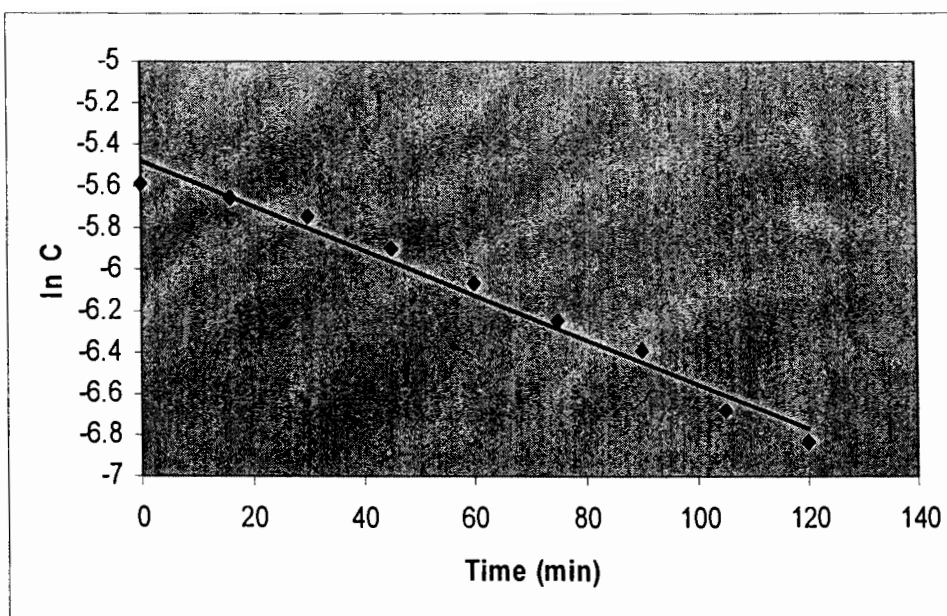


Figure 12 Kinetic plot for pseudo first order reaction of *sec*-phenyl ethyl alcohol with S-naproxen. Fourth measurement of reaction rate constant for R- *sec*-phenyl ethyl alcohol. correlation coefficient $R^2 = 0.98$, reaction rate constant = slope = 0.0108

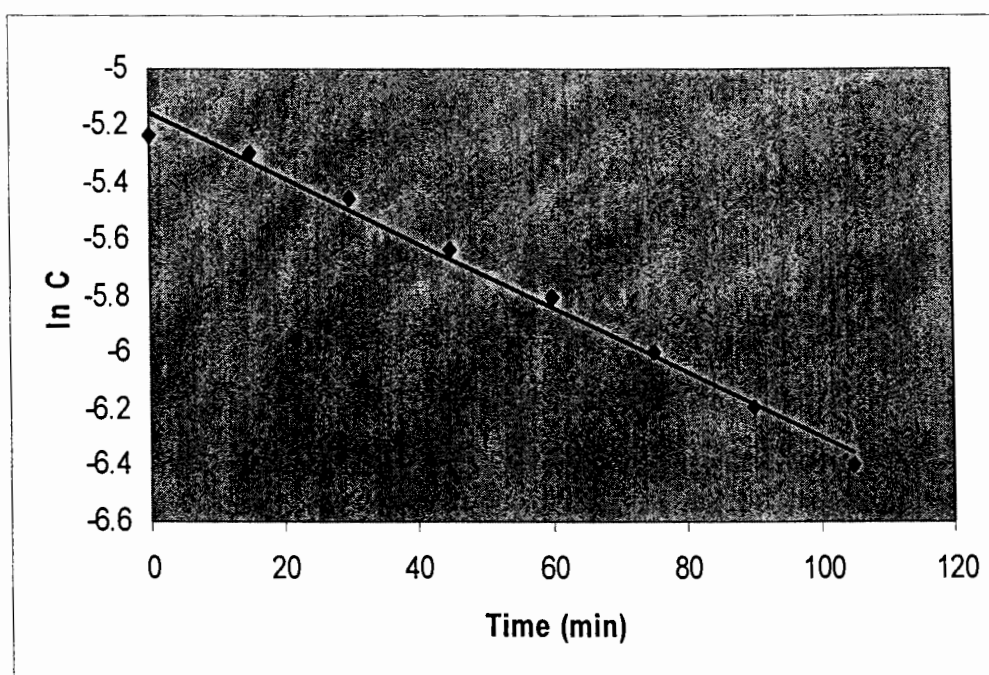


Figure 13 Kinetic plot for pseudo first order reaction of *sec*-phenyl ethyl alcohol with S-naproxen. Fifth measurement of reaction rate constant for R- *sec*-phenyl ethyl alcohol. correlation coefficient $R^2 = 0.99$, reaction rate constant = slope = 0.0114

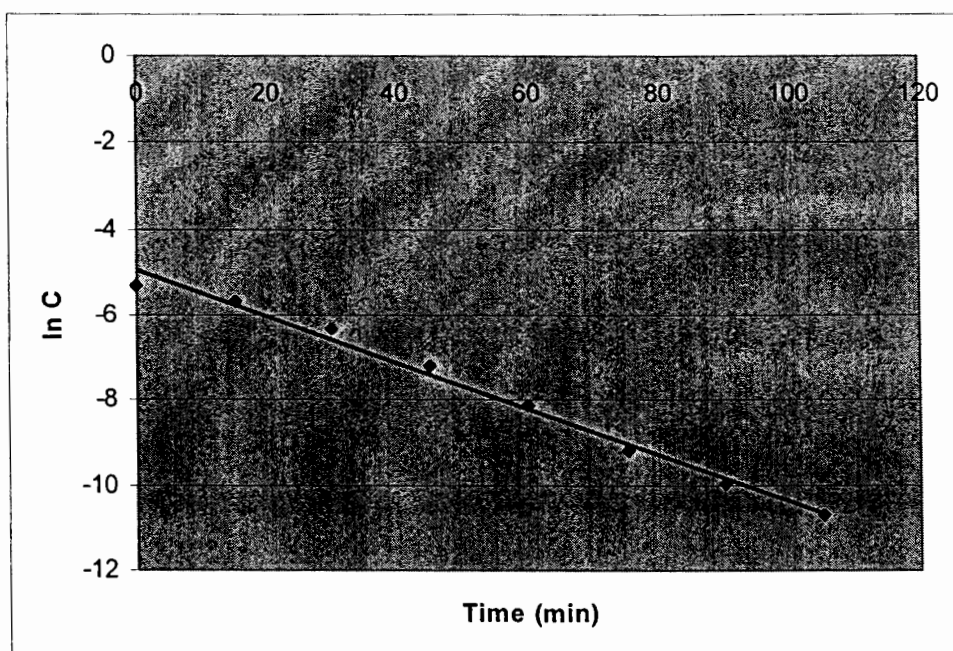


Figure 14 Kinetic plot for pseudo first order reaction of *sec*-phenyl ethyl alcohol with S-naproxen. First measurement of reaction rate constant for S- *sec*-phenyl ethyl alcohol. correlation coefficient $R^2 = 0.99$, reaction rate constant = slope = 0.0544

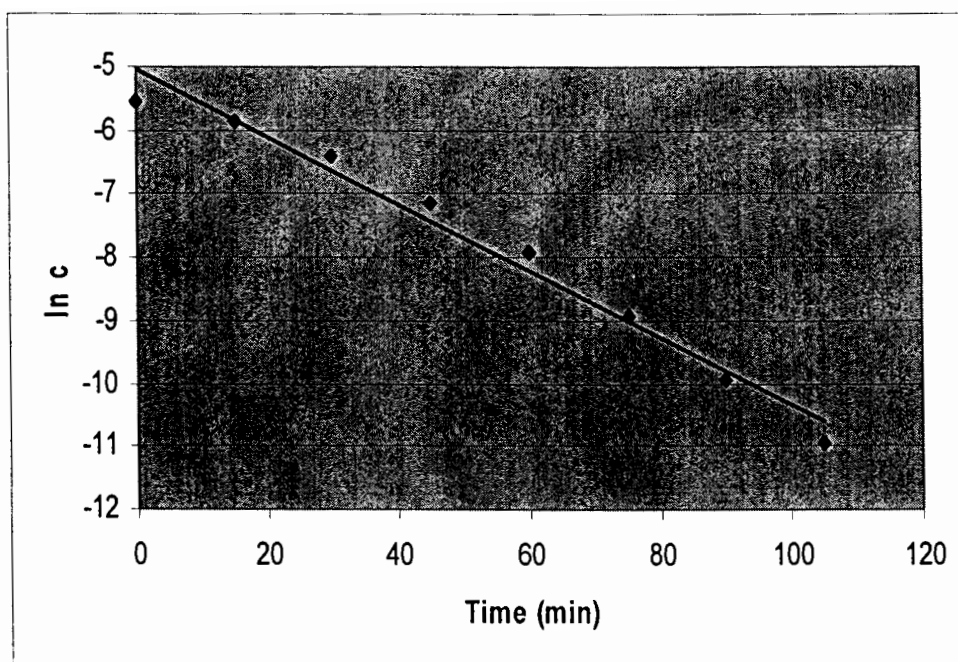


Figure 15 Kinetic plot for pseudo first order reaction of *sec*-phenyl ethyl alcohol with S-naproxen. First measurement of reaction rate constant for S- *sec*-phenyl ethyl alcohol. correlation coefficient $R^2 = 0.98$, reaction rate constant = slope = 0.0529

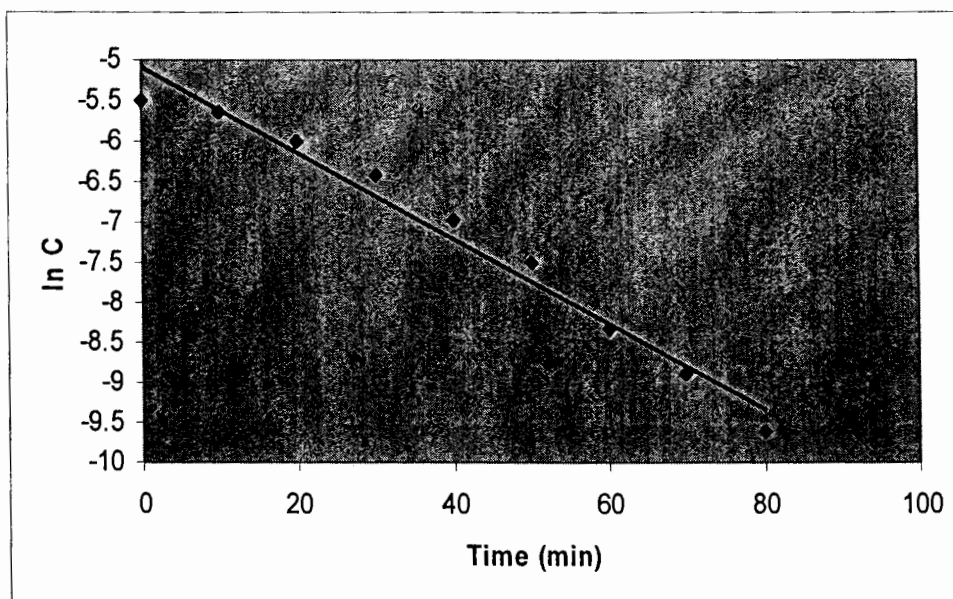


Figure 16 Kinetic plot for pseudo first order reaction of *sec*-phenyl ethyl alcohol with S-naproxen. First measurement of reaction rate constant for S- *sec*-phenyl ethyl alcohol. correlation coefficient $R^2=0.98$, reaction rate constant = slope = 0.0527

Table 3. Reaction rate constants for the reaction of R-*sec*-phenethanol and S- *sec*-phenethanol with S-naproxen

k(mmol/min) for R- <i>sec</i> -phenyl ethanol	k(mmol/min) for S- <i>sec</i> -phenyl ethanol
0.0136	0.0544
0.0114	0.0529
0.0108	0.0527
0.0114	
%RSD: 1.18%	1.70%
Avg. 0.0118	0.0533

The reaction rate constants showed that the S- *sec*-phenyl ethyl alcohol reacts 4.5 times faster than R- *sec*-phenyl ethyl alcohol does. So the reaction is favored to form SS- *sec*-phenyl ethyl alcohol naproxen ester. In the situation where the reaction does not go to the completion, the unreacted alcohol would be predominantly the un-favored enantiomer. This difference is the reason that the percent of RS form, as determined by the *de* was always less than the original *ee*. This implies that the esterification reaction under the current conditions was not proceeding to completion. Thus, a small portion of R *sec*-phenyl ethyl alcohol remains unreacted. Based on these findings, , we decided to study in greater detail the reaction conditions to determine if they can be optimized to drive the reaction to completion. This will be discussed in the next chapter.

§ 2.6 Conclusions

The possible reaction mechanism for derivatization of chiral alcohols with S-naproxen was analyzed. From the pKa range of the α hydrogen which is attached to the chiral center of S-naproxen acid, we know that 4-dimethylaminopyridine is not basic enough to de-protonate the α hydrogen. This therefore is not the primary reason for accuracy problems observed with this derivatization method.

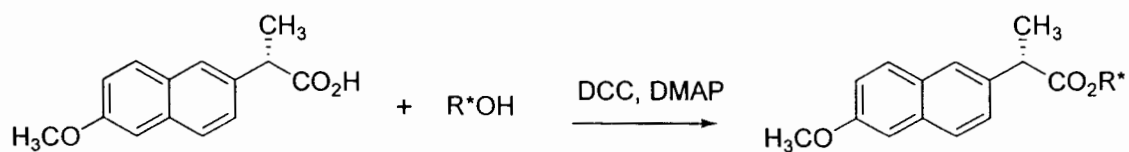
Kinetic studies were performed on the derivatization of *sec*-phenyl ethyl alcohol with S-naproxen. The reaction rate for S-*sec*-phenyl ethyl alcohol was found to be 4.5 time faster than that of R-*sec*-phenyl ethyl alcohol. When the mixture of S and R *sec*-phenyl ethyl alcohol reacts with S-naproxen, the formation of SS *sec*-phenyl ethyl alcohol naproxen ester is preferred. If the derivatization reaction does not go to completion under certain reaction conditions, the residual unreacted alcohol will be the R enantiomer. Therefore, analysis of *de* ratio of resulting ester would not correctly reflect the true *ee* ratio of the starting alcohol. The optimization of esterification reaction of S-naproxen acid with chiral alcohol is therefore critical to obtaining accurate results.

Chapter 3 Optimization of reaction conditions

§ 3.1 Introduction

The kinetic studies provided strong evidence that the accuracy problem of the derivatization method with S-naproxen acid could be attributed to the incomplete reaction with the chiral alcohol. Because the reaction rate of S-alcohol is much larger than that of R-alcohol, the current reaction conditions could not drive the reaction with the R-alcohol to completion. Consequently, the reaction conditions need to be optimized to carry the reaction to completion.

In order to carry one reactant to completion, one can usually increase the concentrations of other reactants. In the derivatization reaction of chiral alcohols with S-naproxen acid, there are three other components as shown in the following reaction scheme:



Among these three reactants, 4-dimethylaminopyridine is the catalyst and increased amounts of it could potentially cause the epimerization of the diastereomeric esters. Thus, the levels

of S-naproxen acid and dicyclohexanecarbodiimide are primary options for the optimization of reaction conditions.

In this chapter, we detail optimization of the reaction conditions to drive the derivatization to completion. The newly optimized reaction conditions were then validated to test the accuracy of the method. In the validation studies, two different chiral alcohols were used as the target molecules. The range of the *ee* ratios of the chiral alcohols used in the validation is wide enough to cover the entire range of analytical possibilities.

§ 3.2 Experimental Section

Reagents

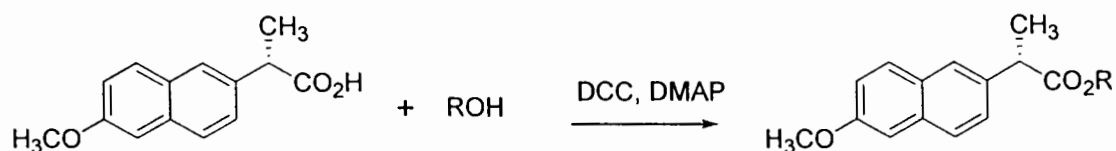
The following chemicals are purchased from Aldrich: S-naproxen acid ((S)-(+)- 6-methoxy- α -methyl-2-naphthaleneacetic acid) with greater than 99% purity and enantiomeric excess ratio; 1,3-dicyclohexylcarbodiimide and 4-dimethylaminopyridine with reagent grade; (S)-(-)-1-phenylethanol, (R)-(+)-1-phenylethanol, (S)-(-)-1-phenylpropanol and (R)-(+)-1-phenylpropanol are purchased from Fluka with greater than 99% purity and and 99% *ee* as ChiralSelect grade.

Chromatographic conditions

All chromatographic studies were performed on Hewlett Packard 1100 HPLC system equipped with a photo diode array UV detector. Data acquisition and treatment was performed with a Perkin Elmer Turbochrom system. The reported chromatographic data is the average of triplicate determinations. The void volume was determined by the first disturbance peak. The mobile phase was a mixture of HPLC grade of acetonitrile and HPLC grade water. HPLC grade acetonitrile was purchased from EM Science and HPLC grade water was obtained from a Pico water purifying system. The percent of diastereomeric ester was calculated based on the peak area ratio of SS- and SR- form of S-naproxen ester.

Derivatization reaction procedure

The reaction for the coupling of S-naproxen with a chiral alcohol is based on the work of Hassner and Alexanian⁵⁹, Neises and Steglich⁶⁰, Ballard, Eller and Knapp⁶⁶ and Kovach⁶⁷ with some modifications.



S-naproxen

Ten mL of anhydrous ether was added to 0.1 mmol of chiral alcohol. Varied amounts of S-naproxen and dicyclohexylcarbodiimide (DCC) and 0.1 equivalent of 4-dimethylaminopyridine(DMAP) were added to the reaction solution. The reaction was stirred for four hours at room temperature. The white precipitate of urea derivative appeared as one of the major side products. HPLC was be used to monitor the reaction progress. Generally, the reaction takes four hours to complete. At the end of the reaction, the reaction mixture was filtered. Then, the reaction solution was washed with diluted HCl solution, saturated sodium bicarbonate solution and HPLC grader water. With appropriate dilution, this solution was ready for diastereomeric analysis by HPLC. For NMR spectroscopy, a preparative TLC technique with silica as the stationary phase and 90% hexane/10% ethyl acetate was used to isolate the pure resulting s-naproxen esters. NMR measurements were made on the purified products to confirm their identity.

In these accuracy studies, *sec*-phenyl ethyl alcohol was the target enantiomers. Enantiomerically pure R- *sec*-phenyl ethyl alcohol and S- *sec*-phenyl ethyl alcohol were mixed in different ratios. After derivatization, the reaction mixture was analyzed by HPLC method and the *de* ratio of the resulting S-naproxen ester was compared to the *ee* ratio of the starting mixture.

§ 3.3 Results and discussion for the optimization studies

For the optimization studies, (\pm) *sec*-phenyl ethyl alcohol is the probe. The first set of reactions was designed to determine the optimal amount of dicyclohexanecarbodiimide. In this set of reactions, the amount of S-naproxen acid was fixed at ten mole equivalents and the amount of the dicyclohexanecarbodiimide varied. The percent of RS- *sec*-phenyl ethyl alcohol naproxen ester was analyzed at the end of reaction. The percent of RS form was then plotted against the mole equivalent of dicyclohexanecarbodiimide (see Figure 17). It was observed that at least five equivalents of dicyclohexanecarbodiimide is needed to carry the reaction of the R-alcohol to the completion.

The second set of reactions was designed to determine the optimal amount of S-naproxen acid. In this set of reactions, the amount of dicyclohexanecarbodiimide was set at eight mole equivalents and the amount of S-naproxen varied. The percent of RS- *sec*-phenyl ethyl alcohol naproxen ester was analyzed at the end of reaction and then plotted against the mole equivalent of dicyclohexanecarbodiimide (see Figure 18). It was determined that ten equivalent of S-naproxen acid is needed to carry the reaction of the R-alcohol to completion.

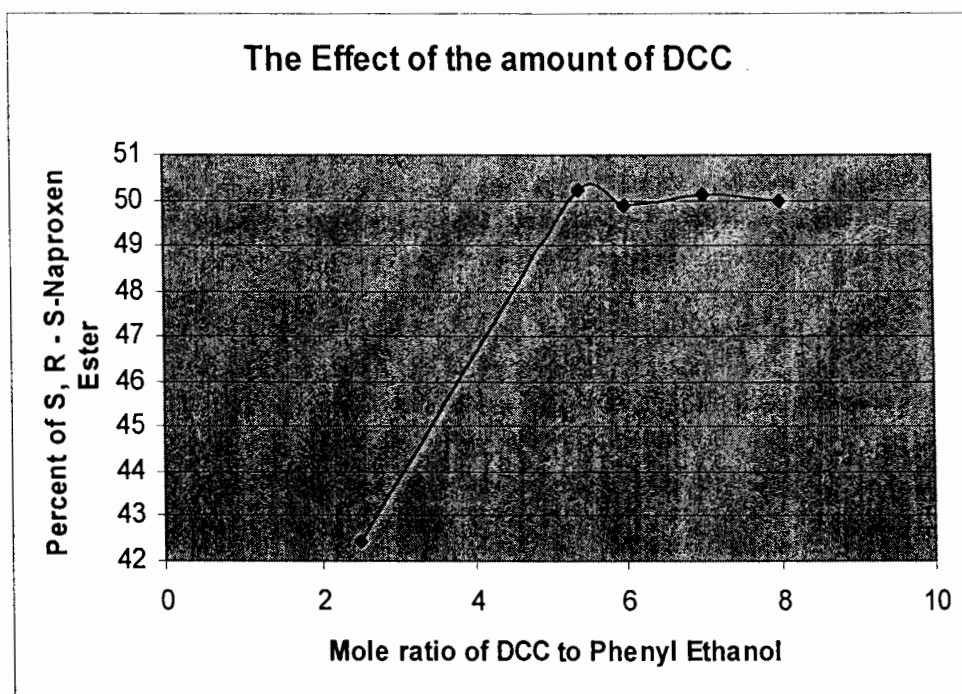


Figure 17 The effect of amount of DCC on the reaction linearity.
Starting material is racemic *sec*-phenethanol. The reactant ratio is:
sec-phenethanol: DMAP : S-naproxen = 1 : 0.1 : 10

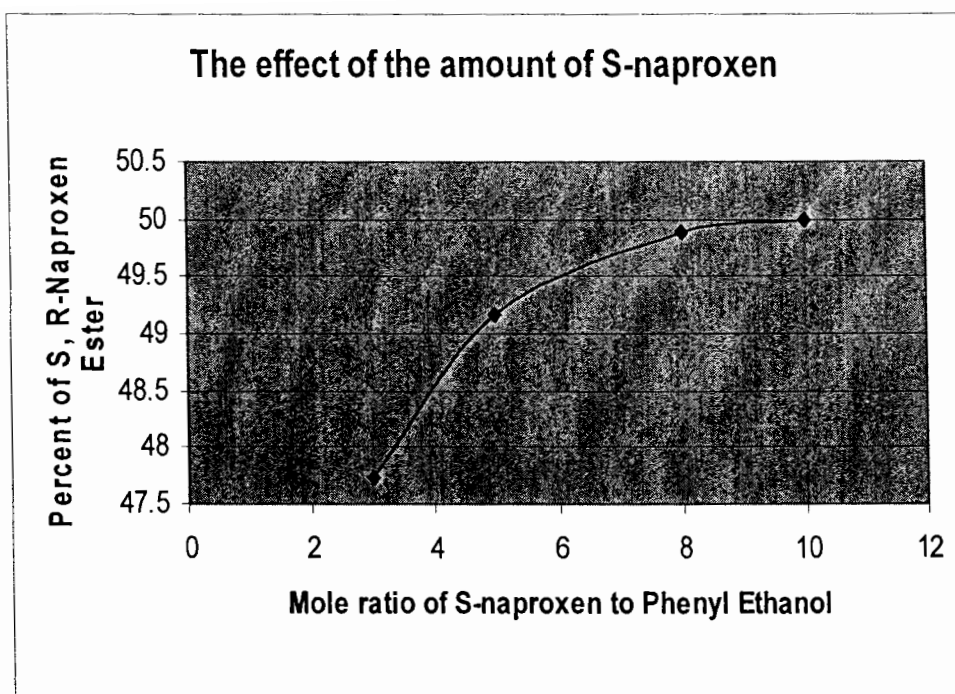


Figure 18 The effect of the amount of S-naproxen on the reaction linearity. Starting material is racemic *sec*-phenethanol. The reactant ratio is: *sec*-phenethanol: DCC : DMAP = 1 : 8 : 0.1

It was found that only when ten equivalents of S-naproxen and at least five equivalents of DCC were charged into reaction system, the R-*sec*-phenethanol can react with S-naproxen to completion. The optimized reactant ratio was determined as chiral alcohol: DCC: DMAP : S-Naproxen = 1 : 8 : 0.1 : 10. Different *ee* ratio mixtures of *sec*-phenethanol and 1-phenyl propanol were used to examine this newly optimized reaction condition. The absolute error between the *ee* ratio of starting material and *de* ratio of the ester product was less than three percent. For the most part, agreement between the *ee* ratio of the starting material and the HPLC *de* analysis is excellent. Over the *ee* range of 1 to 90% (with respect to the R enantiomer), the agreement is larger than 98%. However, further inspection suggests that there are some *ee* ratios where the formation of the SS diastereomer is still favored. For example, for *sec*-phenethanol, the error in the 99% *ee* sample is +2.7% (analysis was performed in triplicate) and shows a slight bias to the SS diastereomer. In addition, for 1-phenylpropanol all errors were in the positive direction, although less than 2%. The results are consistent with a slight imbalance in favor of the SS diastereomer. See Table 4 for *sec*-phenethanol data and Table 5 for 1-phenyl propanol data.

The largest absolute error of this method is 2.7%, when the starting alcohol has 99% R form and 1% S form. An effort was made to improve the results for this *ee* ratio. The amount of S-naproxen acid was increased to 20 mole equivalent and the amount of the SR form of the resulting diastereomers is still 2.7% less than it should be. However, double the amount of reaction solvent was needed to dissolve the S-naproxen acid. This suggests that a 10 mole equivalent solution is saturated with respect to S-naproxen acid. The reaction was performed at 30°C to accelerate the reaction rate. However, the percent of SR form of the

resulting diastereomer was 3.7% less than the starting material. This attempt to improve the percent error clearly went in the wrong direction. From this result, we can conclude that the higher temperature is not going to help solve the accuracy problem. The reaction was also performed in an ice bath for two hours and was brought to room temperature for two hours. The resulting RS diastereomer is about 2.7% less than the starting material. This result matches the result for which the reaction is done in the room temperature. The other set of reaction was done at 0°C for 20 hours. The resulting RS diastereomer is 3.5% less than the starting material. From all these reaction condition studies, we can conclude that the best temperature for this reaction is room temperature which is roughly 20 - 25°C.

Table 4 Linearity study under optimized reactant ratio for the reaction of *sec*-phenyl ethyl alcohol and S-naproxen

% R Enantiomer in Starting Material	% RS diastereomer of naproxen ester	Absolute Error
99.0%	96.3%	+2.7%
88.8%	88.5%	+0.3%
73.6%	74.5%	-0.9%
50.0%	49.9%	+0.1%
25.2%	24.2%	+1.0%
10.0%	10.4%	-0.4%
1.00%	0.99%	+0.01%

Table 5 Linearity study under optimized reactant ratio for the reaction of 1-phenyl propyl alcohol and S-naproxen

% R Enantiomer in Starting Material	% RS diastereomer of naproxen ester	Absolute Error
88.7%	87.7%	+1.0%
74.9%	74.3%	+0.6%
48.6%	48.0%	+0.6%
23.7%	21.7%	+2.0%
9.4%	8.3%	+1.1%

§ 3.4 Conclusions

The derivatization reaction of chiral alcohol with S-naproxen acid was thoroughly studied. The reaction condition was optimized and it was determined that 10 mole equivalents of s-naproxen acid and at least 5 mole equivalents of dicyclohexanecarbodiimide are needed to carry the reaction of the R alcohol to completion. The temperature effect on the reaction was also studied. It is found that higher temperatures do not improve the necessary kinetics for R alcohol. At lower temperature, the reaction is slower than that at room temperature and the reaction of R alcohol does not go to completion. The resulting RS form is lower than the starting material. From these studies, we can conclude that the best temperature for the derivatization of chiral alcohol with S-naproxen acid is room temperature which is roughly 20 - 25°C.

Chapter 4 Diastereomeric separation of S-naproxen esters

§ 4.1 Introduction

The separation of S-naproxen esters is another key factor for the success of this derivatization method. Diastereomers generally exhibit only small differences in their physical and chemical properties. For example, they tend to undergo similar hydrophobic interactions with the stationary phase under reversed-phase chromatographic conditions and these similarities render their separation to be a challenge. The separation of diastereomers mainly relies on small differences in their polar and π - π interactions with the stationary phases and differences in the geometric orientation of the diastereomers toward the stationary phase.

The separation of diastereomers is commonly performed under normal phase conditions^{68, 69}. These normal phase systems commonly employ bare silica, diol, or cyano achiral columns and use solvents that are less polar than the stationary phase as the mobile phase. This separation mode relies mainly on differences in the polar interactions between the analyte and the stationary phase. There are also some reports regarding the separation of diastereomers using reverse-phase HPLC^{47, 70, 71, 72}. Since reversed phase HPLC is a

68 Wang, T.; *J. Chromatogr.*; **1997**, 762, 327

69 Gopal, D.; Grinberg, N.; Dowling, T.; Perpall, H.; Bicker, G. and Tway, P.; *J. Liq. Chromtogr.*; **1993**, 16, 1749

70 Rauwald, H. W. and Beil, A.; *J. Chromatogr.*; **1993**, 639, 359

71 Kirby, D. A.; Miller, C. L. and Rivier, J. E.; *J. Chromatogr.*; **1993**, 648, 257

powerful tool and there is limited research reported in the area of diastereomeric separation, we intended to investigate the separation of S-naproxen esters using the reversed phase mode.

S-naproxen esters have a fused naphthalene ring next to its chiral center. This fused naphthalene ring provides different geometric orientation towards the stationary phase for the diastereomers and make the base-line separation of this type of diastereomers possible for general reversed phase columns. Alkyl alcohols, phenyl alcohols and some fluoro alcohols were used as the target chiral alcohols for this type of separation.

Zirchrom-PBD column had shown excellent separation power for the S-naproxen esters. It also demonstrates very nice separation capability for some positional isomers compared to conventional C18/C8 columns. In this chapter, we discuss these findings.

§ 4.2 Experimental Section

Reagents

The following chemicals are purchased from Aldrich: S-naproxen acid ((S)-(+)- 6-methoxy- α -methyl-2-naphthaleneacetic acid) with greater than 99% purity and enantiomeric excess ratio; 1,3-dicyclohexylcarbodiimide and 4-dimethylaminopyridine with reagent grade; (S)-2-butanol, (R)-2-butanol, (S)-2-pentanol, (R)-2-pentanol, (S)-2-hexanol, (R)-2-hexanol, (S)-2-heptanol, (R)-2-heptanol, (S)-2-octanol and (R)-2-octanol with 99% purity. (S)-(-)-1-phenylethanol, (R)-(+)-1-phenylethanol, (S)-(-)-1-phenylpropanol and (R)-(+)-1-phenylpropanol are purchased from Fluka with greater than 99% purity and 99% *ee* as ChiralSelect grade.

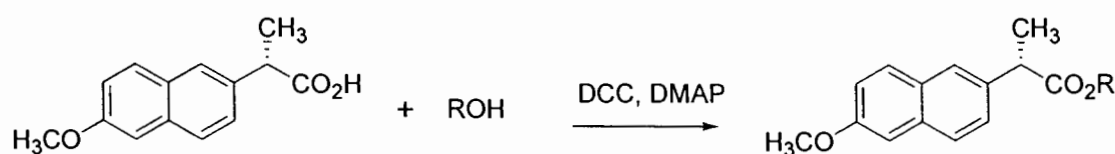
Chromatographic conditions

All chromatographic studies were performed on a Hewlett Packard 1100 HPLC system equipped with a photo diode array UV detector. Data acquisition and treatment was performed with a Perkin Elmer Turbochrom system. The reported chromatographic data is the average of triplicate determinations. The void volume was determined by the first disturbance peak. The mobile phase was a mixture of HPLC grade acetonitrile and HPLC grade water. HPLC grade acetonitrile was purchased from EM Science and HPLC grade water was obtained from a Pico water purifying system. The chromatographic resolution was calculated according to the definition: $R = \frac{2(t_{p2} - t_{p1})}{W_{p2} + W_{p1}}$, where t_{p1} is the retention time for peak one and t_{p2} is the retention time for peak two; W_{p1} is the peak width at the base for peak

one and W_{p2} is the peak width at base of peak two. The percent of diastereomeric ester was calculated based on the peak area ratio of SS- and SR- forms of S-naproxen ester.

Derivatization reaction procedure

The reaction for the coupling of S-naproxen with a chiral alcohol is based on the work of Hassner and Alexanian⁵⁹, Neises and Steglich⁶⁰, Ballard, Eller and Knapp⁶⁶ and Kovach⁶⁷ with some modifications as discussed in the previous section.



S-naproxen

Ten ml of anhydrous ether was added to 0.1mmol of chiral alcohol. Then ten mole equivalents of S-naproxen and eight equivalents of dicyclohexylcarbodiimide (DCC) and 0.1 equivalents of 4-dimethylaminopyridine(DMAP) were added to the reaction solution. The reaction was stirred for four hours at room temperature. The white precipitate of urea derivative appeared as a side product. HPLC was used to check the reaction progress. Generally, the reaction takes four hours to complete. At the end of reaction, the reaction mixture was filtered. Then, the reaction solution was washed with 0.1N HCl solution, saturated sodium bicarbonate solution and HPLC grade water. With appropriate dilution, this solution was ready for the diastereomeric analysis by HPLC.

For NMR spectroscopy, a preparative TLC technique with silica as the stationary phase and 90% hexane/10% ethyl acetate was used to isolate the pure resulting s-naproxen esters. NMR measurements were made of the purified the products to confirm their identity.

§ 4.3 Results and discussion

In these studies, alkyl alcohols, phenyl alcohols and some fluoro alcohols were used as the test chiral alcohols. Through extensive HPLC method optimization, baseline separations for these S-naproxen esters were achieved. The resolution data are listed in Table 6. Generally, the percent of organic modifier (acetonitrile) was controlled so that the retention time of the diastereomers could be less than fifty minutes with reasonable resolution. See Figures 19 to 27 for the LC conditions and typical chromatograms. From our observation, there is a general trend that the Zirchrom-PBD column exhibited better resolution with the solutes that has a benzene ring on the alcohol portion. In cases where conventional C18 columns could not resolve the diastereomers, the Zirchrom-PBD column was usually able to do so.

According to a previous report⁷³, analytes with a large size difference between the groups attached to the chiral center will give improved resolution. We have found that the resolution of alkyl alcohols increases as the molecular size increase. From 2-butanol to 2-octanol, the resolution increases from 1.4 to 4.3 under similar HPLC conditions. These results confirm the previous report⁷³. It was also reported in the literature that the distance between the asymmetric centers should be minimal¹. Generally, the ideal distance should be less than three bonds⁷⁴. We tested some alcohols with chiral centers five carbons away (such

73. H. C. Rose; R. L. Stern; and B. L. Karger; *Anal. Chem. Chim. Acta*, **1966**, 38, 469

74. Rauwald, H. W. and Beil, A.; *J. Chromatogr.*, **1993**, 639, 359

Table 6 Resolution data for diastereomeric separations of S-naproxen esters

Compound Names	Resolution from LC Separation
(±)-2-butanol S-naproxen ester ^a	1.39
(±)-2-pentanol S-naproxen ester ^a	2.35
(±)-2-hexanol S-naproxen ester ^a	2.62
(±)-2-heptanol S-naproxen ester ^a	3.63
(±)-2-octanol S-naproxen ester ^a	4.34
(±)-3-methyl-2-cyclohexen-1-ol S-naproxen ester ^b	1.72
(±)-3-phenyl-1-butanol S-naproxen ester ^b	1.22
(±)-2-trifluorooctanol S-naproxen ester ^b	1.83
(±)-(trifluoromethyl) benzyl alcohol S-naproxen ester ^b	2.35
(±)- <i>sec</i> -phenethanol S-naproxen ester ^b	4.69
(±)-1-phenyl-propanol S-naproxen ester ^b	2.88

a. YMC ODS-AM 4.6 x 250mm x 5 µm column was utilized for the purpose of separation

b. ZirChrom-PBD 4.6 x 150 mm x 3 µm column was utilized for the purpose of separation

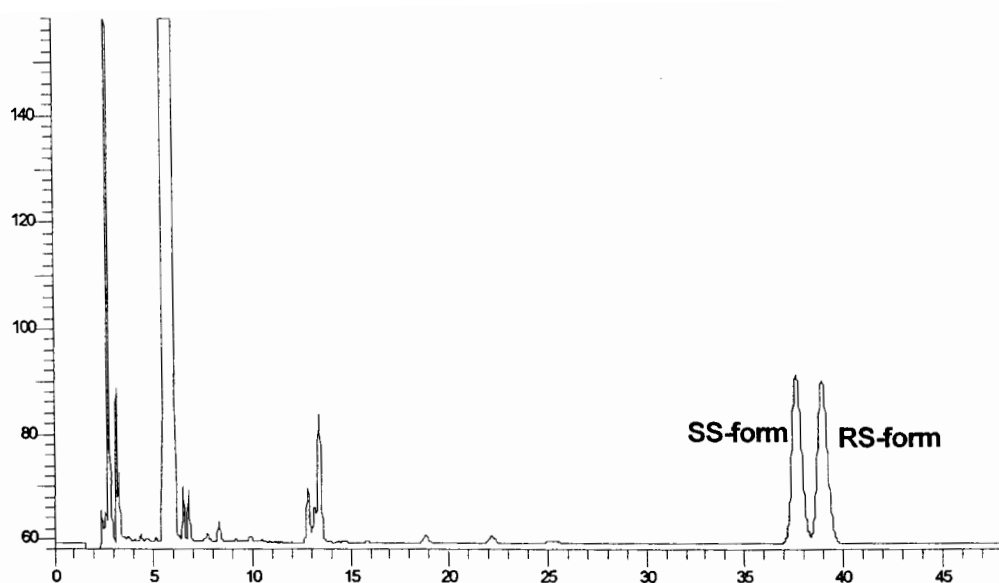


Figure 19 The HPLC separation of R,S-butanol S-naproxen ester

LC Condition:

Column: YMC – ODS AM , 4.6 x 250 mm x 5 μ m;

Mobile phase: 55 : 45 / ACN : Water;

Temperature: 35 °C;

Wavelength: 230 nm

Flow rate: 1.0 ml/min

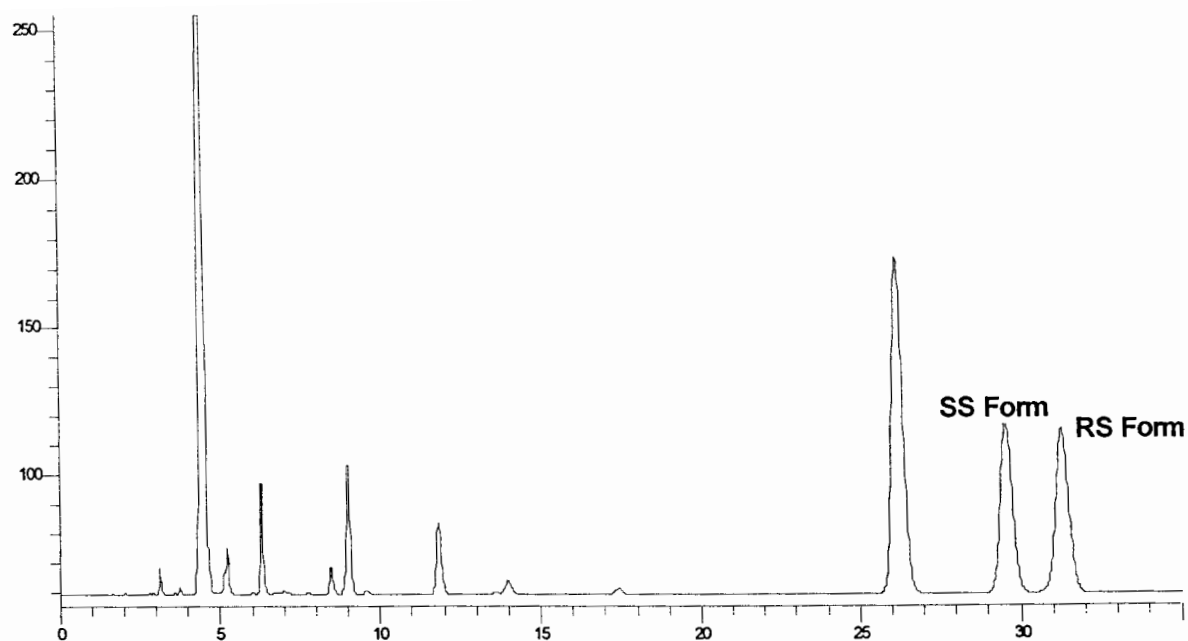


Figure 20 The HPLC separation of R,S-pentanol S-naproxen ester

LC Condition:

Column: YMC – ODS AM , 4.6 x 250 mm x 5 μ m;

Mobile phase: 68 : 32 / ACN : Water;

Temperature: 35 °C;

Wavelength: 230 nm

Flow rate: 1.0 ml/min

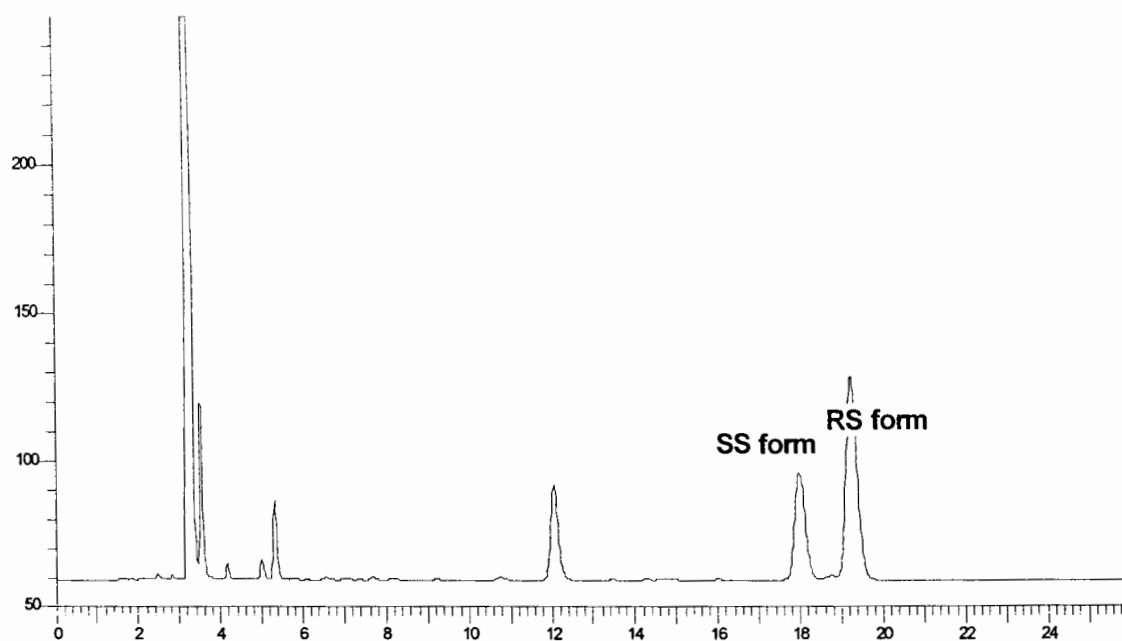


Figure 21 The HPLC separation of R,S-hexanol S-naproxen ester

LC Condition:

Column: YMC – ODS AM , 4.6 x 250 mm x 5 μ m;

Mobile phase: 70 : 30 / ACN : Water;

Temperature: 35 °C;

Wavelength: 230 nm

Flow rate: 1.2 ml/min

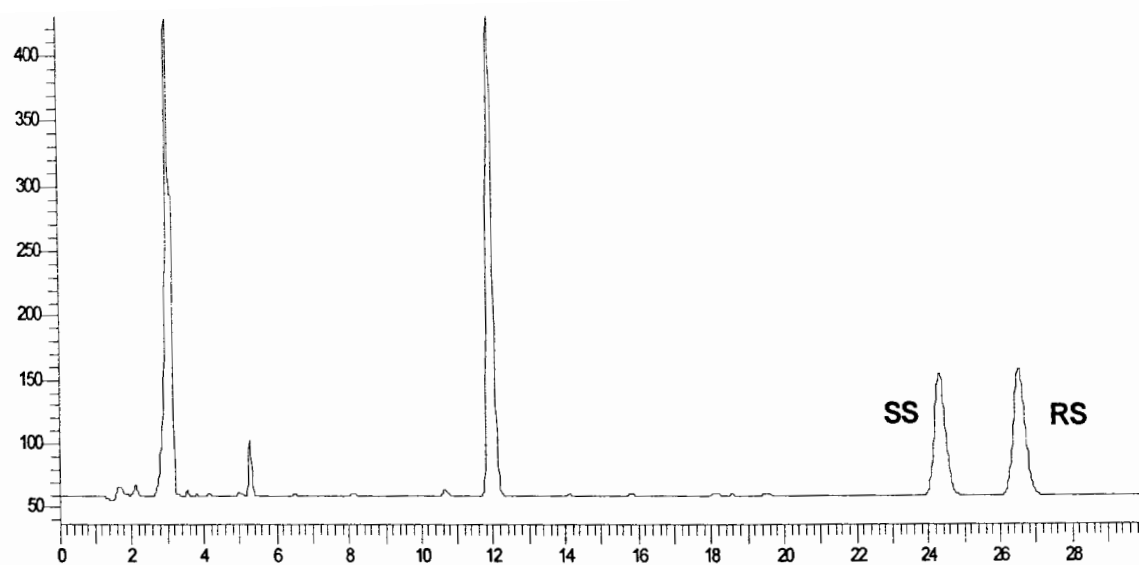


Figure 22 The HPLC separation of R,S-heptanol S-naproxen ester

LC Condition:

Column: YMC – ODS AM , 4.6 x 250 mm x 5 μ m;

Mobile phase: 70 : 30 / ACN : Water;

Temperature: 35 °C;

Wavelength: 230 nm

Flow rate: 1.2 ml/min

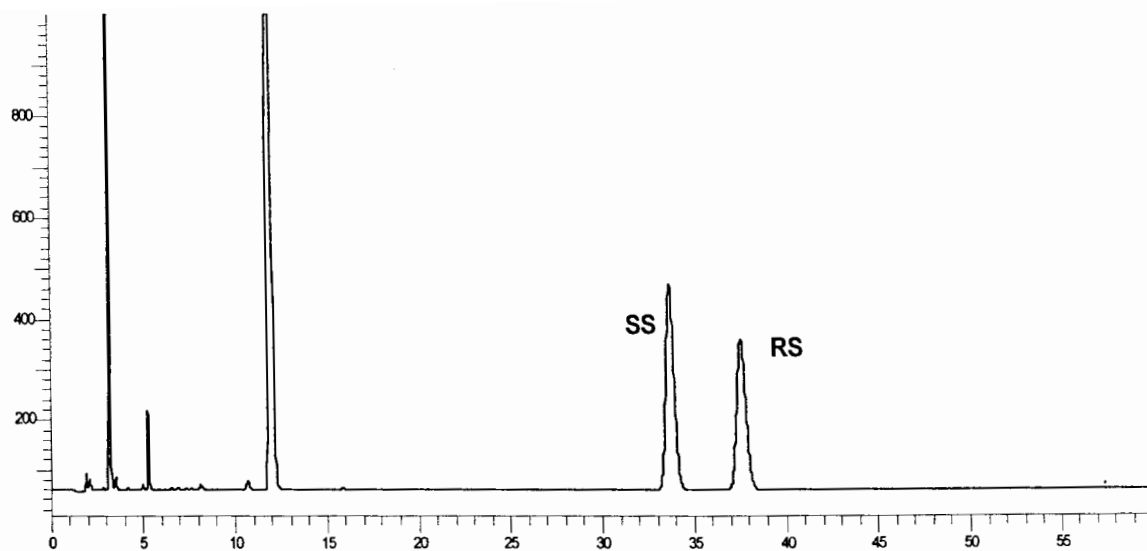


Figure 23 The HPLC separation of R,S-octanol S-naproxen ester

LC Condition:

Column: YMC – ODS AM , 4.6 x 250 mm x 5 μ m;

Temperature: 35 °C;

Mobile phase: 70 : 30 / ACN : Water;

Wavelength: 230 nm;

Flow rate: 1.2 ml/min

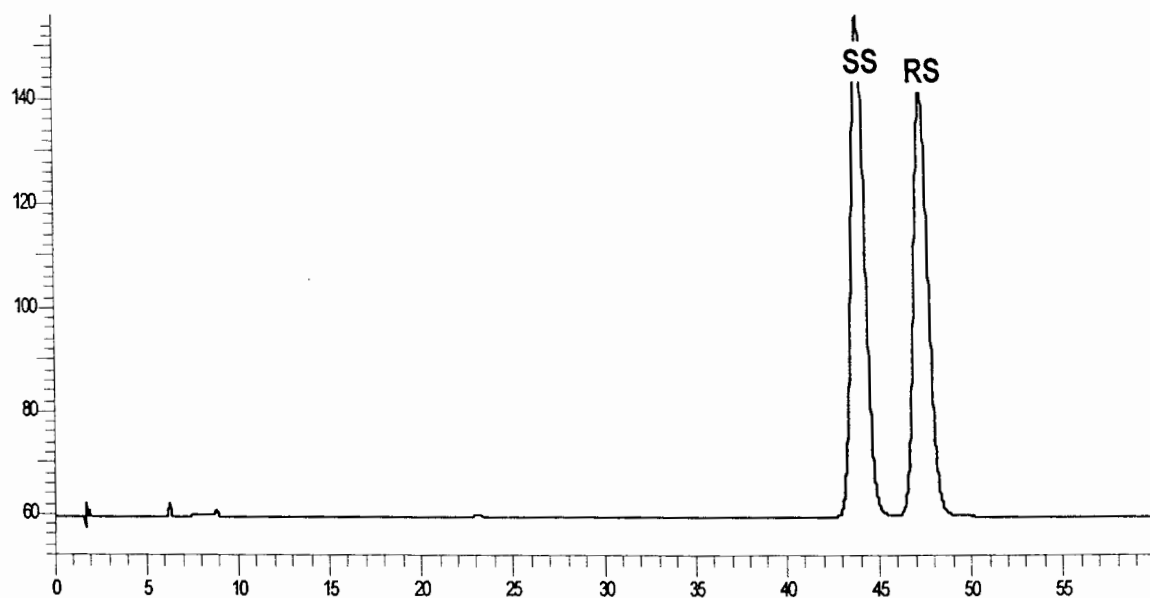


Figure 24 The HPLC separation of R,S-trifluoro methyl benzyl alcohol S-naproxen ester
LC Condition:

Column: Zirchrom-PBD , 4.6 x 150 mm x 3 μ m;
Mobile phase: 50 : 50 / ACN : Water;
Temperature: 40 °C;
Wavelength: 230 nm
Flow rate: 0.9 ml/min

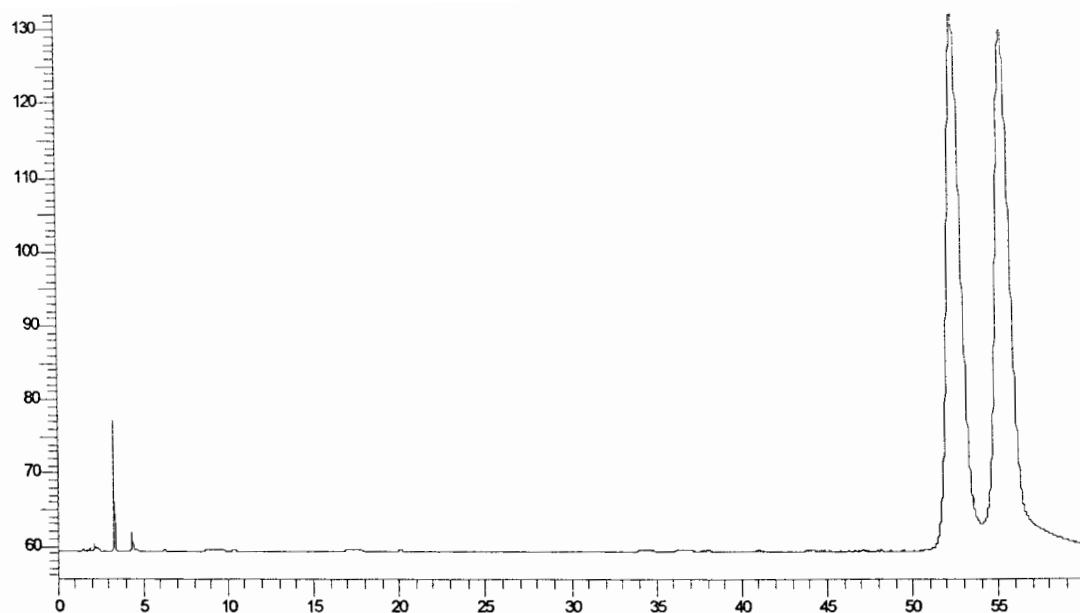


Figure 25 The HPLC separation of R,S-trifluoro octanol-2 S-naproxen ester
LC Condition:

Column: Zirchrom-PBD , 4.6 x 150 mm x 3 μ m;

Mobile phase: 40 : 60 / ACN : Water;

Temperature: 40 °C;

Wavelength: 230 nm;

Flow rate: 1.0 ml/min

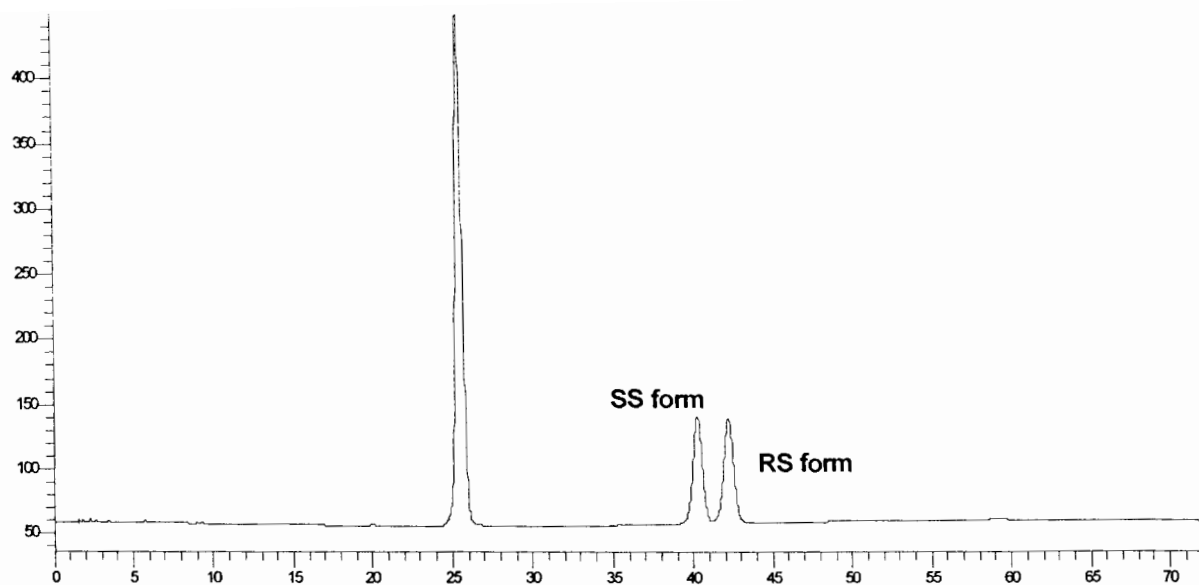


Figure 26 The HPLC separation 3-methyl-2-cyclohexene-1-ol S-naproxen ester

LC Condition:

Column: Zirchrom-PBD , 4.6 x 150 mm x 3 μ m;

Mobile phase: 35 : 65 / ACN : Water;

Temperature: 40 °C;

Wavelength: 230 nm;

Flow rate: 1.0 ml/min

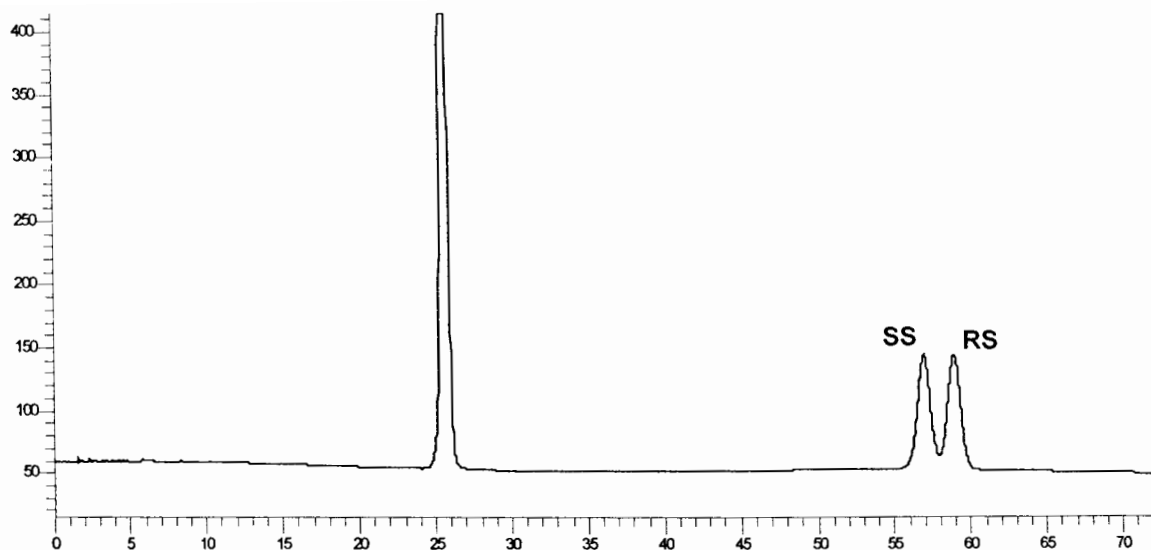


Figure 27 The HPLC separation 20phenyl-butanol-1 S-naproxen ester

LC Condition:

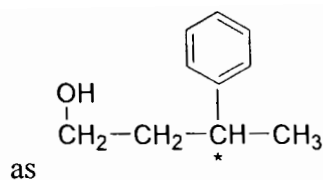
Column: Zirchrom-PBD , 4.6 x 150 mm x 3 μ m;

Mobile phase: 35 : 65 / ACN : Water;

Temperature: 40 $^{\circ}$ C;

Wavelength: 230 nm;

Flow rate: 1.0 ml/min



) from each other. Partial resolution was achieved (See Figure 20 for chromatogram). If the chiral centers are farther than six carbons, no resolution was observed for S-naproxen esters. The racemate of (\pm)-3-methyl-2-cyclohexen-1-ol was used as an example of allylic alcohol with a ring structure and its S-naproxen ester showed acceptable HPLC resolution. As a rough guideline, resolution of 1.5 is an indication of two well separated peaks. The only compounds that show poor separation (not baseline) are 2-butanol ($R=1.39$), 3-phenyl-1-butanol ($R = 1.22$) and 2-trifluorooctanol ($R = 1.83$). This data demonstrates that base line separation for S-naproxen ester can be achieved by reverse phase HPLC method. This method provides a useful alternative analytical method for the chiral analysis for small chiral alcohols, especially alcohols without a UV chromophore.

4.4 Isomeric selectivity of Zirchrom-PBD column

Zirconia based polybutadiene is a new type of commercially available polymer-based reversed phase. Unlike conventional silica based phases, this phase offers excellent acid, base, and thermal stabilities. Our results have shown that this column often provides greater separation ability as compared to conventional C18 and C8 phases for the separation of positional isomers, structurally related isomers, and *trans/cis* isomers. For example, structural isomers, such as butyl benzene isomers, give better separation (see Table 7). Also, *trans/cis* stilbenes were used to compare the Zirchrom-PBD column versus conventional C8/C18 columns. Mobile phase composition was adjusted for all columns to give similar retention factors for both solutes for a fair comparison. The selectivity values (defined as the

ratio of the capacity factor, $\alpha = k'_A/k'_B$) are 1.102, 1.036 and 1.048 for Zirchrom-PBD, YMC ODS-AM and Zorbax SB-C8 columns, respectively. Separation was better using the Zirchrom column.

For the tests of positional isomers, (2, 4)-, (2, 5)-, (2, 6)- and (3, 4)- difluorobenzyl amine were used as chromatographic solutes. It was noticed that both conventional C18 column and Zirchrom-PBD column gave baseline resolution. However, zirconia based PBD column exhibited sharper peaks. This is attributed to the fact that zirconia has less hydrogen bonding capacity than silica (see Figure 28). In order to have a fair comparison of the HPLC resolution data, similar capacity factors k' were achieved by adjusting the mobile phase composition.

Table 7. Isomer selectivities for Zirchrom-PBD, C8 and C18 columns

	PBD Column ^b	C8 Column ^c	C18 Column ^d
n-butyl benzene	1.000 ^a	1.000 ^a	1.000 ^a
sec-butyl benzene	1.215	1.082	1.126
t-butyl benzene	1.502	1.199	1.303

- a. By definition: $\alpha = k'_1/k'_2$. n-butyl benzene is the reference
- b. Column dimension: 4.6 x 150 mm x 3 μ m
- c. Column dimension: 4.6 x 150 mm x 3.5 μ m; brand name: Zorbax SB-C8
- d. Column dimension: 4.6 x 150 mm x 3 μ m; brand name: YMC ODS-AM

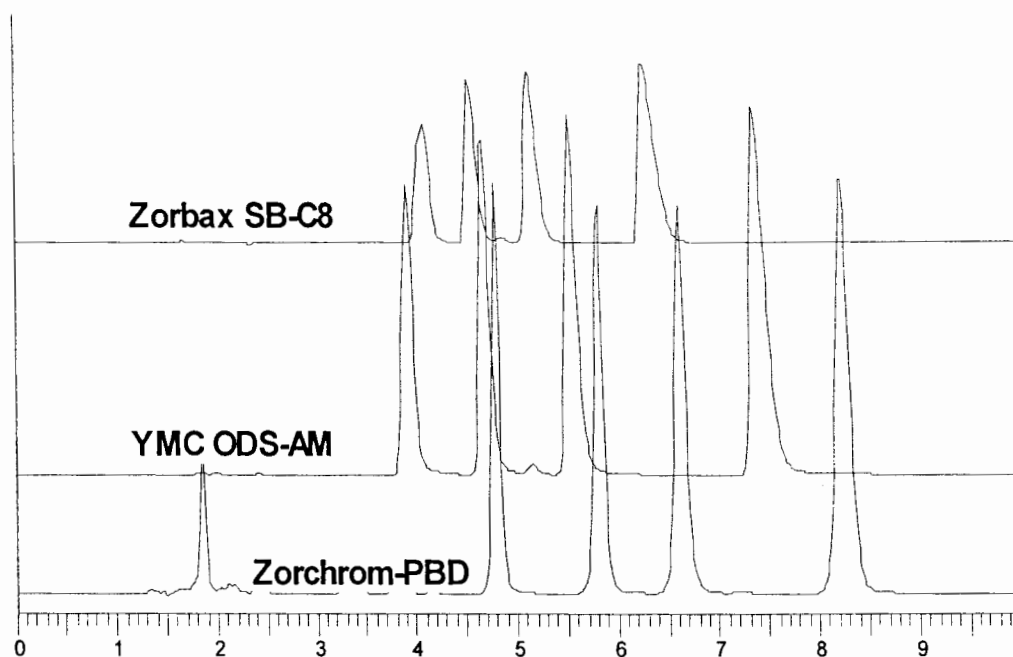


Figure 28 Isomeric selectivity of (2, 4)-, (2, 5)-, (2, 6)- and (3, 4)-difluorobenzyl amine in Zorchrom-PBD column, YMC ODS-AM column and Zorbax SB-C8 column
Elution order for all columns is 2,6-, 2,5-, 2, 4- and 3, 4-difluorobenzyl amine

Other positional isomers were also used to test the Zirchrom-PBD column. It was found that the elution order is not necessarily the same as that of C18 phases. For example, the elution order of 2, 4-, 2, 5- and 3, 4-difluorotoluene is 2, 5-, 3, 4- and 2, 4- difluorotoluene for both C18 column and Zirchrom-PBD columns. However, the elution order of 2, 4-, 2, 5- and 3, 4-difluoroanisole is 2, 5-, 2, 4- and 3, 4-difluoroanisole with the C18 column and 2, 4-, 2, 5- and 3, 4-difluoroanisole is 2, 4-, 2, 5- and 3, 4-difluoroanisole. The data are summarized in Table 8. At this time, there is no theory which can explain the elution order.

This study allowed us to identify possible reasons for better/improved selectivity of Zirchrom-PBD columns with the S-naproxen ester diastereomers. The main reasons include the better hydrophobic selectivity and high polarity of the Zirchrom-PBD column. In addition, we discovered a few interesting advantages of the Zirchrom-PBD column in separations of some regio isomers of common aromatic compounds and aromatic amines (see Table 8 for resolution data). However, this advantage is not a general property of the Zirchrom-PBD column. Thus, we decided not to pursue additional separation studies.

Table 8 Isomeric separation data for both C18 and Zirchrom-PBD

Compound	C18 column		Zirchrom-PBD column	
	elution order	resolution	elution order	resolution
2,4-difluorotoluene	3	1.7	2	3.7
2,5-difluorotoluene	1	N/A	1	N/A
3,4-difluorotoluene	2	0.9	1	Co-elute

Compound	C18 column		Zirchrom-PBD column	
	elution order	resolution	elution order	resolution
2,4-difluoroanisole	1	N/A	2	1.2
2,5-difluoroanisole	1	N/A	1	N/A
3,4-difluoroanisole	2	5.3	3	12.5

Compound	C18 column		Zirchrom-PBD column	
	elution order	resolution	elution order	resolution
2,4-difluoronitrobenzene	3	15.4	1	N/A
2,5- difluoronitrobenzene	1	N/A	2	2.1
3,4- difluoronitrobenzene	2	1.4	3	6.1

Compound	C18 column		Zirchrom-PBD column	
	elution order	resolution	elution order	resolution
2-methylacetophenone	2	Co-elute	1	N/A
3-methylacetophenone	2	1.34	2	12.4
4-methylacetophenone	1	N/A	3	1.1

Compound	C18 column		Zirchrom-PBD column	
	elution order	resolution	elution order	resolution
2-trifluoromethylacetophenone	1	N/A	1	N/A
3-trifluoromethylacetophenone	2	6.7	1	coelute
4-trifluoromethylacetophenone	4	1.8	3	2.8

§ 4.4 Conclusions

The diastereomeric separation of S-naproxen esters was studied thoroughly. We demonstrated that reversed phase HPLC is a powerful tool to separate the S-naproxen esters. Both C18 and Zirchrom-PBD can provide good resolution for the diastereomeric esters. It is also important to point out that the large size difference in groups which are attached to the chiral center of either the S-naproxen acid portion or the chiral alcohol portion can enhance the HPLC resolution. We have also demonstrated that small alkyl alcohol S-naproxen esters, such as diastereomeric *sec*-butanol S-naproxen ester can easily be separated by reverse phase HPLC, while the diastereomeric *sec*-butanol Mosher's ester cannot be separated in similar HPLC conditions. This is one important advantage of S-naproxen acid over Mosher's reagent. However, if the chiral center of the alcohol is far away (six bonds away) from the chiral center of S-naproxen acid, then the HPLC separation is not possible under the current chromatographic conditions.

Isomeric separations by Zirchrom-PBD column were also studied. We have found that Zirchrom-PBD column can provide good HPLC resolution for certain isomers. This column has no silanophilic interaction with amino groups and has very nice peak shape for amino compounds. This characteristic is a big advantage over typical C18/C8 columns that undergo silanophilic interactions with basic solutes and for which an acidified mobile phase was needed to improve the peak shape. We can conclude that Zirchrom-PBD column is a good choice for diastereomeric and isomeric separations.

Chapter 5 NMR Measurements for S-naproxen Ester

§ 5.1 Introduction

Nuclear resonance magnetic (NMR) spectroscopy has been used to determine chiral purity for over thirty years. The general procedure consists of derivatization of the analyte with an optically pure auxiliary reagent. The proton NMR spectra of the resulting diastereomeric derivatives have different chemical shifts. The ratio of the peak heights of R and S form of the resulting diastereomers can be used to determine the enantiomeric excess ratio of the analyte. The difference of the chemical shifts between the R and S form and relative position can also be used to determine the absolute configuration of the original analyte.

Methoxyphenylacetic acid (Mosher's acid) is one of the auxiliary reagents which are most commonly used for derivatization of secondary chiral alcohols^{75, 76, 77}. Recently, 9-anthrylmethoxyacetic acid and related compounds have been introduced in this area^{78, 79, 80, 81, 82, 83, 84}.

75. Dale, J. A.; Dull, D. L.; Mosher, H. S.; *J. Org. Chem.*; **1969**, *34*, 2543

76. Dale, J. A.; Mosher, H. S.; *J. Am. Chem. Soc.*; **1973**, *95*, 512

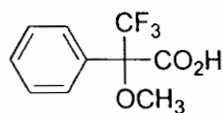
77. Sullivan, G. R.; Dale, J. A.; Mosher, H. S.; *J. Org. Chem.*; **1973**, *38*, 2143

78. Latypov, S. K.; Seco, J. M.; Quiñoá, E and Riguera, R. *J. Org. Chem.*; **1995**, *60*, 504

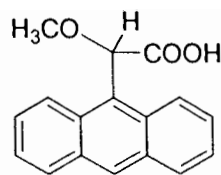
79. Seco, J. M.; Quiñoá, E and Riguera, R. *Tetrahedron*, **1997**, *53*, 8541

80. Seco, J. M.; Latypov, S.; Quiñoá, E and Riguera, R.; *Tetrahedron Lett.*; **1994**, *35*, 2821

81. Ferreiro, M. J.; Latypov, S. K.; Quiñoá, E and Riguera, R.; *Tetrahedron: Asymmetry*, **1996**, *7*, 2195



R, S-Mosher's acid



R, S- 9-anthrylmethoxyacetic acid

S-Naproxen acid has a similar structure as methoxyphenylacetic acid and 9-anthrylmethoxyacetic. These compounds all possess one or more aromatic rings attached to the chiral center. The aromatic rings can provide large chemical shifts in NMR spectra to neighboring diastereotopic hydrogens. Therefore, the resulting diastereomeric esters, derivatized by these types of reagents, usually have large chemical shift differences and the ratio of the chemical shifts of R and S forms can accurately reflect the enantiomeric excess ratio of the starting alcohols.

In this chapter, alkyl alcohols are used as the target starting material and the NMR spectra of these S-naproxen esters are measured. The chemical shift difference between the R form and S form were measured to investigate whether S-naproxen acid could be used as a derivatization reagent for the purpose of determination of enantiomeric excess ratio of chiral alcohols.

82. Latypov, S. K.; Ferreiro, M. J.; Quiñoá, E and Riguera, R.; *J. Am. Chem. Soc.*; **1998**, *120*, 4741

83 . Seco, J. M.; Quiñoá, E and Riguera, R.; *J. Org. Chem.*; **1999**, *64*, 4669

84 Seco, J. M.; Tseng, L. H.; Godejohann, M.; Quiñoá, E and Riguera, R.; *Tetrahedron: Asymmetry*; **2002**, *13*, 2149

§ 5.2 Experimental section

5.1. Reagents

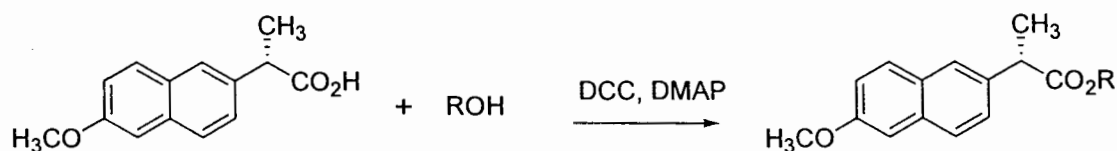
The following chemicals are purchased from Aldrich: S-naproxen acid ((S)-(+)- 6-methoxy- α -methyl-2-naphthaleneacetic acid) with greater than 99% purity and enantiomeric excess ratio; 1,3-dicyclohexylcarbodiimide and 4-dimethylaminopyridine with reagent grade; R and S form of 2-butanol, 2-pentanol, 2-hexanol, 2-heptanol and 2-octanol are purchased from Flucos with greater than 99% purity.

5.2. Chromatographic conditions

All chromatographic studies were performed on a Hewlett Packard 1100 HPLC system equipped with a photo diode array UV detector. Data acquisition and treatment was performed with a Perkin Elmer Turbochrom system. The reported chromatographic data is the average of triplicate determinations. The void volume was determined by the first disturbance peak. The mobile phase was a mixture of HPLC grade of acetonitrile and HPLC grade water. HPLC grade acetonitrile was purchased from EM Science and HPLC grade waster was obtained from a Pico water purifying system. The percent of diastereomeric ester was calculated based on the peak area ratio of SS- and SR- form of S-naproxen esters.

5.3. Derivatization reaction procedure

The reaction for the coupling of S-naproxen with a chiral alcohol is based on the work of Hassner and Alexanian⁵⁹, Neises and Steglich⁶⁰, Ballard, Eller and Knapp⁶⁶ and Kovach⁶⁷ with some modification.



S-naproxen

Ten mLs of anhydrous ether was added to 0.1mmol of chiral alcohol, then three equivalents of S-naproxen, three equivalents of dicyclohexylcarbodiimide (DCC) and 0.1 equivalents of 4-dimethylaminopyridine(DMAP) was added to the reaction solution. The reaction was stirred for four hours at room temperature. A white precipitate of urea derivative appeared as one of the major side products. HPLC can be used to check the reaction progress. Generally, the reaction takes four hours to complete. At the end of the reaction, the reaction mixture was filtered. Then, the reaction solution was washed with dilute HCl solution, saturated sodium bicarbonate solution and HPLC grade water. With appropriate dilution, this solution was ready for diastereomeric analysis by HPLC. For the S-naproxen esters made for this paper, a preparative TLC technique was used to purify the reaction mixtures for NMR spectroscopy. Silica plate was used as the stationary phase and 90% hexane/10% ethyl acetate was used as mobile phase for the preparative TLC technique to isolate the pure resulting s-

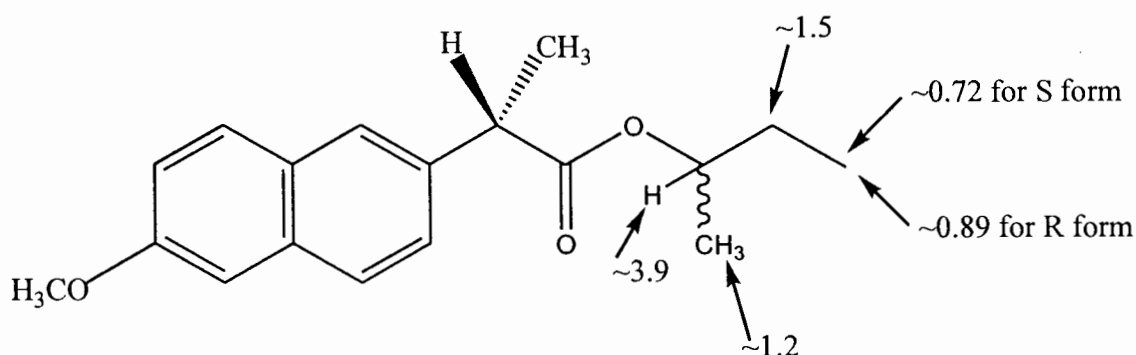
naproxen esters. NMR measurements were made on the purified the products to confirm the product structures. A Bruker 400 NMR was used as the NMR spectrometer. Deuterated chloroform was the solvent.

§ 5.3 Results and Discussion

Nuclear magnetic resonance spectrometry is one of the common absorption spectrometry techniques. Under appropriate conditions, in a magnetic field, a sample can absorb electromagnetic radiation in the radio frequency region at frequencies governed by the characteristics of the sample. Absorption is a function of certain nuclei in the molecule. Only the nuclei with spin number of $\frac{1}{2}$ and a uniform spherical charge distribution can absorb electromagnetic radiation. Among them, ^1H is the most popular nuclei for the NMR measurements. A plot of the frequencies of the absorption peaks versus peak intensities constitutes an NMR spectrum. The difference in the absorption position of a particular proton from the absorption position of a reference proton is called the chemical shift of the particular proton. Proton NMR spectrum measures the chemical shift differences of hydrogen atoms.

Protons that are interchangeable through an axis of symmetry are homotopic. Homotopic means that the hydrogens are chemical shift equivalent in any environment whether achiral or chiral. Protons that are interchangeable through any other symmetry operation are called enantiotopic (nonsuperimposable mirror images), and these are chemical shift equivalent only in an achiral environment. Noninterchangeable geminal protons are called diastereotopic and they are not necessarily chemical shift equivalent in any environment. Before the derivatization with S-naproxen acid, the hydrogens (under lined) in alkyl alcohol, such as butanol $\text{CH}_3\text{CH}(\text{OH})\underline{\text{CH}_2}\underline{\text{CH}_3}$, are enantiotopic. After the derivatization reaction with S-naproxen, the introduction of another chiral center makes the

above enantiotopic hydrogens become diastereotopic hydrogens (see the following scheme). They are not chemical shift equivalent. The chemical shifts of the alkyl alcohol in S form and R form will be different. This difference makes the chiral analysis for derivatized alcohols possible.



S-naproxen 2-butanol ester

Scheme D

Alkyl alcohols, such as 2-butanol, pentanol, hexanol, heptanol and octanol, are derivatized by S-naproxen acid. The resulting diastereomeric esters are measured by NMR spectroscopy. It is found that the largest chemical shift difference occurs in the methyl group which is the last methyl group in the alkyl alcohols. This is likely due to the folding of the alkyl chain of the alkyl alcohols. The shielding effect of naphthalene ring current is different for the S form and R form diastereomers, because the folding angle could be different for S

form and R form diastereomers. From the chemical data, we know that the S form is more shielded than the R form. The difference between the S form and R form of the S-naproxen esters is at least 1 ppm (see Table 9). That means the last methyl peaks of S form and R form are baseline separated from each other. This large difference of chemical shifts provides an accurate means for the chiral analysis of S-naproxen derivatized esters. The comparison of NMR *de* analysis results, LC *de* analysis results and the starting material *ee* ratio are listed in Table 10. From the results we know that NMR data can match LC analysis very well in the range up to 75% *ee* (with ~ 5% error). At higher *ee* ratio range, the NMR results are well off from the original data. This is mainly due to the lower sensitivity of NMR methodology. Generally, a 10% error is considered acceptable in NMR integration. However, smaller and broader peaks are more difficult to integrate causing a higher error.

Table 9. Chemical shift differences for S-naproxen alkyl alcohol esters

Compounds	Chemical shift for R, S Form	Chemical shift for S, S Form	Δ
2-Butanol S-Naproxen Ester	0.875 ppm	0.725 ppm	0.150 ppm
2-pentanol S-Naproxen Ester	0.895 ppm	0.756 ppm	0.139 ppm
2-Hexanol S-Naproxen Ester	0.862 ppm	0.691 ppm	0.171 ppm
2-Heptanol S-Naproxen Ester	0.863 ppm	0.729 ppm	0.134 ppm
2-Octanol S-Naproxen Ester	0.871 ppm	0.777 ppm	0.094 ppm

Table 10. Comparison of LC analysis results with NMR analysis results

% R Enantiomer by Weighing	LC Results	NMR Ratio	% error
9.42%	8.34%	13.8%	+ 4.4 %
23.7%	21.7%	25.1%	+ 1.4 %
48.6%	48.0%	49.9%	+1.3 %
74.9%	74.3%	75.0%	+ 0.1 %
88.7%	87.6%	79.7%	- 9.0 %

§ 5.4 Conclusions

The NMR spectra of alkyl alcohols were measured. The chemical shift differences of S-naproxen diastereomeric esters were recorded. It is found that the largest chemical shift difference occurs in the methyl group which is the last methyl group in the alkyl alcohols, instead of the methyl groups which are the closer to the chiral center of the S-naproxen site. This is likely due to the folding effect of the alkyl chain toward to the naphthalene ring. The chemical shift differences between the S form and R form of S-naproxen esters are at least 0.1 ppm. This large difference makes the quantitation of *de* ratio of diastereomeric S-naproxen ester by NMR spectroscopy possible. The results of NMR *de* analysis of S-naproxen esters were compared to the LC *de* analysis of S-naproxen esters and the *ee* ratio of the starting material. It was found that the NMR *de* analysis of S-naproxen esters is very accurate in the medium *ee* range. When the *ee* ratio is too high, the low sensitivity of NMR method gives higher error for the analysis.

Part II

Kinetic Study of the Epimerization of Trityloxymethylbutyrolactol by High Performance Liquid Chromatography

Chapter 1 Introduction

Investigations into dynamic molecular processes and determination of their kinetic parameters are frequently performed through the utilization of dynamic spectroscopic techniques (NMR, ESR, IR)^{85, 86, 87, 88, 89}. These kinetic parameters can also be determined chromatographically, specifically for two species that can interconvert on a chromatographic time scale and can be separated chromatographically^{90, 91, 92, 93, 94, 95, 96, 97, 98, 99, 100, 101, 102, 103}.

85 W. Stewart, T. Siddall, *Chem. Rev.* **1970**, *70*, 517

86 L. Jackman, "Dynamic Nuclear Magnetic Resonance Spectroscopy", Academic Press, New York, **1975**.

87 J. Sandstrom, "Dynamic NMR Spectroscopy", Academic Press, London, **1982**

88 K. Ingold, J. Walton, *Acc. Chem. Res.*, **1989**, *22*, 8

89 F. Grevels, J. Jache, W. Klotzbucher, C. Kruger, K. Seegovel, Y. Tsay, *Angew. Chem. Int. Ed. Engl.* **1987**, *26*, 885

90 M. Lebl, V. Gut, *J. Chromatogr.*, **1983**, *260*, 478

91 W. Melander, H. Lin, C. Horvath, *J. Phys. Chem.*, **1984**, *88*, 4527

92 J. Jacobson, W. Melander, G. Vaisnys, C. Horvath, *J. Phys. Chem.*, **1984**, *88*, 4536

93 M. Hearn, A. S. Hodder, M. Aguilar, *J. Chromatogr.*, **1985**, *327*, 47

94 W. Melander, J. Jacobson, C. Horvath, *J. Chromatogr.*, **1986**, *359*, 3

95 R. Hanai, S. Endo, A. Wada, *Biophys. Chem.*, **1986**, *25*, 27

96 R. Hanai, A. Wada, *J. Chromatogr.*, **1987**, *394*, 273

97 B. Stephan, H. Zinner, F. Kastner, A. Mannschreck, *Chimia*, **1990**, *10*, 336

98 M. Crespo, J. Veciana, *Angew. Chem. Int. Ed.*, **1991**, *30*, 74

99 M. Jung, V. Schurig, *J. Am. Chem. Soc.*, **1992**, *114*, 523

100 K. Cabrera, M. Jung, M. Fluck, V. Schurig, *J. Chromatogr. A*, **1996**, *731*, 315

101 C. Wolf, W. Pirkle, C. Welch, D. Hochmuth, W. Konig, G. Chee, J. Charlton, *J. Org. Chem.*, **1997**, *62*, 5208,

This chemical interconversion can occur during sample preparation or on-column and may be influenced by the mobile phase or the stationary phase. The types of reactions that may occur include acid or base catalyzed reactions and isomerization reactions^{104, 105, 106, 107, 108, 109, 110, 111}. The same phenomena were also observed for NMR spectroscopy^{86, 87}.

Chromatographic retention of a species, in its simplest form, is a factor of the equilibrium constant for its distribution between the mobile and stationary phase. Interconversion of species, however, leads to the establishment of a secondary equilibrium. When an eluate is subjected to a secondary equilibrium, its retention is a weighted average of the two species¹¹². If the rate of interconversion is slow compared to the chromatographic process two resolved peaks are observed due to the occurrence of little or no interconversion. If the rate of interconversion is fast compared to the chromatographic process, only one peak is observed due to the extensive interconversion. However, if the interconversion is on a

102 J. Oxelbark, S. Allenmark, *J. Org. Chem.*, **1999**, *64*, 1483

103 O. Trapp, V. Schurig, *J. Am. Chem. Soc.*, **2000**, *122*, 1424

104 D. Henderson, C. Horvath, *J. Chromatogr.*, **1986**, *368*, 203

105 M. Moriyaasu, A. Kato, Y. Hasimoto, *J. Chem. Soc. Perkin Tran.*, **1986**, *2*, 515

106 D. Henderson, J. Mello, *J. Chromatogr.*, **1990**, *499*, 79

107 S. Gustafsson, B. Eriksson, I. Nilsson, *J. Chromatogr.*, **1990**, *506*, 75

108 K. Brogle, R. Ornaf, D. Wu, P. Palermo, *J. Pharm. Biomed. Anal.*, **1999**, *19*, 669

109 H. Trabelsi, S. Bouabdallah, S. Sabbah, F. Raouafi, K. Bouzouita, *J. Chromatogr. A*, **2000**, *871*, 189

110 R. LoBrutto, Y. Bereznitski, T. Novak, L. DiMichele, L. Pan, M. Journet, J. Kowal, N. Grinberg, *J. Chromatogr. A*, **2003**, *995*, 67

111 O. Trapp, V. Schurig, *Chirality*, **2002**, *465*, 14

112 A. Martin, *Biochem. Soc. Symp.*, **1949**, *3*, 4

similar time scale to that of the chromatographic process, band spreading and peak distortion may be observed. On-column interconversion of a species is usually characterized by tailing of the less retained peak and fronting of the more retained peak. Tailing of the less retained peak occurs as this species is converted to the more retained species. Conversely fronting of the more retained peak occurs as this species is converted to the less retained species. The two peaks may be joined by an elevated baseline (see Figure 29). This elevated baseline represents species which have undergone at least one interconversion cycle.

The determination of rate constants for interconversion in chromatographic processes is generally undertaken with computer simulations using primarily three different models. The continuous flow model^{91, 92, 113, 114, 115} is derived from chemical engineering principles. It utilizes a dimensionless Damköhler number (Da) representing the ratio of time constants for bulk mass transport and chemical reaction. The Damköhler number is derived from the first moment (center of mass) and second moment (variance) of the peak and the rate constants are subsequently obtained. The theoretical plate model^{99, 100, 116, 117} considers each theoretical plate as a distinct discrete reactor. At each plate the species interconvert and are distributed between the mobile and stationary phase. The mobile phase is then shifted onto the next

113 S. Langer, J. Yurchak, J. Patton, *Ind. Eng. Chem.*, **1969**, 61, 10

114 D. Henderson, C. Horvath, *J. Chromatogr.*, **1985**, 349, 211

115 *J. Liq. Chromatogr.*, **1998**, 2089, 21

116 W. Burkle, H. Karfunkel, V. Schurig, *J. Chromatogr.*, **1984**, 288, 1

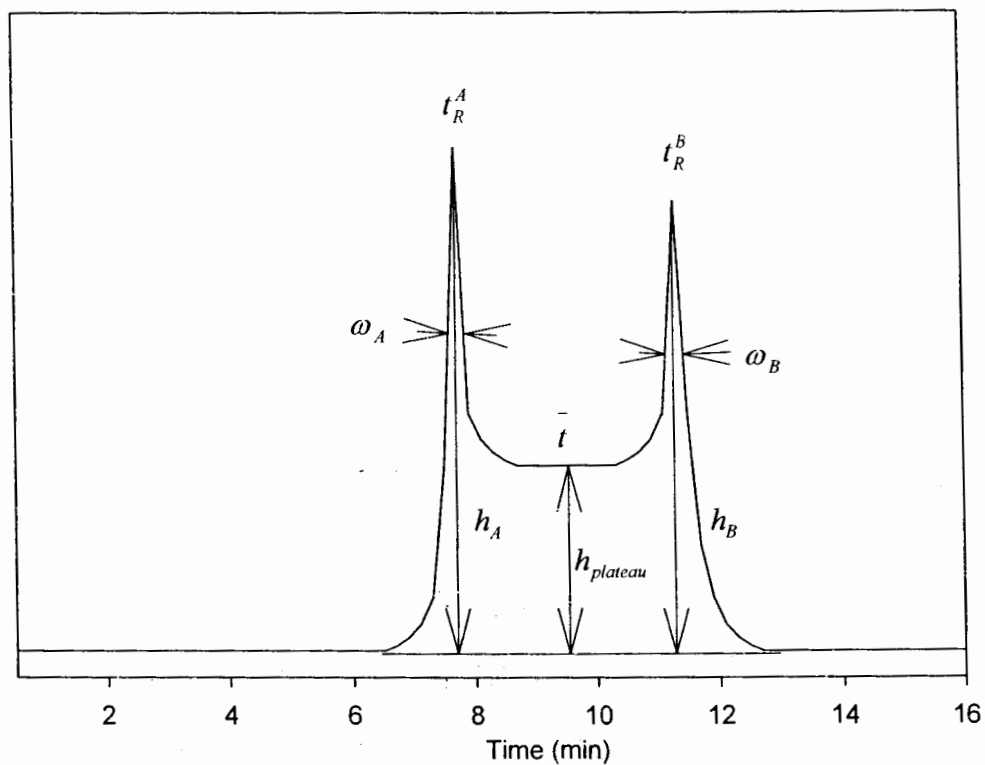


Figure 29. Example of an elution profile of an interconverting species with the experimental parameters needed for calculation of rate constants and the Arrhenius constant.

plate. The stochastic model^{97, 118, 119} describes the chromatographic process using time dependent distribution functions. The elution profile is a summation of the distribution functions of the non-interconverted species and the probability density functions of the interconverted species.

More recently Trapp and Schurig¹²⁰ have been able to obtain rate constants without the use of computer simulations. They utilized an approximation function to directly calculate interconversion rate constants and Gibbs activation energies. The input parameters were retention times of the two species, their peak widths, and the relative plateau height between the two peaks. Trapp's method has been utilized in this study for a kinetic study of the epimerization of trityloxymethyl butyrolactol. It is known that lactols can undergo ring opening and closing in solution. This phenomenon has been observed in carbohydrates such as glucose. Ring opening of trityloxymethyl butylrolactol in solution leads to inversion at the stereogenic center where the hydroxyl group is located (see Figure. 30). Under appropriate chromatographic conditions the resulting interconversion is manifested through peak broadening, plateau formation, and peak coalescence. Like typical interconversion of stereoisomers, this epimerization constitutes a reversible first order reaction^{116, 121}.

118 R. Keller, J. Giddings, *J. Chromatogr.*, 1960, 3, 205

119 J. Veciana, M. Crespo, *Angew. Chem. Soc.*, **1927**, 49, 2554

120 O. Trapp, V. Schurig, *J. Chromatogr. A*, **2001**, 911, 167

121 M. Resit, B. Testa, P. Carrupt, M. Jung, V. Schurig, *Chirality*, **1995**, 7, 396.

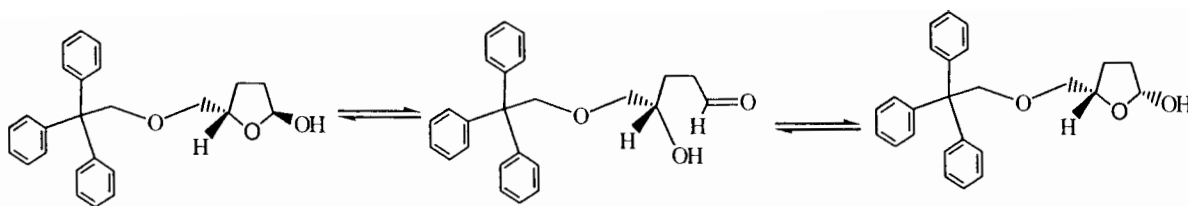


Figure 30. Epimerization of Butyrolactol.

Rate constants and the activation energy for interconversion were determined at varied flow rates, temperatures, and chromatographic conditions. Additionally optimal conditions were identified to achieve either improved separation of the interconverting species or to have them co-elute as one peak.

Chapter 2 Theoretical Aspects

§ 2.1 General Aspects

Stereoisomerization, i.e., enantiomerization, epimerization and diastereomerization, constitutes a reversible first-order reaction as shown below, which arises from the inter-conversion of a stereogenic center in a particular molecule.



This type of stereomerization may lead to peak broadening, plateau-formation, and finally peak coalescence^{103, 104}, depending on the stereochemical stability of the compound of interest.

Until recently, there was no simple way to calculate the stereoisomerization rate constants and Gibbs activation energy. There are several models, such as theoretical plate model, stochastic model and continuous flow model, which were developed to simulate the elution profile. These models provided basic relationships of stereoisomerization reaction rate constants with other chromatographic parameters, such as capacity factor, peak height, plateau height and peak width. These relationships finally lead to the direct calculation of stereoisomerization reaction rate constants by using only chromatographic parameters.

§ 2.2 Theoretical Plate Model

The theoretical model assumes that all steps proceed repeatedly in separate uniform sections of a multicompartmentalized column consisting of N plates^{122, 123, 124}. Every theoretical plate is considered as a distinct chemical reactor^{99, 103, 116, 125}. There are three steps which are performed in every plate: 1) distribution of the stereoisomers A and B between the stationary phase and mobile phase, 2) the stereoisomerization process in both phases, and 3) shifting of the mobile phase to the next plate (see Figure 31).

Stereoisomer A and B are distributed into mobile phase and stationary phase according to eqs. (2.1) and (2.2):

$$\begin{aligned}A_m &= \frac{1}{1 + k'_A} (A_m^0 + A_s^0) \\ B_m &= \frac{1}{1 + k'_B} (B_m^0 + B_s^0)\end{aligned}\tag{2.1}$$

$$\begin{aligned}A_s &= \frac{k'_A}{1 + k'_A} (A_m^0 + A_s^0) \\ B_s &= \frac{k'_B}{1 + k'_B} (B_m^0 + B_s^0)\end{aligned}\tag{2.2}$$

122 A. Martin, R. Synge, *Biochem. J.*; **1941**, 35, 1358

123 L. Craig, *J. Biol. Chem.* **1944**; 155, 519

124 D. Bassett, H. Habgood, *J. Phys. Chem.*; **1960**, 64, 769

125 J. Kallen, E. Heilbronner, *helv. Chim. Acta*, **1960**, 43, 489

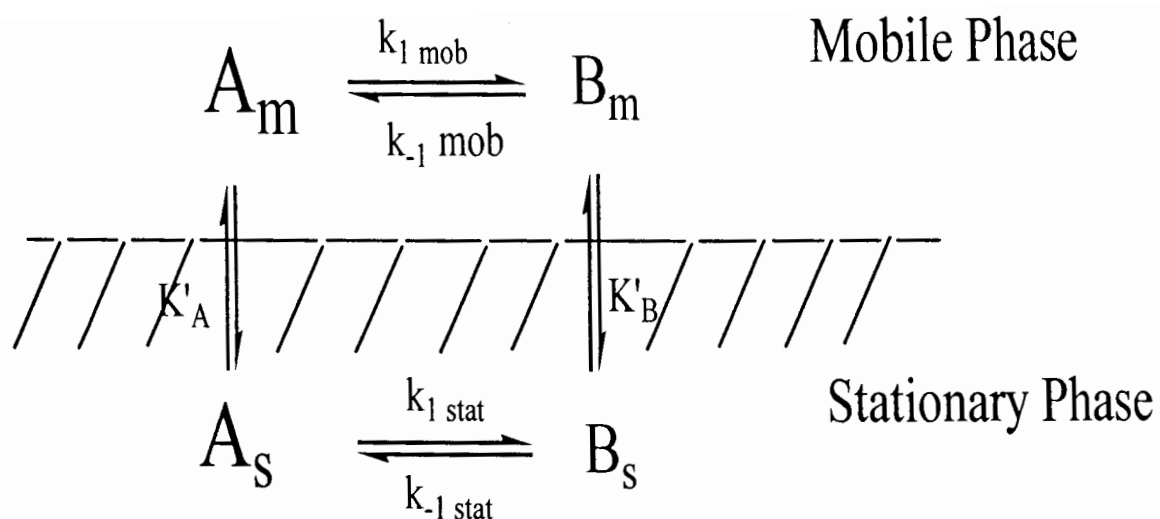


Figure 31 Equilibria in a theoretical plate: A is the first eluted stereoisomer and B is the second eluted stereoisomer, k is the rate constant and K' is the phase distribution constant

where $A_m, B_m, A_s,$ and $B_s,$ are the concentrations of the stereoisomer A and B at equilibrium;

A_m^0, A_s^0, B_m^0 and B_s^0 are the initial concentration; k_A' and k_B' are the capacity factors of A and

B and are calculated from $k' = (t_R - t_m) / t_m$, where t_R is the retention time and t_m is the void time.

The equilibrium constant, K^{Stat} , in the stationary phase depends on the two phase-distribution constant K_A' and K_B' :

$$K^{Stat} = \frac{K_B'}{K_A'} = \frac{k_B'}{k_A'} = \frac{k_1^{Stat}}{k_{-1}^{Stat}} \frac{k_{-1}^{mob}}{k_1^{mob}} \quad (2.3)$$

This equation implies that the backward rate constant k_{-1}^{Stat} is determined for a given values of k_1^{Stat} , k_A' , and k_B' . Also, k_1^{Stat} differs from k_{-1}^{Stat} when k_B' and k_A' are different, i.e., when the stereoisomers are separated by the stationary phase. Thus, no overall isomerization will occur as the second eluted stereoisomer is depleted to a greater extent to its longer residence time in the column. The forward and backward rate constants in the mobile phase must be equal. Since the mobile phase does not have the ability to separate them. k_1^{mob} / k_{-1}^{mob} will be unity. Eq (2.3) can be simplified as

$$K^{Stat} = \frac{K_B'}{K_A'} = \frac{k_B'}{k_A'} = \frac{k_1^{Stat}}{k_{-1}^{Stat}} \quad (2.4)$$

Stereoisomerization is a reversible first-order reaction. The rate of this reversible first-order can be expressed as follow:

$$\frac{dx}{dt} = k_1^{Stat} ([A_0] - [X]) - k_{-1}^{Stat} ([B_0] + [X]) \quad (2.5)$$

where the amount $[X]$ is the change of A and B. By using the initial conditions, eq. (2.5) can be solved by integration:

$$[A] = \frac{k_{-1}^{Stat}}{k_1^{Stat} + k_{-1}^{Stat}} ([A_0] + [B_0]) + \frac{k_1^{Stat} [A_0] - k_{-1}^{Stat} [B_0]}{k_1^{Stat} + k_{-1}^{Stat}} e^{-(k_1^{Stat} + k_{-1}^{Stat}) \Delta t} \quad (2.6)$$

The amount of B can be calculated from the mass balance of $[A_0] + [B_0] = [A] + [B]$.

The apparent rate constant and the kinetic activation energy of stereoisomerization can be obtained by iterative comparison of experimental and simulated chromatograms. For computer simulation of elution profiles, the rate constants in the mobile phase and stationary phase cannot be differentiated. The apparent rate constants are weighted by the retention factors k_A' and k_B' . They are defined as ¹²⁶:

$$\begin{aligned} k_1^{app} &= \frac{1}{1 + k_A'} k_1^{mob} + \frac{k_A'}{1 + k_A'} k_1^{Stat} \\ k_{-1}^{app} &= \frac{1}{1 + k_B'} k_{-1}^{mob} + \frac{k_B'}{1 + k_B'} k_{-1}^{Stat} \end{aligned} \quad (2.7)$$

Based on this theory, Bürkle et al. developed the first simulation program in 1984¹¹⁶. The simulation procedure furnishes the apparent rate constants. If k^{mob} and k^{Stat} are very similar, k_{-1}^{app} and k_1^{app} can be directly used for the simple estimation of activation energy for the interconverting reaction.

126 J. Veciana, M. I. Crespo, *Angew. Chem., Int. Ed. Engl.*; **1991**, 30, 74

§ 2.3 Stochastic Model

The stochastic model uses mathematical distribution function to describe chromatographic behavior of an interconvertible species. This model¹¹⁸ is based on the simulation of Gaussian distribution functions $\Phi_i(t')$ [$i = A, B$], the running time t' and a time-dependent probability density function $\Psi_i(t')$. This model describes the chromatography stereoisomerization as an elution profile. The elution profile $p(t)$ for an stereoisomerization process during the separation process is defined by the sum of the distribution functions $\Phi_A(t')$ and $\Phi_B(t')$ of the non-interconverted stereoisomers and the probability density functions $\Psi_A(t')$ and $\Psi_B(t')$ of the interconverted stereoisomers A and B:

$$P(t) = \Phi_A(t') + \Phi_B(t') + \Psi_A(t') + \Psi_B(t') \quad (2.8)$$

$$\text{The mass balance for this process is: } c_A^0 + c_B^0 = c_{A'} + c_{B'} + c_{A''} + c_{B''} \quad (2.9)$$

The peak shape of non-converting stereoisomers can be approximately considered as ideal linear chromatography. Therefore, the concentration profile can be expressed as a Gaussian distribution function. The standard deviation σ of the Gaussian distribution function is calculated from the theoretical plate number N or the half peak width ϖ_h as eqs. (2.10a, b):

$$\sigma^2 = \frac{t_R^2}{N} \quad (2.10a)$$

$$\sigma = \frac{\varpi_h}{\sqrt{8 \ln 2}} \quad (2.10b)$$

The concentration-time area of the non-interconverting stereoisomers can be calculated from the irreversible first-order kinetics with the apparent reaction rate constant, k_{-1}^{app} and k_1^{app} , and the initial concentration-time area, c^0 , as following:

$$c_{A'}(t_R^A) = c_A^0 e^{-k_1^{app} t_R^A} \quad (2.11a)$$

$$c_{B'}(t_R^B) = c_B^0 e^{-k_{-1}^{app} t_R^B} \quad (2.11b)$$

Combination of eq.2.10 and eq.2.11 gives the time-dependent Gaussian distribution function of the non-interconverted stereoisomers A' and B' which can be expressed as follows:

$$\Phi(t, t_R^i, \sigma_i, c_i') = \Sigma \frac{c_i'}{\sigma_i \sqrt{2\pi}} e^{-(t_i - t_R^i)^2 / 2\sigma_i^2} \quad (2.12)$$

The concentration profile of the interconverted stereoisomers A'' and B'' is calculated according to the derivations of Giddings¹¹⁸ and Kramer¹²⁷. A probability density function which is proportional to the concentration profile \bar{c}_i (eq. 2.13a) is used. The retention times of the stereoisomers t_R^A and t_R^B , the apparent rate constant k_{-1}^{app} and k_1^{app} , and the initial concentration of the stereoisomers are required as input parameters for the calculation.

$$\bar{c}_i(t) = (S_1 + S_2) \bullet e^{-(k_1^{app} - k_{-1}^{app})t} \quad (2.13a)$$

S_1 and S_2 are the peak areas for form A and B at any retention time as shown in Figure 31 and their values are shown as eq. (2.13b) and eq.(2.13c):

$$S_1 = (c_A k_1^{app} + c_B k_{-1}^{app}) \sum_{j=0}^{\infty} \frac{(k_1^{app} \bullet k_{-1}^{app} t^2)^j}{j! j!} \quad (2.13b)$$

127 R. Kramer, *J. Chromatogr.*, **1975**, 107, 241

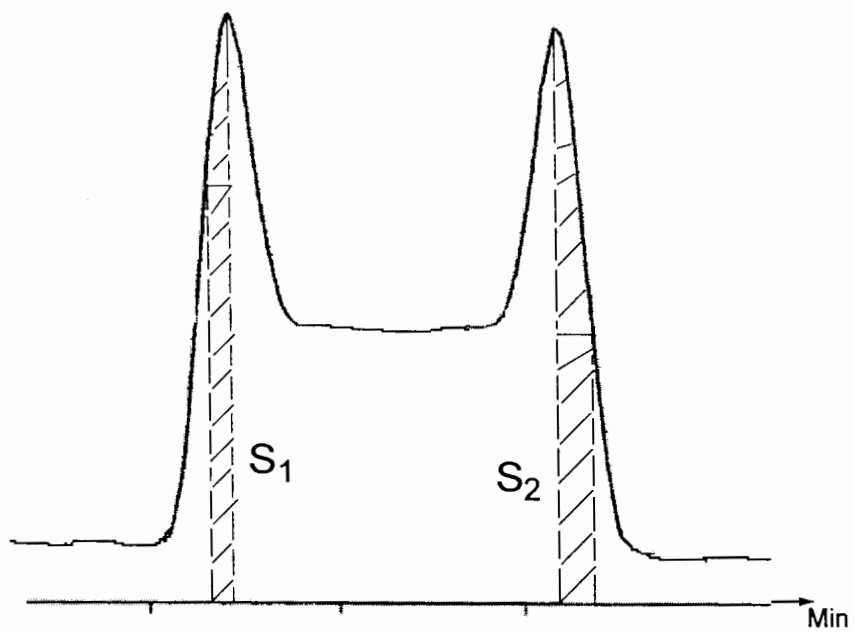


Figure 32 Definition for S.

$$S_2 = k_1^{app} k_{-1}^{app} (c_A \frac{t_R^A \bullet (t_R^B - t)}{t_R^B - t_R^A} + c_B \frac{t_R^B - t_R^A \bullet t_R^B}{t_R^B - t_R^A}) \sum_{j=0}^{\infty} \frac{(k_1^{app} \bullet k_{-1}^{app} t^2)^j}{(j+1)! j!} \quad (2.13c)$$

When the contribution approaches zero, the terminating condition for the variable j in expressions S_1 and S_2 will be achieved. The function \bar{c}_i is only a concentration profile for an ideal or linear chromatographic separation. Thus, a distribution function, which agrees with both the solution mass balance and the theoretical plate theory, is needed for the situations of peak distortion such as peak broadening and tailing. Therefore, the concentration profile \bar{c}_i is fragmented in arbitrary intervals and replaced by distribution curves using retention time t_R^A and t_R^B , and the mean plate number N_{AB}

($N_{AB} = (N_A + N_B)/2$), see eq. (2.14).

$$\Psi(t, t') = \sqrt{\frac{N_{AB}}{2\pi}} \int_{t_R^A}^{t_R^B} \bar{c}_i e^{-N_{AB}/2 \bullet (t-t')^2/t^2} \frac{1}{t} dt \quad (2.14)$$

where t' is the running time and t is the integration variable.

The computer simulation program based on the stochastic model has been applied for the determination of enantiomerization barriers for several systems^{118, 126, 127, 128, 129, 130}. Generally, the computer simulation program based on the theoretical plate model needs longer calculation time¹³¹. However, the results generated by these two independent models

128 A. Mannschreck, H. Zinner, N. Pustet, *Chimia*, **1989**, *43*, 165

129 B. Stephan, H. Zinner, F. Kastner, *Chimia*, **1990**, *10*, 336

130 R. Kramer, *J. Chromatogr.*, **1975**, *107*, 253

131 O. Trapp, G. Schoetz, V. Schurig, *Chirality*, **2001**, *13*, 403

are in very good agreement^{132, 133}. These two models were combined in the computer program ChromWin^{103, 134} and this simulation program allows a fast and efficient simulation and evaluation of experimental chromatograms without restrictions referring to plate numbers, N.

132 G. Schoetz, O. Trapp, V. Schurig, *Enantiomer*, **2000**, 5, 391

133 G. Schoetz, O. Trapp, V. Schurig, *Anal. Chem.*, **2000**, 72, 2758

134 O. Trapp, V. Schurig, *Comput. Chem.*, **2001**, 26, 187

Chapter 3 Approximate Function for the Calculation of Rate Constants

The above two models are frequently used for the computer simulation of dynamic chromatography. Considering the cost and availability of the software and the computer, a direct calculation is much preferred in certain circumstances and possibly more convenient. In 1975, Kramer¹²⁷ attempted to derive an equation to calculate the reaction rate constants, k_1 , from chromatographic parameters. However, the recursive simulation was still necessary to refine the reaction rate constant.

In 2001, Trapp and Schurig¹²⁰ derived an approximation function, based on the stochastic model, which allows for the calculation of rate constants (k_1) of enantiomerization for a racemic mixture directly from chromatographic parameters, such as retention times of both A and B forms (t_R^A and t_R^B), peak widths at half height (w_A and w_B) and the relative plateau height (h_{plateau}) (Figure 29) . No computer simulation was required. The epimerization of butyrolactol is a reversible first order reaction and the same data treatment can be employed to calculate the rate constants for this process. The elution profile $P(t')$ for interconverting epimers during the separation process can be expressed by the following equation:

$$P(t') = \Phi_A(t') + \Phi_B(t') + \Psi_A(t') + \Psi_B(t') \quad (3.1)$$

Where, $\Phi_A(t')$ and $\Phi_B(t')$ are the two distribution functions of the non-interconverted epimers, and $\Psi_A(t')$ and $\Psi_B(t')$ are the probability density functions of the interconverted epimers. Since the time dependent concentration profile, $\bar{c}(t')$, is Gaussian-modulated, the distribution functions $\Phi_A(t')$ and $\Phi_B(t')$ of the non-interconverted epimers A and B can be calculated according to the following:

$$\Phi_i(t') = \frac{c_i'}{\sigma_i \sqrt{2\pi}} e^{-\frac{(t'-t_R)^2}{2\sigma_i^2}} \quad \text{and} \quad \sigma_i = \frac{w_i}{\sqrt{8 \ln 2}} \quad \text{with } i = \{A, B\} \quad (3.2)$$

where w_i is the peak width at fifty percent of peak height and t_R is the retention time. The concentration-time area of the non-interconverted epimers, c_i' , can be calculated from first-order kinetics with the reaction rate k , reaction time t , and the initial concentration-time area c_i^0 :

$$c_i' = c_i^0 e^{-kt} \quad \text{with } i = \{A, B\} \quad (3.3)$$

The concentration profile $\Psi(t')$ of interconverting species can be calculated by the Gaussian modulation of the concentration function $\bar{c}_{\text{boxcar}}(t')$ with the integration variable t and the running time t' :

$$\Psi(t') = \frac{\bar{c}_{\text{boxcar}}(t')}{\sqrt{\pi}} \int_{t_1}^{t_2} \sqrt{\frac{N}{2}} e^{-\frac{N}{2} \left(\frac{t-t'}{t}\right)^2} \frac{1}{t} dt \quad (3.4)$$

$$\bar{c}_{boxcar}(t_R^A \leq t' \leq t_R^B) = \frac{c_{plateau}}{t_R^B - t_R^A} = \frac{c_A^0 - c_A' + c_B^0 - c_B'}{t_R^B - t_R^A} \quad (3.5)$$

Eq. (3.4) can be simplified as follows:

$$\Psi(v) = \frac{\bar{c}_{boxcar}(t')}{\sqrt{\pi}} \int_{v_1}^{v_2} \frac{e^{-v^2}}{1 - \sqrt{\frac{2}{N}} v} dv = \frac{\bar{c}_{boxcar}}{\sqrt{\pi}} \lim_{N \rightarrow \infty} \int_{v_1}^{v_2} \frac{e^{-v^2}}{1 - \sqrt{\frac{2}{N}} v} dv \quad (3.6)$$

$$v = \sqrt{\frac{N}{2}} \frac{t - t'}{t} \quad (3.7a)$$

$$\frac{dv}{dt} = \sqrt{\frac{N}{2}} \frac{t'}{t^2} \quad (3.7b)$$

$$t = \frac{t'}{1 - \sqrt{\frac{2}{N}} v} \quad (3.7c)$$

The integral was calculated numerically. It was noted that this integral converges at the retention times t_R^A and t_R^B to a value of 0.5. For low plate numbers, the solution of the integral is corrected by empirically adding $1/\sqrt{2\pi N}$ to 0.5 at the retention time t_R^A and empirically subtracting $1/\sqrt{2\pi N}$ from 0.5 for t_R^B . At the time-middle,

\bar{t} ($\bar{t} = (t_R^A + t_R^B) / 2$), the solution of the integral is approximate 1.0. The following

represents the solution of the concentration profile at times t_R^A , t_R^B and \bar{t} :

$$\begin{aligned}\Psi(t_R^A) &\approx (0.5 + \frac{1}{\sqrt{2\pi N}}) \bar{c}_{boxcar}(t_R^A) \\ \Psi(t_R^B) &\approx (0.5 - \frac{1}{\sqrt{2\pi N}}) \bar{c}_{boxcar}(t_R^B) \\ \Psi(\bar{t}) &\approx 1.0 \bar{c}_{boxcar}(\bar{t})\end{aligned}\tag{3.8a, b, c}$$

The calculation of the concentrations $c(t')$ at the retention times t_R^A , t_R^B and \bar{t} of the interconversion profile is done by combining the contributions of the distribution functions $\Phi_A(t')$, $\Phi_B(t')$ and the concentration profile $\Psi(t')$ as follows:

$$\begin{aligned}c(t_R^A) &= \Phi_A(t_R^A) + \Psi(t_R^A) + \Phi_B(t_R^A) \\ &= (0.5 - \frac{1}{\sqrt{2\pi N}}) \frac{c_A^0 + c_B^0}{t_R^B - t_R^A} (1 - e^{-k_1^{approx} t_R^A}) + \frac{c_A^0}{\sigma_A \sqrt{2\pi}} e^{-k_1^{approx} t_R^A} + \frac{c_B^0}{\sigma_B \sqrt{2\pi}} e^{-k_1^{approx} t_R^A} e^{-\frac{(t_R^A - t_R^B)^2}{2\sigma_B^2}} \\ c(t_R^B) &= \Phi_A(t_R^B) + \Psi(t_R^B) + \Phi_B(t_R^B) \\ &= (0.5 + \frac{1}{\sqrt{2\pi N}}) \frac{c_A^0 + c_B^0}{t_R^B - t_R^A} (1 - e^{-k_1^{approx} t_R^A}) + \frac{c_A^0}{\sigma_A \sqrt{2\pi}} e^{-k_1^{approx} t_R^A} e^{-\frac{(t_R^A - t_R^B)^2}{2\sigma_A^2}} + \frac{c_B^0}{\sigma_B \sqrt{2\pi}} e^{-k_1^{approx} t_R^A} \\ c(\bar{t}) &= \Phi_A(\bar{t}) + \Phi_B(\bar{t}) + \Psi(\bar{t}) \\ &= \frac{c_A^0 + c_B^0}{t_R^B - t_R^A} (1 - e^{-k_1^{approx} t_R^A}) + \frac{c_A^0}{\sigma_A \sqrt{2\pi}} e^{-k_1^{approx} t_R^A} e^{-\frac{(t_R^A - t_R^B)^2}{8\sigma_A^2}} + \frac{c_B^0}{\sigma_B \sqrt{2\pi}} e^{-k_1^{approx} t_R^A} e^{-\frac{(t_R^A - t_R^B)^2}{8\sigma_B^2}}\end{aligned}\tag{3.9a, b, c}$$

Since h_{plateau} is defined as the ratio of the concentration at the middle-time \bar{t} and the concentration of the higher peak at the retention times t_R^A and t_R^B , k_1^{approx} can be calculated as the following two cases:

(i) when $c(t_R^A)$ is higher than $c(t_R^B)$, h_{plateau} is defined as $h_{\text{plateau}} = 100 \frac{c(\bar{t})}{c(t_R^A)}$. Substitution

of this expression with eq. (9a) and eq.(9c) gives the final approximation function for k_1^{approx} :

$$\begin{aligned}
 k_1^{\text{approx}} = & -\frac{1}{t_R^A} \ln \left[\frac{(c_A^0 + c_B^0)}{(t_R^A - t_R^B)} \left(1 - \frac{h_{\text{plateau}}}{100} \left(0.5 + \frac{1}{\sqrt{2\pi} N} \right) \right) \right] \\
 & + \frac{1}{t_R^A} \ln \left[\frac{(c_A^0 + c_B^0)}{(t_R^A - t_R^B)} \left(1 - \frac{h_{\text{plateau}}}{100} \left(0.5 + \frac{1}{\sqrt{2\pi} N} \right) \right) + c_A^0 \frac{0.01 h_{\text{plateau}} - e^{-\frac{(t_R^B - t_R^A)^2}{8\sigma_A^2}}}{\sigma_A \sqrt{2\pi}} \right. \\
 & \left. + c_B^0 \frac{0.01 h_{\text{plateau}} e^{-\frac{(t_R^A - t_R^B)^2}{2\sigma_B^2}} - e^{-\frac{(t_R^A - t_R^B)^2}{8\sigma_B^2}}}{\sigma_B \sqrt{2\pi}} \right] \quad (3.10)
 \end{aligned}$$

(ii) when $c(t_R^B)$ is higher than $c(t_R^A)$,

$$\begin{aligned}
 k_1^{\text{approx}} = & -\frac{1}{t_R^A} \ln \left[\frac{(c_A^0 + c_B^0)}{(t_R^A - t_R^B)} \left(1 - \frac{h_{\text{plateau}}}{100} \left(0.5 - \frac{1}{\sqrt{2\pi} N} \right) \right) \right] \\
 & + \frac{1}{t_R^A} \ln \left[\frac{(c_A^0 + c_B^0)}{(t_R^A - t_R^B)} \left(1 - \frac{h_{\text{plateau}}}{100} \left(0.5 - \frac{1}{\sqrt{2\pi} N} \right) \right) + c_B^0 \frac{0.01 h_{\text{plateau}} - e^{-\frac{(t_R^B - t_R^A)^2}{8\sigma_B^2}}}{\sigma_B \sqrt{2\pi}} \right. \\
 & \left. + c_A^0 \frac{0.01 h_{\text{plateau}} e^{-\frac{(t_R^A - t_R^B)^2}{2\sigma_A^2}} - e^{-\frac{(t_R^A - t_R^B)^2}{8\sigma_A^2}}}{\sigma_A \sqrt{2\pi}} \right] \quad (3.11)
 \end{aligned}$$

This approximation function of k_1^{approx} was validated¹²⁰ by using a dataset of 15625 chromatograms. The data set was evaluated with the approximate function equations and the calculated rate constants were compared to the rate constants obtained from the computer simulation. It was found to give an average error of $\pm 11.7\%$ for the approximated rate constant, k_1^{approx} and the deviation of the Gibbs activation energy was $\pm 0.11RT$.

Chapter 4 Determination of Reaction Rate Constant and the Arrhenius Constant

§ 4.1 Introduction

The above mathematical model is relatively simple model for the calculation of the on-column stereoisomerization rate constant. It can be estimated by using simple chromatographic data, such as retention time, peak width, and relative height of the plateau. After the estimation of apparent reaction rate constant, the stereoisomerization energy barrier can be determined by Arrhenius equation. Since the publication of this research¹²⁰, no other research report has confirmed this result. It is our intention to test this mathematical formula for the estimation of the on-column isomerization reaction rate constant. Trityloxymethyl butyrolactol was chosen as a model molecule that can undergo on-column epimerization. The peak shape of this compound exhibits the typical profile of an on-column isomerization plateau at a certain temperature range (see Figure 33 for example chromatogram) and fits the requirements which include the existence of the plateau between two peaks, for the Trapp and Schrig's model. In this chapter, detailed chromatographic studies and mathematic studies will be reported.

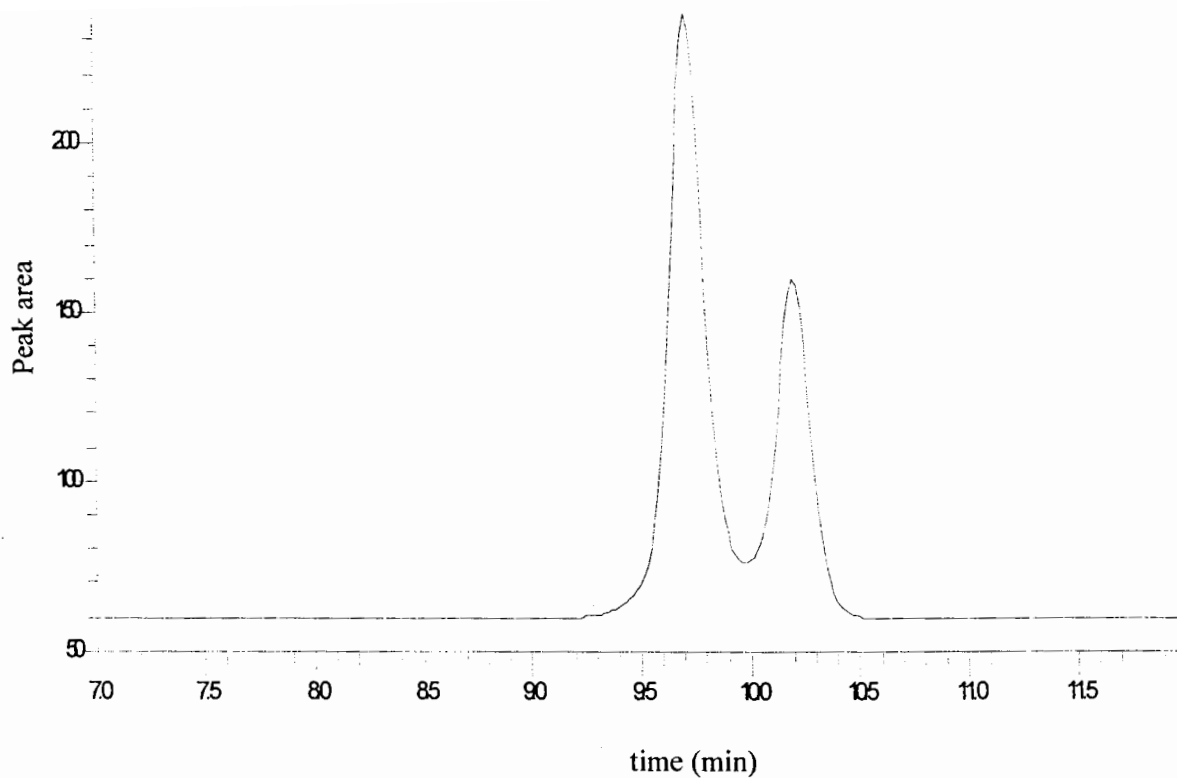


Figure 33 Typical chromatogram for trityloxymethyl Butyrolactol.
Chromatography conditions: Column: YMC-ODS AM column,
4.6 x 150 mm x 3 μ m, Mobile phase: 35% water / 65% Acetonitrile,
Flow rate: at 1 ml/min, temperature: 5°C, detection wavelength: 210 nm,
diluent: 50% water/50% Acetonitrile

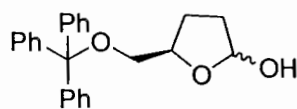
§ 4.2 Experimental Section

Synthesis

1 mmol of S (+)- γ -(trityloxymethyl)- γ -butyrolactone, purchased from Sigma Aldrich, was reacted with 5 mmol of DIBAL at -78°C in methylene chloride to generate the corresponding butyrolactol. After one hour the reaction was quenched with aqueous ammonium chloride. The organic layer was collected and the methylene chloride evaporated off. The butyrolactol was purified by prep-HPLC. The identity of the purified product was confirmed by NMR spectroscopy.

NMR

The ^1H NMR spectra (see Figure 1) of the synthesized butyrolactol was recorded on a 400 MHz Bruker NMR.



spectrometer for verification.

A

Compound A (mixture of 2

diastereomers, $\sim 1:1$). ^1H NMR (400 MHz, CDCl_3), δ 7.48-7.00 [m, 30 H, (15 H for each diastereomer, same below), Ph-H], 5.62 (br d, $J = 3.6$ Hz, 1 H, CH_2OH), 5.32 (br d, $J = 3.1$ Hz, 1 H, CH_2OH), 4.45 (m, 1 H, $\text{CHCH}_2\text{OC Ph}_3$), 4.27 (m, 1 H, $\text{CHCH}_2\text{OC Ph}_3$), 3.30 (dd, $J = 3.8$ and 9.8 Hz, 1 H, $\text{Ph}_3\text{COCH}_a\text{H}_b$), 3.22 (dd, $J = 4.8$ and 9.8 Hz, 1 H, $\text{Ph}_3\text{COCH}_a\text{H}_b$), 3.11 (d, $J = 4.8$ Hz, 2 H, $\text{Ph}_3\text{COCH}_a\text{H}_b$), and 2.15-1.95 (m, 8 H, CH_2CH_2). ^{13}C NMR (100 MHz, CDCl_3), δ (mixture of $\sim 1:1$ diastereomers) 144.14, 143.88, 128.87, 128.80, 127.89, 127.82, 127.14, 127.00, 99.09, 98.86, 79.46, 77.79, 66.85, 66.24, 34.31, 32.96, 29.75, 26.02, and

25.20. Additionally the distribution constant for the two epimers of butyrolactol in solution were determined by NMR for the –CHOH group. The ratio is 1.0 for the peaks of CHOH at chemical shift 5.62 and 5.32

Chromatographic Conditions

All chromatographic studies were performed on a Hewlett Packard 1100 HPLC system equipped with a photo diode array UV detector. Data acquisition and treatment was performed with a Perkin Elmer Turbochrom system. The reported chromatographic data is the average of triplicate determinations at a detection wavelength of 210 nm. The column dead volume was determined by using deuterated methanol as a dead volume marker as reported by Knox¹³⁵.

Chromatographic separation was performed on a 3 μ m YMC-pack ODS-AM column (150 x 4.6 mm). The eluent was HPLC grade acetonitrile and HPLC grade water. HPLC grade acetonitrile was purchased from Sigma-Aldrich Co. HPLC grade water was obtained from a Picotech water purifying system. Chromatographic runs were performed at 5, 10, 15, 20, and 25 °C. At each temperature point, five flow rates were studied to ensure accuracy and precision.

135 J. Knox, R. Kaliszan, *J. Chromatogr.*, **1985**, 349, 211,

§ 4.3 Calculation of Apparent Reaction Rate Constant

According to Trapp and Schurig¹²⁰, the on-column interconversion reaction rate can be estimated as following:

$$\begin{aligned}
 k_1^{approx} = & -\frac{1}{t_R^A} \ln \left[\frac{(c_A^0 + c_B^0)}{(t_R^A - t_R^B)} \left(1 - \frac{h_{plateau}}{100} \left(0.5 + \frac{1}{\sqrt{2\pi N}} \right) \right) \right] \\
 & + \frac{1}{t_R^A} \ln \left[\frac{(c_A^0 + c_B^0)}{(t_R^A - t_R^B)} \left(1 - \frac{h_{plateau}}{100} \left(0.5 + \frac{1}{\sqrt{2\pi N}} \right) \right) + c_A^0 \frac{0.01h_{plateau} - e^{-\frac{(t_R^B - t_R^A)^2}{8\sigma_A^2}}}{\sigma_A \sqrt{2\pi}} \right. \\
 & \left. + c_B^0 \frac{0.01h_{plateau} e^{-\frac{(t_R^A - t_R^B)^2}{2\sigma_B^2}} - e^{-\frac{(t_R^A - t_R^B)^2}{8\sigma_B^2}}}{\sigma_B \sqrt{2\pi}} \right]
 \end{aligned}$$

if the peak height of form A (see Figure 28) is higher than that of form B. In the case that the stationary phase stabilizes the form B more than A form, the peak height of form B is going to be higher than that of form A. The formula is changed to following:

$$\begin{aligned}
 k_1^{approx} = & -\frac{1}{t_R^A} \ln \left[\frac{(c_A^0 + c_B^0)}{(t_R^A - t_R^B)} \left(1 - \frac{h_{plateau}}{100} \left(0.5 - \frac{1}{\sqrt{2\pi N}} \right) \right) \right] \\
 & + \frac{1}{t_R^A} \ln \left[\frac{(c_A^0 + c_B^0)}{(t_R^A - t_R^B)} \left(1 - \frac{h_{plateau}}{100} \left(0.5 - \frac{1}{\sqrt{2\pi N}} \right) \right) + c_B^0 \frac{0.01h_{plateau} - e^{-\frac{(t_R^B - t_R^A)^2}{8\sigma_B^2}}}{\sigma_B \sqrt{2\pi}} \right. \\
 & \left. + c_A^0 \frac{0.01h_{plateau} e^{-\frac{(t_R^A - t_R^B)^2}{2\sigma_A^2}} - e^{-\frac{(t_R^A - t_R^B)^2}{8\sigma_A^2}}}{\sigma_A \sqrt{2\pi}} \right]
 \end{aligned}$$

From above two equations, the on-column epimerization rate constant can be estimated by using simple chromatographic data. All the chromatographic parameters, such as retention time t_R^A and t_R^B , peak width w_i , and theoretical plate number N can be obtained from Turbochrom software report, except the peak height and the plateau height. The plateau height and peak height have to be measured by ruler as shown in Figure 34.

Five temperature points were taken for the measurements of k_1^{approx} in order to determine the activation energy for this epimerization. According to C. Horváth's^{91, 92}, the peak shape could change at different flow rate, when this type interconversion exists in a chromatographic system. Thus, five flow-rate points were taken for each temperature point to ensure the accuracy of the data. Since the two epimers are present at equal concentrations in the diluent, as indicated earlier by NMR data, c_A^0 and c_B^0 are assumed to be 0.5. The theoretical plate number in the equation was measured by using butyrolactone. It was injected in the chromatographic runs for each condition, and its theoretical plate number was used for the calculation of k_1^{approx} . There are two reasons for using butyrolactone's theoretical plate number instead of butyrolactol's. First, this compound has very similar structure and functional groups as butyrolactol. Secondly, it does not undergo interconversion in either diluent or on-column and, thus, peak broadening due to interconversion is excluded from the non-reaction broadening¹¹³. The raw data are listed in Table 11-15.

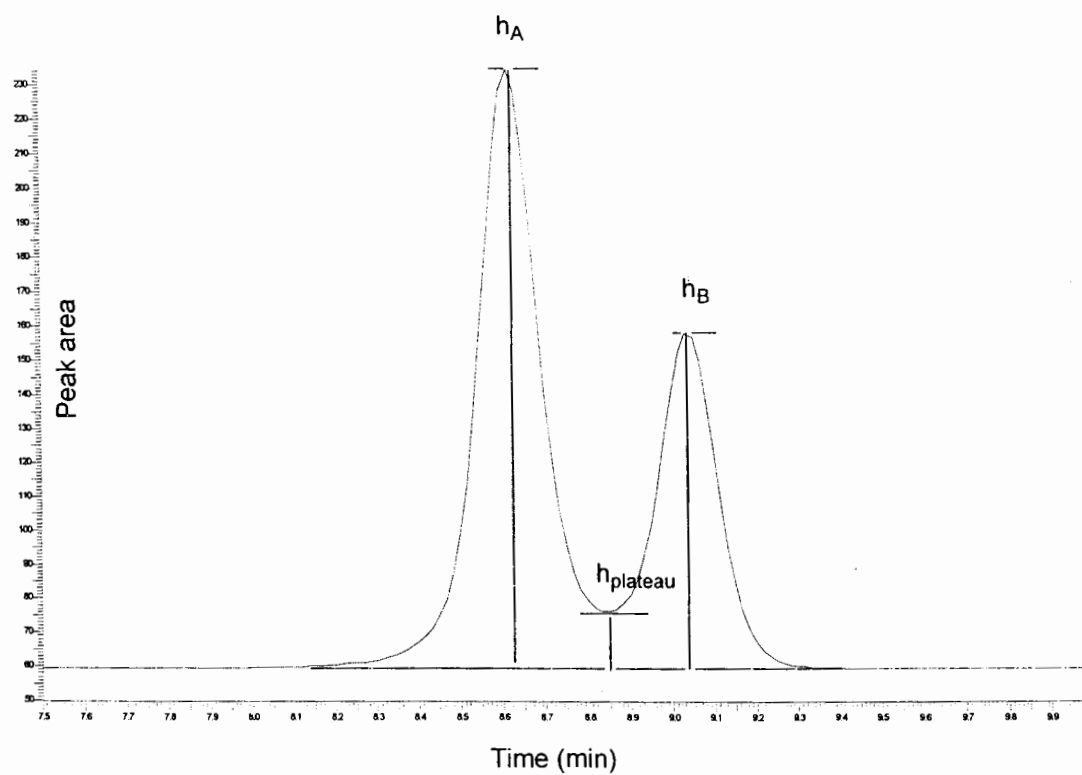


Figure 34 Measurement of peak heights for trityloxymethyl butylrolactol $h = h_{\text{plateau}} / h_A$

The calculated results for k_1^{approx} are listed in Table 16. Some of the data for k_1^{approx} was out of range according to Q test. When this occurred, that specific datum for k_1^{approx} was ignored for the calculation of average k_1^{approx} . Since the ring structure of butyrolactol is similar to that of carbohydrates, the ring opening and closing reaction rates for both should be of similar magnitude. Reported isomerization rates of common carbohydrates are comparable to the rates measured in this study¹³⁶ (See Table 17). It is found that the value calculated by using the approximate function is very close the isomerization rate of common carbohydrates. A previous study of interconversion of muramyl dipeptide¹³⁷ also reported similar results.

136 B. Capon, W. G. Overend, *Advances in Carbohydrate Chemistry and Biochemistry*, 15, 11, 1960

137 M. Lebl, and V. Gut, *J. Chromatogr.*, 1983, 260, 478,

Table 11. The chromatographic data for 5°C

Flow Rate (ml/min)	t_R^A (min)	t_R^B (min)	Half peak width for A(sec)	Half peak width for B(sec)	Relative plateau height	Theoretical number, N	k_1^{approx} ($\times 10^{-4}$, s^{-1})
1.1	7.065	7.412	8.07	8.20	0.1053	16748.52	1.54
1.0 ^a	7.864	8.256	8.08	8.88	0.0990	17905.5	2.19
0.9	8.625	9.051	9.39	9.45	0.0946	18176.31	1.99
0.8	9.710	10.196	10.34	10.38	0.0913	18978.55	1.84
0.7	11.095	11.654	11.66	11.75	0.0927	20334.23	1.70
						Avg.	1.74

a. Rejected by Q test at 95% confidence interval

Table 12. The chromatographic data for 10°C

Flow Rate (ml/min)	t_R^A (min)	t_R^B (min)	Half peak width for A(sec)	Half peak width for B(sec)	Relative plateau height	Theoretical number, N	k_1^{approx} ($\times 10^{-4}$, s^{-1})
1.1	6.837	7.155	7.56	7.48	0.0925	17606.92	2.00
1.0	7.508	7.859	8.12	8.03	0.0936	18663.45	2.03
0.9	8.358	8.750	8.89	8.79	0.0917	19529.03	1.90
0.8 ^a	9.372	9.814	9.83	9.67	0.0918	20364.88	1.79
0.7 ^a	10.715	11.224	11.14	10.94	0.0926	21396.3	1.65
						Avg.	1.98

a. Rejected by Q test at 95% confidence interval

Table 13. The chromatographic data for 15°C

Flow Rate (ml/min)	t_R^A (min)	t_R^B (min)	Half peak width for A(sec)	Half peak width for B(sec)	Relative plateau height	Theoretical number, N	k_1^{approx} ($\times 10^{-4}$, s^{-1})
1.1	6.648	6.940	7.46	7.30	0.124	18211.87	2.35
1.0	7.315	7.638	8.06	7.89	0.121	18846.19	2.27
0.9	8.112	8.471	8.81	8.58	0.120	198464.68	2.17
0.8	9.11	9.516	9.83	9.54	0.123	20508.05	2.09
0.7 ^a	10.389	10.854	11.12	10.82	0.129	21249.64	2.01
						Avg.	2.22

a. Rejected by Q test at 95% confidence interval

Table 14. The chromatographic data for 20°C

Flow Rate (ml/min)	t_R^A (min)	t_R^B (min)	Half peak width for A(sec)	Half peak width for B(sec)	Relative plateau height	Theoretical number, N	k_1^{approx} ($\times 10^{-4}$, s^{-1})
1.1	6.522	6.796	7.63	7.36	0.166	17780.76	2.50
1.0	7.163	7.463	8.26	7.98	0.163	18575.85	2.34
0.9	7.958	8.294	9.06	8.76	0.17	19633.24	2.51
0.8	8.951	9.331	10.14	9.83	0.176	20408.79	2.45
0.7	10.24	10.674	11.57	11.30	0.186	21169.75	2.30
						Avg.	2.42

Table 15. The chromatographic data for 25°C

Flow Rate (ml/min)	t_R^A (min)	t_R^B (min)	Half peak width for A(sec)	Half peak width for B(sec)	Relative plateau height	Theoretical number, N	k_1^{approx} ($\times 10^{-4}$, s ⁻¹)
1.1	6.370	6.621	8.19	8.82	0.326	18319.92	2.75
1.0	6.990	7.267	8.86	9.76	0.323	18512.21	2.71
0.9	7.759	8.068	9.77	10.92	0.321	19015.90	2.52
0.8	8.732	9.081	10.89	12.00	0.311	19668.26	2.37
0.7	9.974	10.374	12.41	13.70	0.321	20338.81	2.33
						Avg.	2.54

Table 16. The calculated k_1^{approx} value

Temperature (°)	$k_1^{approx} (10^{-4} \text{ s}^{-1})$	SD(10^{-4} s^{-1})
25	2.54	0.02
20	2.42	0.01
15	2.22	0.01
10	1.98	0.01
5	1.77	0.02

Table 17. Literature reported interconversion reaction rate constants for Carbohydrates. Data are from reference 136.

Sugar	Reaction Rate Constant ($\times 10^{-4}$ at 20°, sec ⁻¹)
α -D-Glucose	2.43
β -D-Glucose	2.40
α -D-Mannose	6.64
β -D- Mannose	6.83
α -D-Xylose	7.79
α -D-Lyxose	21.8
β -D-Lyxose	22.7
α -Lactose•H ₂ O	1.81
β -Lactose	1.79
β -Maltose	2.02

§ 4.4 Arrhenius Activation Energy

As one of the most important tools for the investigation of reaction mechanisms, the Arrhenius equation was employed for the determination of the rate of a reaction as a function of temperature. From the Arrhenius equation, which represents the relationship between the rate constant k and the activation energy of the reaction, the activation energy of this reaction can be calculated.

$$\ln k = -E_a / RT + \text{constant}$$

Where E_a is the activation energy and R is the gas constant. The plot of $\ln k$ vs. the reciprocal of the absolute temperature is a straight line with a slope of E_a / R . This plot is shown in Figure 35. The correlation coefficient for this straight line is 0.990 and the calculated activation energy for this isomerization reaction is 10.3 Kcal / mol.

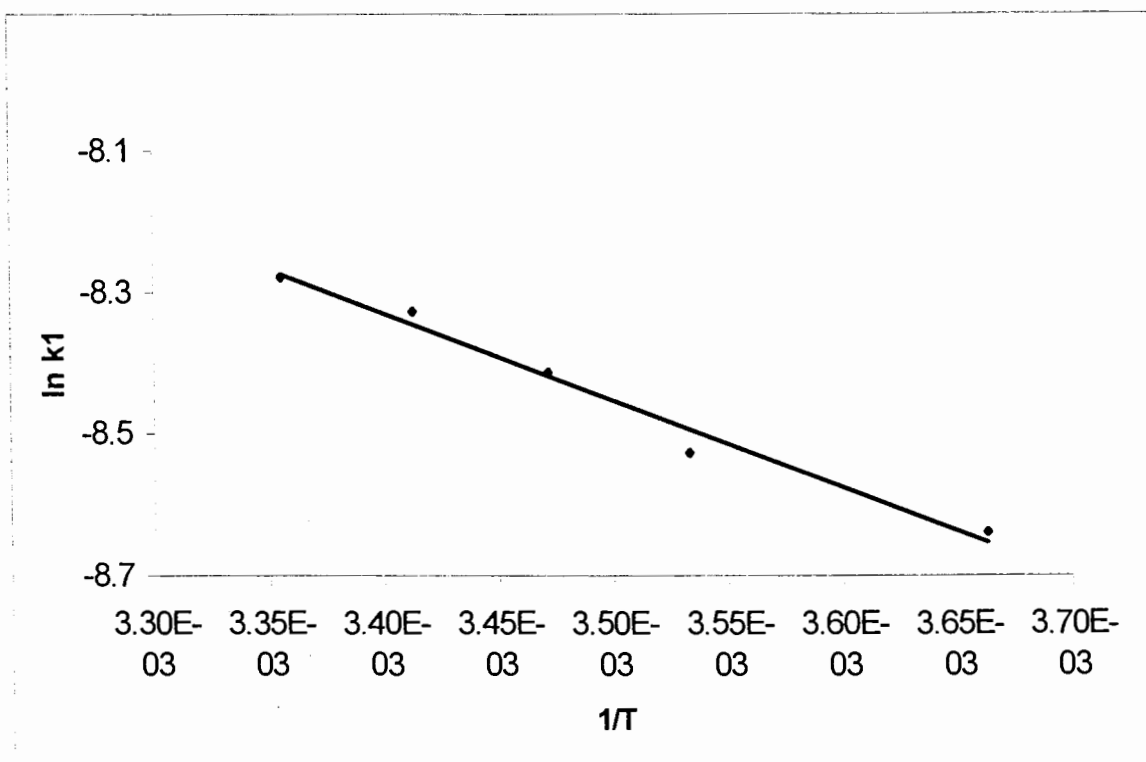


Figure 35 The Arrhenius plot for trityloxymethyl butyrolactol (ODS –AM 4.6 x 150 mm x 3.5 μ m column)

Chapter 5 Peak Shape Studies for the Inter-conversion Reactions

§ 5.1 Introduction

For an inter-converting compound, it is desirable to obtain a single sharp peak for overall impurity and quantitative analysis. Chromatographic conditions have a large effect on the peak shape when on-column interconversion occurs. Peak resolution is observed if the rate of chemical conversion is slow compared to the chromatographic exchange process. If the rate of chemical conversion is fast relative to the chromatographic exchange process only one peak is observed. There are two general means that can lead to the achievement of such goal. One way is to accelerate the inter-conversion rate by either an increase in the reaction temperature, which can be achieved easily by increasing the column temperature, or by adding catalyst to the mobile phase to enhance the inter-conversion reaction. Another way is to slow down the chromatographic process and by decreasing the flow rate of the mobile phase. Thus, parameters such as flow rate, pH of the mobile phase and temperature can be varied to obtain the ideal peak shape. In this chapter, detailed studies of chromatographic parameters on the effect of peak shape are reported.

§ 5.2 The flow-rate effect on the peak shape

The effect of flow-rate on the peak shape was observed by several other research groups. Horváth *et al.* had reported this observation as early as 1982¹³⁸. In their paper⁹¹, a group of chromatograms (see Figure 36) demonstrates this effect. Flow-rate usually does not have such big effect on peak shape for linear chromatography. However, when there is a secondary equilibrium existing in the chromatographic system, the peak shapes of these inter-converting species can change dramatically. When the inter-conversion rate is faster than the chromatographic rate, the chromatographic system cannot detect the inter-conversion. Therefore, only one peak is observed in the chromatogram. When the inter-conversion rate is slower than the chromatographic rate, two individual peaks will be observed. When the inter-conversion rate is about the same as the chromatographic rate, two peaks linked with elevated baseline or a distorted peak will be observed. In the research of Horváth *et al.*, different peak shapes have been observed at different flow-rates. Trabelsi *et al.*¹³⁹ have reported similar observations. At higher flow-rates, two bimodal peaks corresponding to the inter-converting species was obtained. At lower flow-rates, a single peak was obtained (see Figure 37) due to the longer relaxation time.

In our studies, chromatograms of butyrolactol obtained at the flow-rates of 0.2, 0.4, 0.6, 0.8 and 1.0 ml/min with a mobile phase consisting of a mixture of water/acetonitrile (35/65, v/v) at 5°C are shown in Figure 38. At the lower flow-rate of 0.2 ml/min, a single

138 W. R. Melander, J. Jacobson, C. Horvath, *J. Chromatogr.*, **1982**, 234, 269,

139 H. Trabelsi, S. Bouabdallah, S. Sabbah, F. Raouafi, K. Bouzouita, *J. Chromatogr.*

A, **2000**, 871, 189

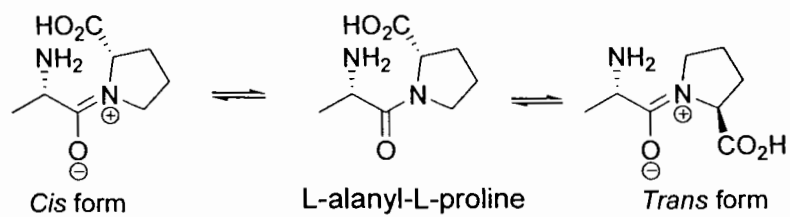
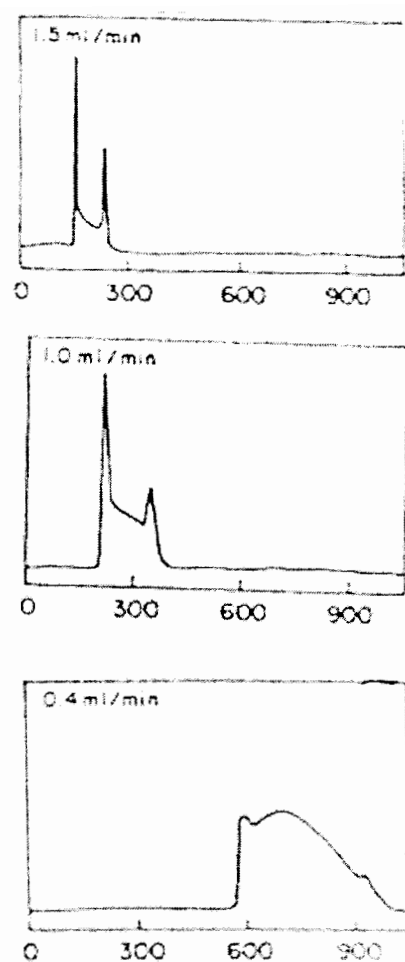
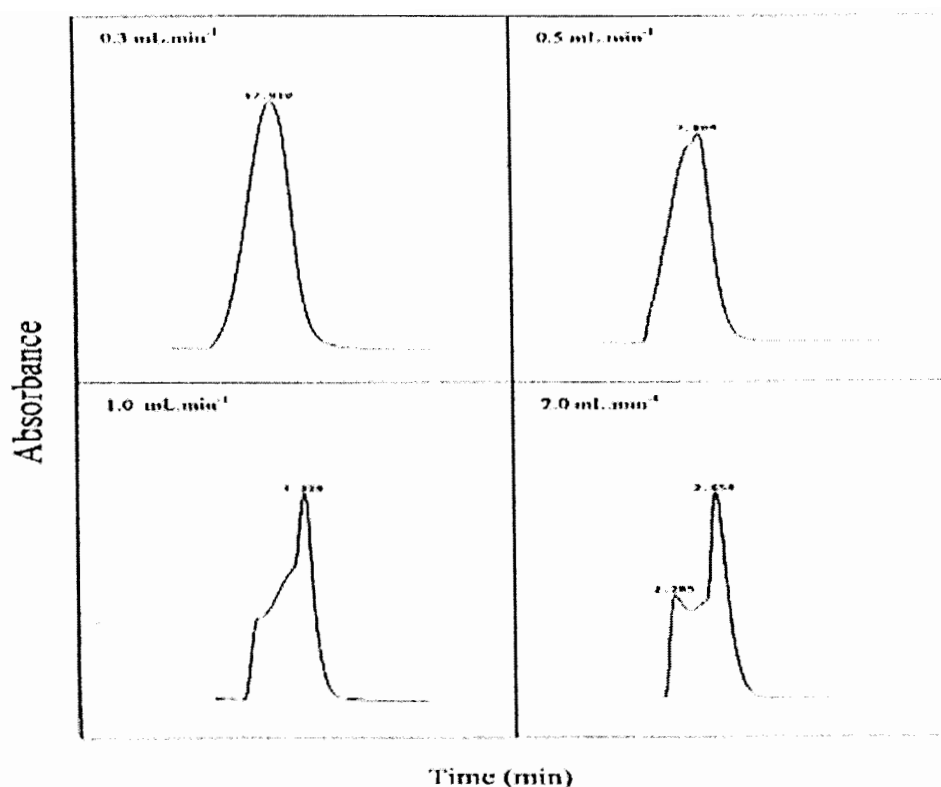


Figure 36 The flow-rate effect on the peak shape of cis-trans proline inter-conversion. Column: Partisil ODS 4.6 x 250 mm x 5 μ m, mobile phase: 0.050 M phosphate buffer at 1.5 ml/min. The figure is re-produced from reference 91.



The following is the structure of enalapril. The isomerization reaction of this compound is similar to that of alanyl-proline.

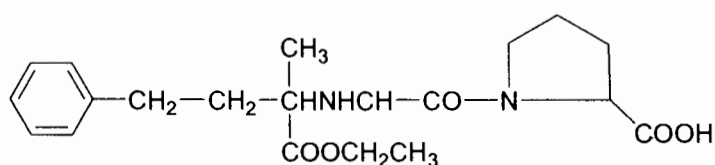
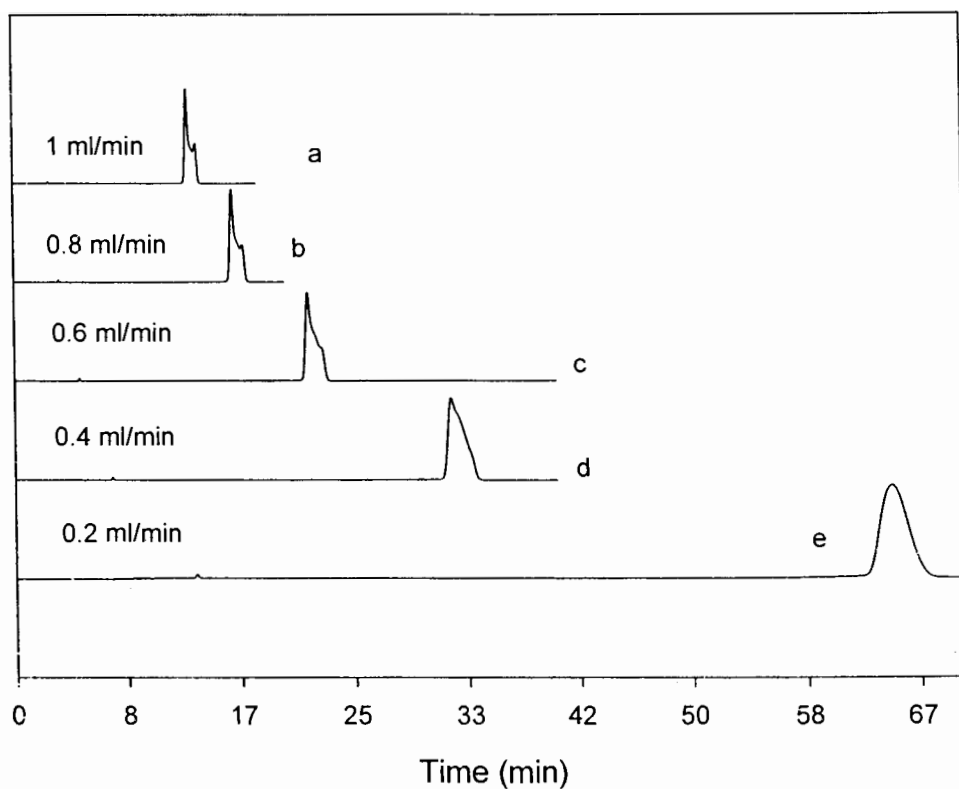


Figure 37 The flow-rate effect on the peak shape of enalapril inter-conversion. Mobile phase: phosphate buffer at pH = 2.0-acetonitrile at 60: 40/v:v; flow-rate: 1.0 ml/min; Column: Sulpelco LC 18, 4.6 x 250 mm x 5 μ m. The figure is re-produced from reference [139].

wide peak is obtained, as the interconversion rate is fast relative to the chromatographic process. At higher flow-rates, a bimodal peak corresponding to the epimers was observed due to the fact that the interconversion rate is slower relative to the chromatographic process. This peak shape change is not due to a decrease of column efficiency at lower flow-rate. The reference compound trityloxymethyl butyrolactone was injected at each chromatographic condition. We have found that the theoretical plate numbers reported from Turbochrom system suitability data only decreased from about 24,600 to about 24,000, when flow-rate decreased from 1 ml/min to 0.2 ml/min. Such small change in theoretical plate number cannot be counted upon as the main factor of such a dramatic change in peak shape.



- A) From a to c, the interconversion rate is slow with respect to the flow rate. Two peaks are observed.
 B) From d to e, the inter-conversion rate is fast with respect to flow rate. One
 C) peak is observed.

Figure 38 Effect of flow-rate on the peak shape of trityloxymethyl butyrolactol (ODS 4.6 x 250 mm x 5 μ m column, 35 : 65 /water: acetonitrile, 5°C)

§ 5.3 Column temperature effect on the peak shape

The influence of the temperature on the peak shape for the inter-conversion species is very large, since temperature is one of the key factors that affect the reaction rate. For an endothermic reaction, increasing temperature can increase the reaction rate. The influence of the stereoisomerization on peak shape is governed by the rate of isomerization with respect to the time scale of HPLC elution. Faster isomerization rates and relatively long retention times would most likely result in a single peak⁹¹. It was reported that L-ananyl-L-proline has two peaks linked with elevated baseline at 25°C and has a single peak with tailing at 40°C (see Figure 39). H. Trabelsi *et al.* also reported similar results in their paper¹³⁹, the temperature study on the peak shape of enalapril (see Figure 40) yielded different peak shapes at different temperatures. The dramatic change in peak shape at different temperatures can only be explained by on-column inter-conversion. At higher temperatures, the isomerization reaction of the amide bond is faster than at lower temperatures. Therefore, the peak shape becomes sharper at higher temperature, as the time-scale of the chromatographic system does not allow for detection of the inter-conversion.

In our studies, the influence of temperature on the peak shape of butyrolactol was investigated at several column temperatures while keeping other parameters constant. Figure 40 shows that the increase of temperature led to a significant improvement in the peak shape. This effect is attributed to an increase of the interconversion rate for the two epimers at higher temperature, eventually resulting in a single peak. The retention time

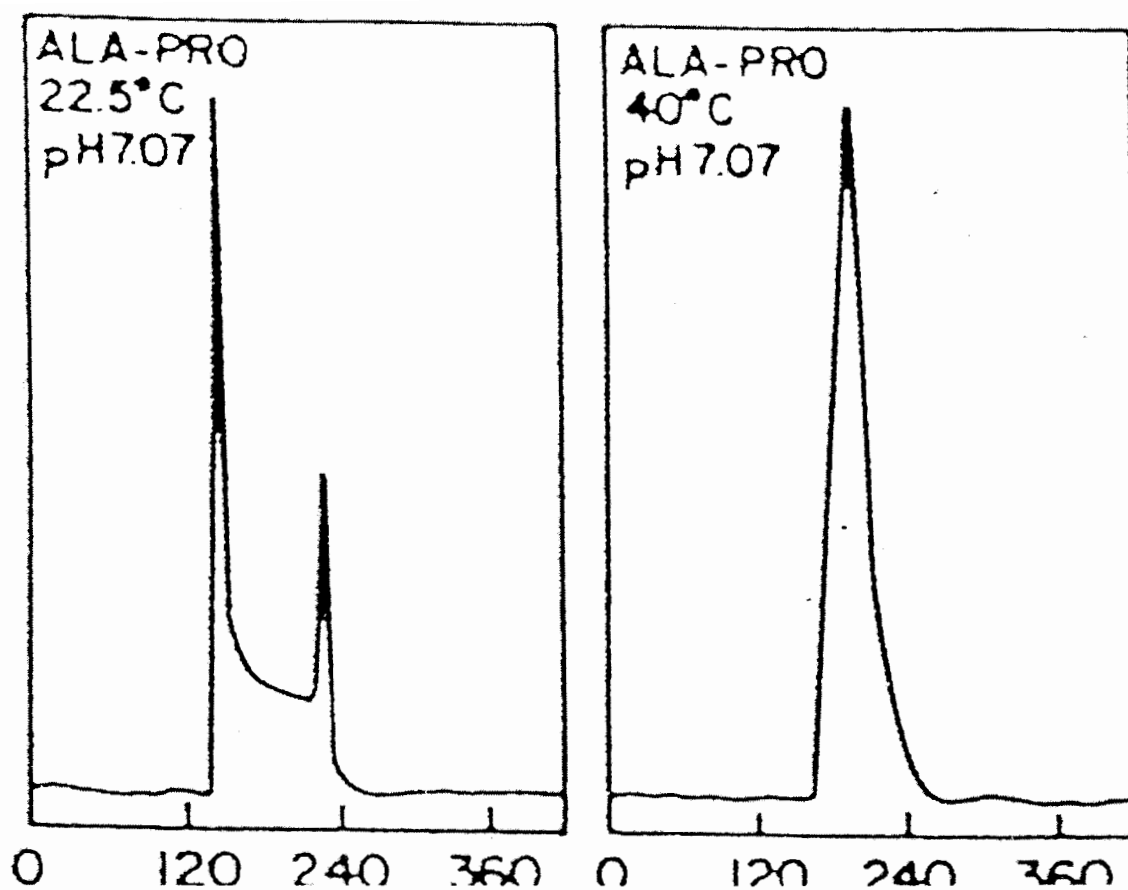


Figure 39 The temperature effect on the peak shape of L-alanyl-L-proline.
Chromatographic condition: Column: Partisil ODS 4.6 x 250 mm x 5 μ m,
mobile phase: 0.050 M phosphate buffer at 1.5 ml/min.
X axis unit is seconds and Y axis is peak area.
The figure is re-produced from reference [92].

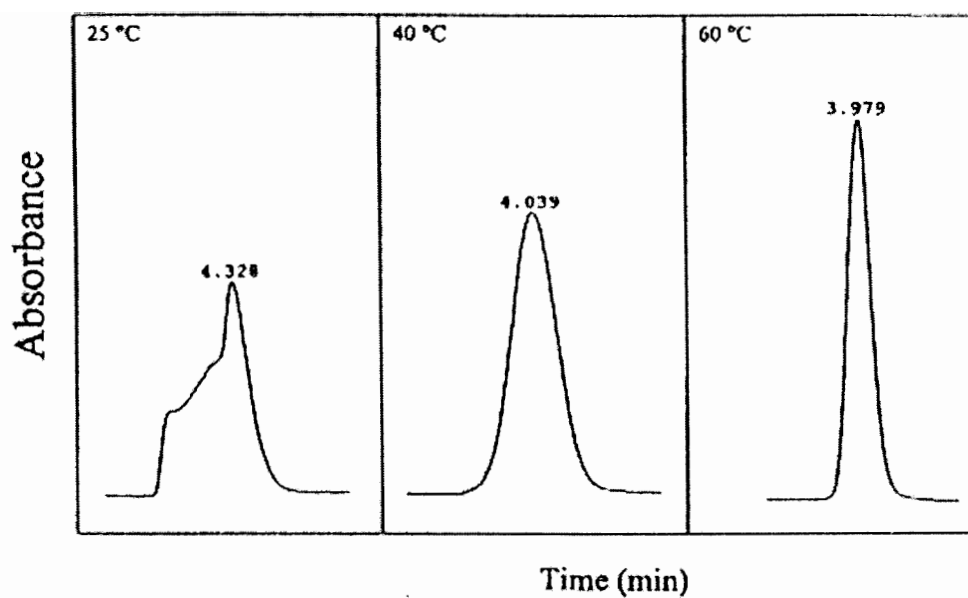


Figure 40 Effect of column temperature on the peak shape and retention of enalapril.
Mobile phase: phosphate buffer at pH = 2.0, acetonitrile at 60: 40/v:v;
flow-rate: 1.0 ml/min; Column: Sulpelco LC 18, 4.6 x 250 mm x 5 μ m.
The figure is re-produced from reference [139].

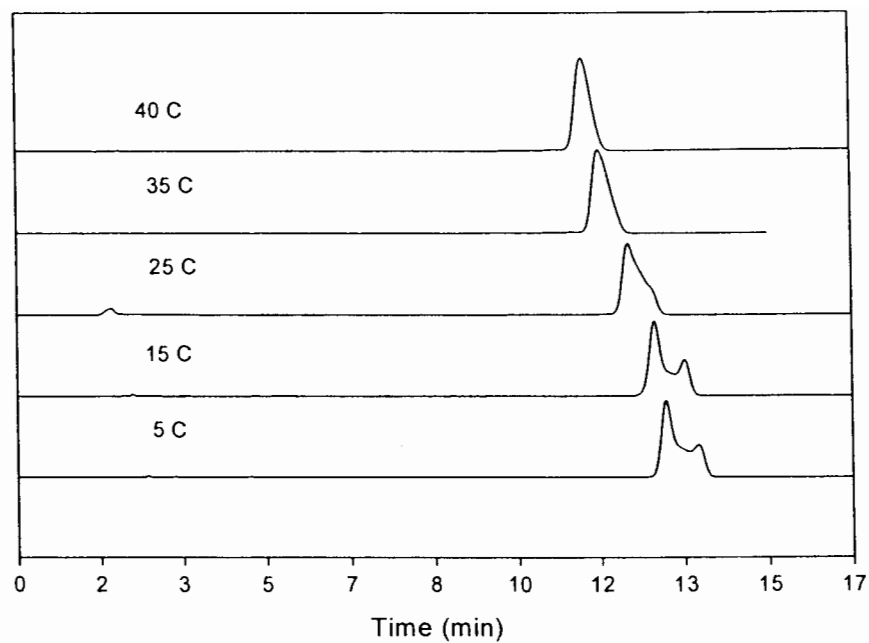


Figure 41 Effect of temperature on the peak shape of trityloxymethyl butyrolactol (ODS- AM 4.6 x 250 mm x 5 μ m column, 35 : 65 /water: acetonitrile, 1 ml/min)

for butyrolactol changed significantly while varying the temperature. This phenomenon is different from that observed for proline-containing substances, which have relatively smaller change in retention time, reflecting a larger enthalpic contribution to retention for butyrolactol¹³⁸.

§ 5.4 Mobile phase pH effect on the peak shape

The reaction rate can vary in different environments. The solution pH is an important parameter to vary for a pH dependent reaction. The ring opening process for lactol compounds can be catalyzed by both hydrogen ions and hydroxyl ions. In carbohydrate chemistry, this process is called mutarotation. The catalysis mechanisms for both hydrogen ion and hydroxyl ion are listed in Figure 42 and 43.

As reported in 1927¹⁴⁰, Brönsted and *et al.* had reported the total reaction constant has three contributions - an intrinsic, an acid catalysis and a base catalysis reaction constant in aqueous solutions:

$$k = k_0 + k_{OH} \times C_{OH} + k_H \times C_H$$

where C_{OH} and C_H are the concentrations of hydrogen and hydroxyl ion, respectively. From the above equation, we can conclude that at certain mobile phase pH, the inter-conversion rate of lactol can reach a minimum. Harron *et al.* studied cyclic hemiacetal reactions of hydroxyl benzaldehydes¹⁴¹. They reported similar results and had made a curve of $\log k$ vs. solution pH (see Figure 44). From the curve, we know that the ring opening and closing reactions for lactol compounds have slowest rate at pH around 4 to 5. From these data, we know that the

140 J. N. Brönsted and E. A. Guggenheim, *J. Am. Chem. Soc.*, **1927**, *49*, 2554

141 J. Harron, R. A. McClelland, C. Thankachan and T. T. Tidwell,
J. Org. Chem., **1981**, *46*, 903

inter-conversion rate of lactol will be minimized around pH 4 – 5. This means that the peak shape of interconverting species will be much sharper at other pH ranges.

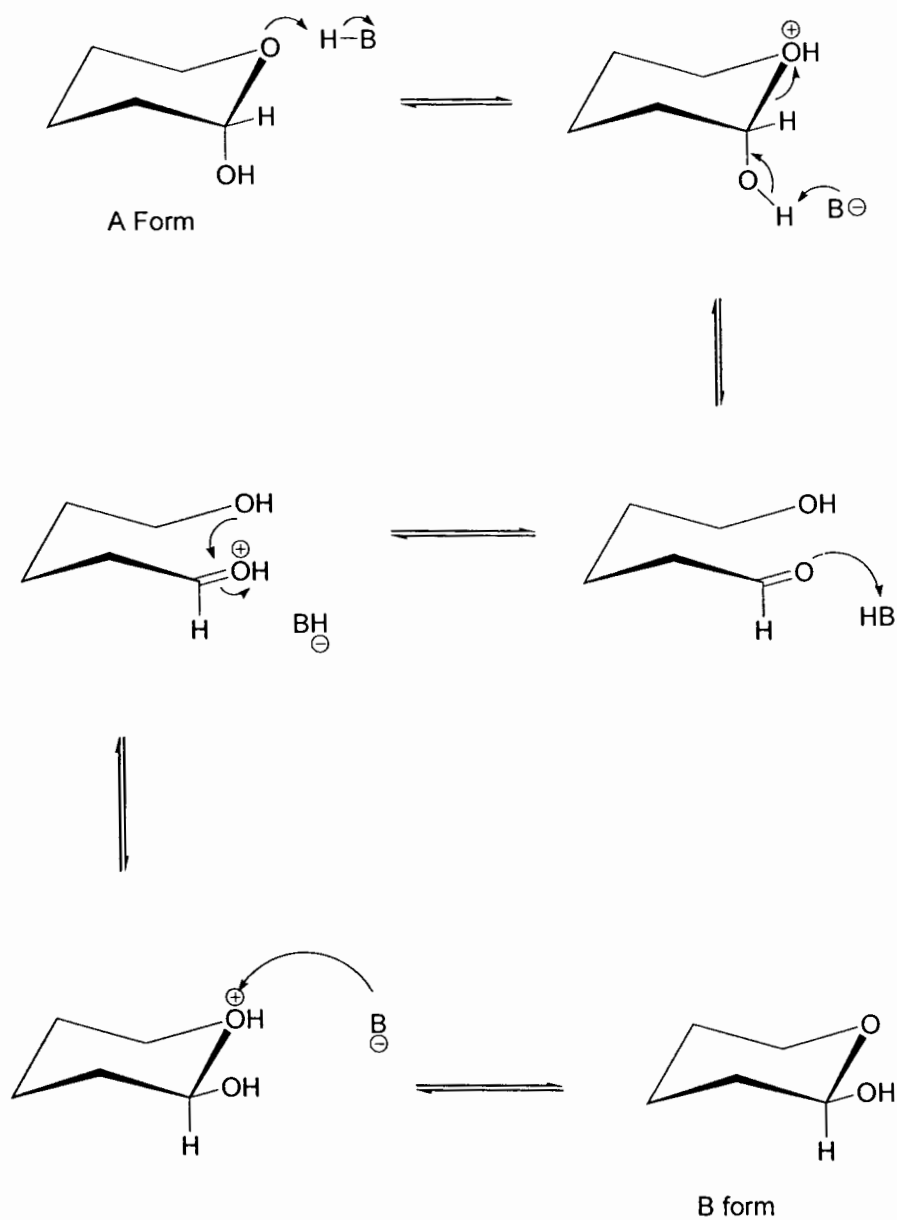


Figure 42. The reaction mechanism for the acid catalyzed epimerization reaction of lactols

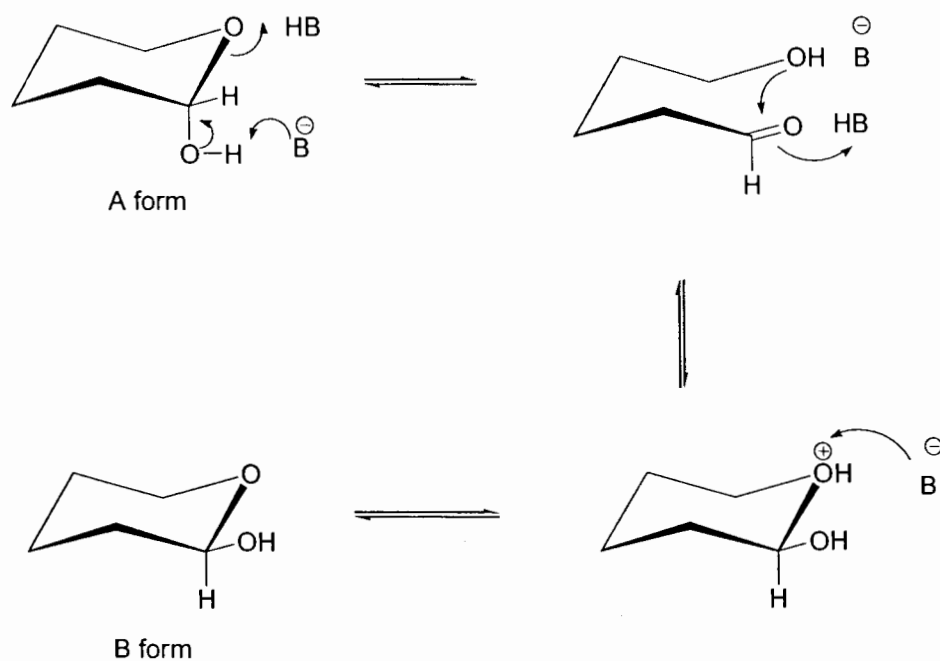


Figure 43 The reaction mechanism for the base catalyzed epimerization reaction of lactols

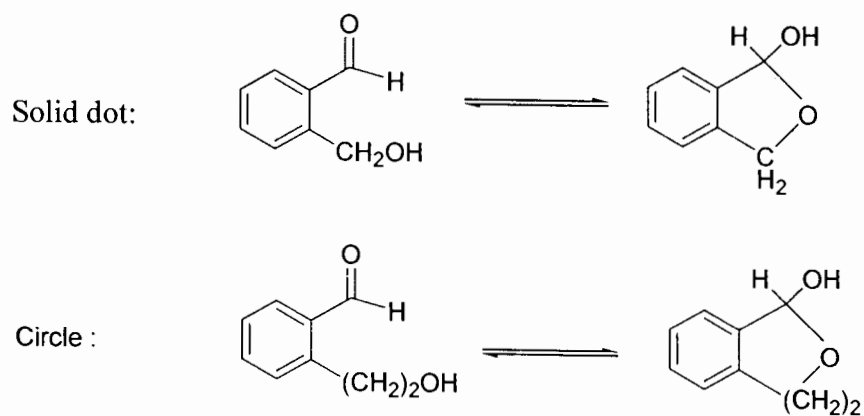
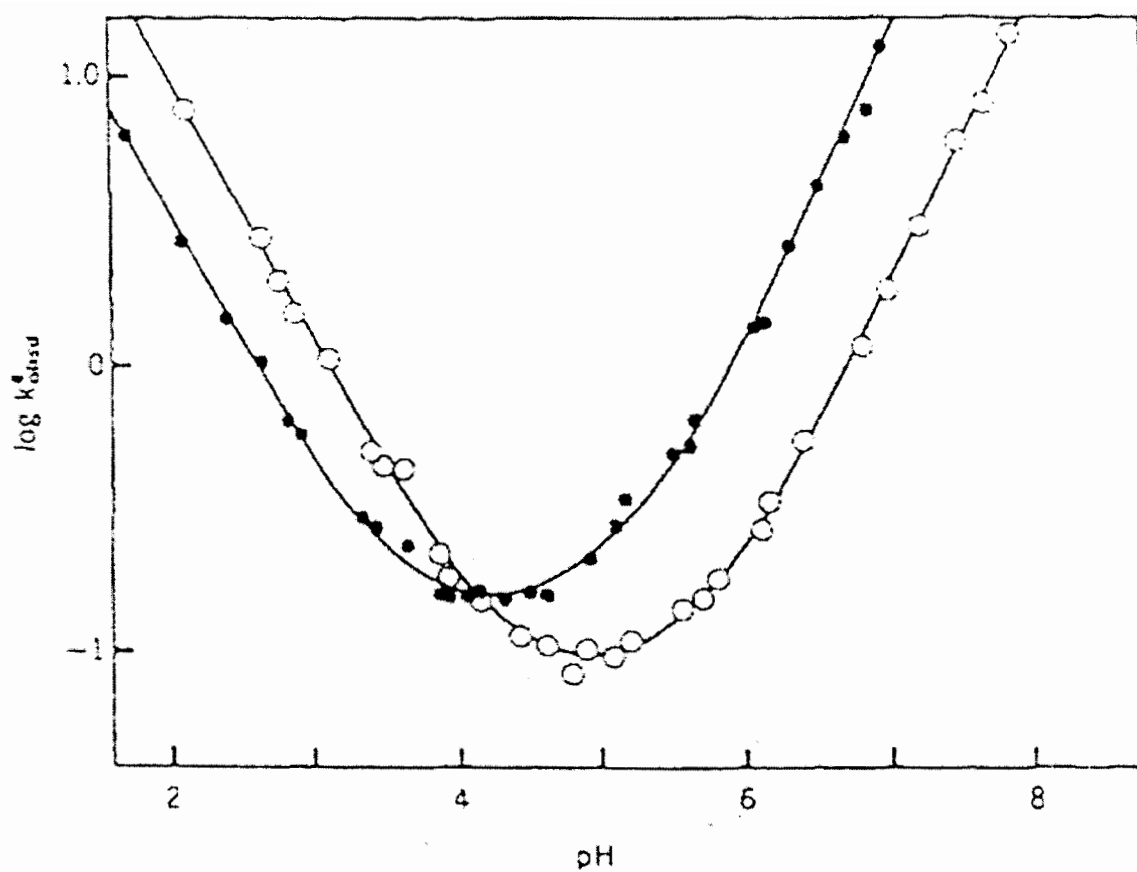


Figure 44 Reaction rate constant for some hydroxyl benzaldehyde.
It is re-produced from reference [141].

In our studies, the influence of phosphate buffer pH on the peak shape was investigated by using a mobile phase consisting of 10 mM phosphate buffer-acetonitrile (35/65 v/v) at a temperature of 25°C and a flow rate of 1 ml/min. Figure 45 shows that at either a higher or lower pH, a single peak of butyrolactol was observed. At intermediate pH (~ 4.5), two peaks for butyrolactol were observed. The reason for these phenomena is that both acid and base can accelerate the ring opening process¹⁴⁰, thus increasing the interconversion rate for the two epimers. A previous study¹⁴¹ also points out that this type of interconversion has the slowest reaction rate in the pH 3 to 5 region.

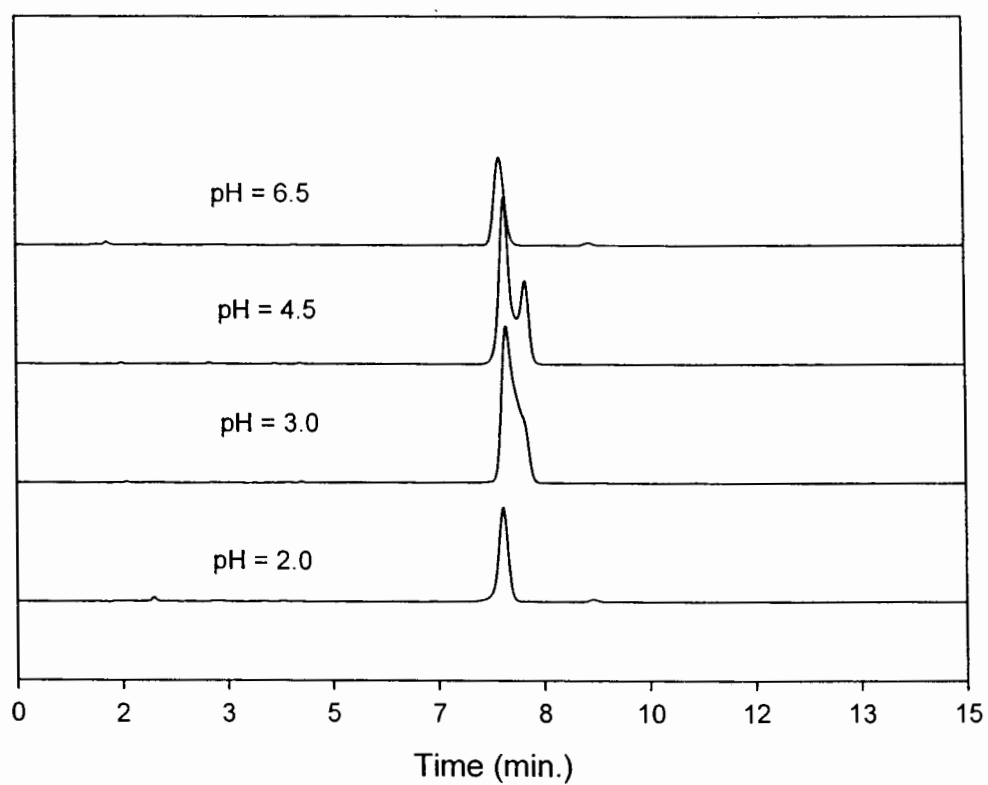


Figure 45. Effect of pH on the peak shape of trityloxymethyl butyrolactol (ODS – AM 4.6 x 150 mm x 3 μ m column, 35 : 65 /water: acetonitrile, 1 ml/min, temperature 25°C).

Chapter 6 Conclusions

In the second part of this research, the theoretical aspects of the on-column stereoisomerization reaction were studied. The formulas for computer simulation programs for the on-column stereoisomerization were introduced. Based on the theory, we have learned that the stereoisomerization reaction which includes enantiomerization, epimerization and diastereomerization are all first order reactions. In chromatographic systems, the overall reaction rate is the summation of the reaction rate in both mobile phase and stationary phase.

The chromatograms of the species which are able to isomerize in the column tend to have different shapes according to its reaction rate and the chromatographic conditions. If the rate of interconversion is slow compared to the chromatographic process two resolved peaks are observed due to the occurrence of little or no interconversion. If the rate of interconversion is fast compared to the chromatographic process, only one peak is observed due to the rapid interconversion. However, if the interconversion is on a similar time scale to that of the chromatographic process, band spreading and peak distortion may be observed. On-column interconversion of a species is usually characterized by tailing of the less retained peak and fronting of the more retained peak. Tailing of the less retained peak occurs as this species is converted to the more retained species. Conversely fronting of the more retained peak occurs as this species is converted to the less retained species. The two peaks may be joined by an elevated baseline.

The approximate function for the direct calculation of an on-column inter-conversion reaction rate as introduced by Trapp and Schurig is based on a stochastic model. In this model, the elution profile $P(t')$ for interconverting epimers during the separation process can be expressed by two distribution functions of the non-interconverted epimers and the probability density functions of the interconverted epimers. The probability density functions can be expressed by an ideal Gaussian distribution function and the probability density functions are expressed by a modulated Gaussian function. After mathematical simplification, the equation to determine the approximate reaction rate constant is derived.

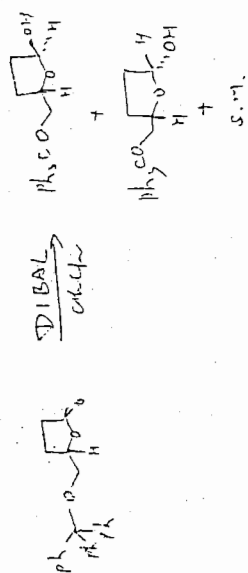
In our studies, the approximation function developed by Trapp and Schurig was successfully used to directly calculate interconversion rate constants and Gibbs activation energies for the inter-conversion of butyrolactol on a chromatographic column. A possible epimerization reaction mechanism was proposed. The effect of this epimerization on the chromatogram of inter-converting species was thoroughly studied. It was demonstrated that temperature, pH and flow rate are major parameters that can influence the peak shape of the inter-converting species. These parameters can be manipulated so that a single peak can be obtained for the inter-converting species to enhance accurate quantitation.

Appendix

NMR Spectrum

NMR Spectrum of Trityloxymethylbutyrolactol

nmc400b h-1



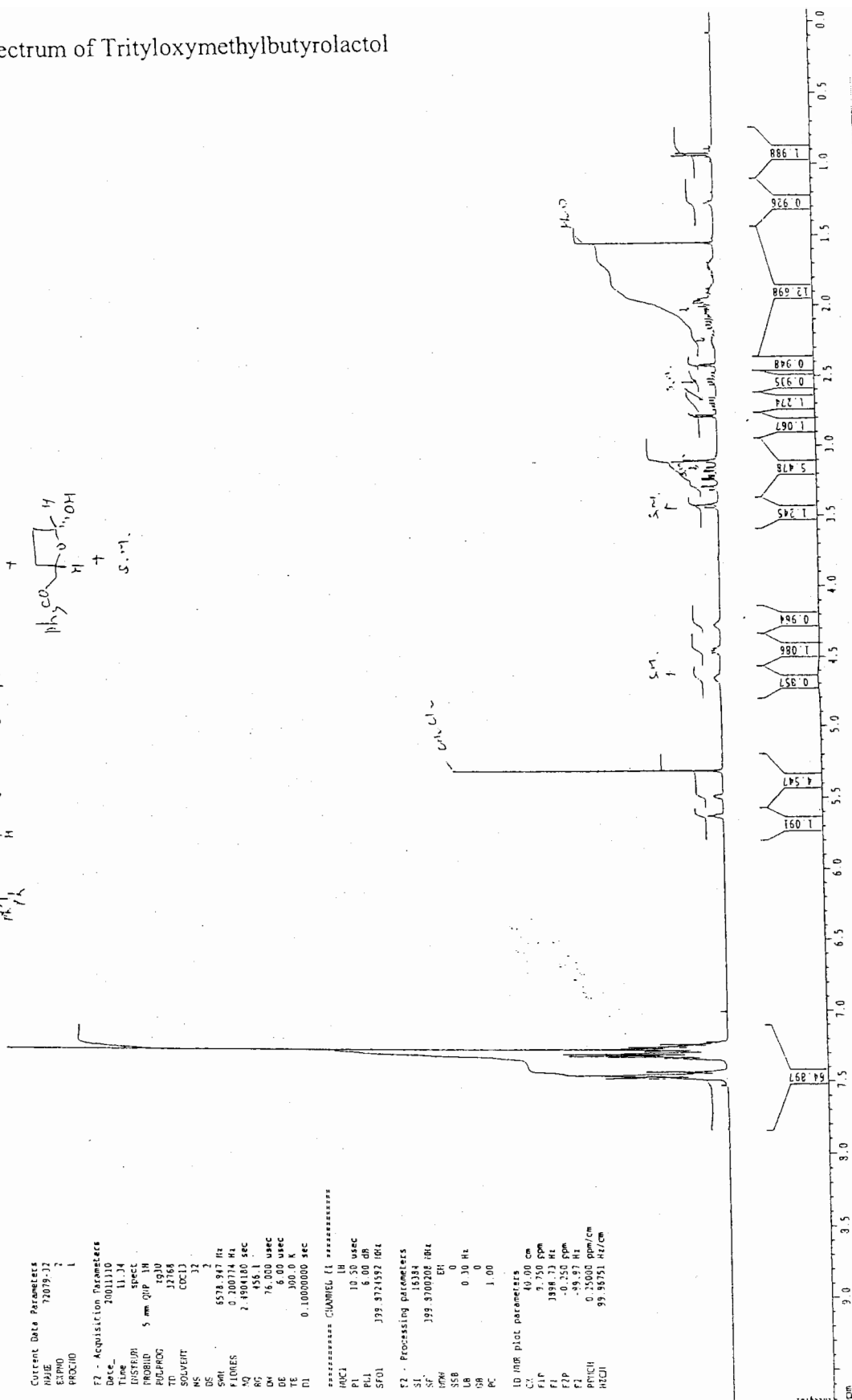
Current Data Parameters
 NAME 72019-12
 EXPNO 2
 PROCNO 1

F2 - Acquisition Parameters
 Date_ 20011110
 Time 11.34
 INSTRUM spect
 PROBHD 5 mm QNP 1H
 PULPROG zgpg30
 TD 32768
 SOLVENT CDCl₃
 NS 32
 DS 2
 SWH 6578.947 Hz
 FIDRES 0.200714 Hz
 AQ 2.4904100 sec
 RG 458.1
 DV 76.000 usec
 DE 1.500 usec
 TE 300.0
 TI 0.10000000 sec

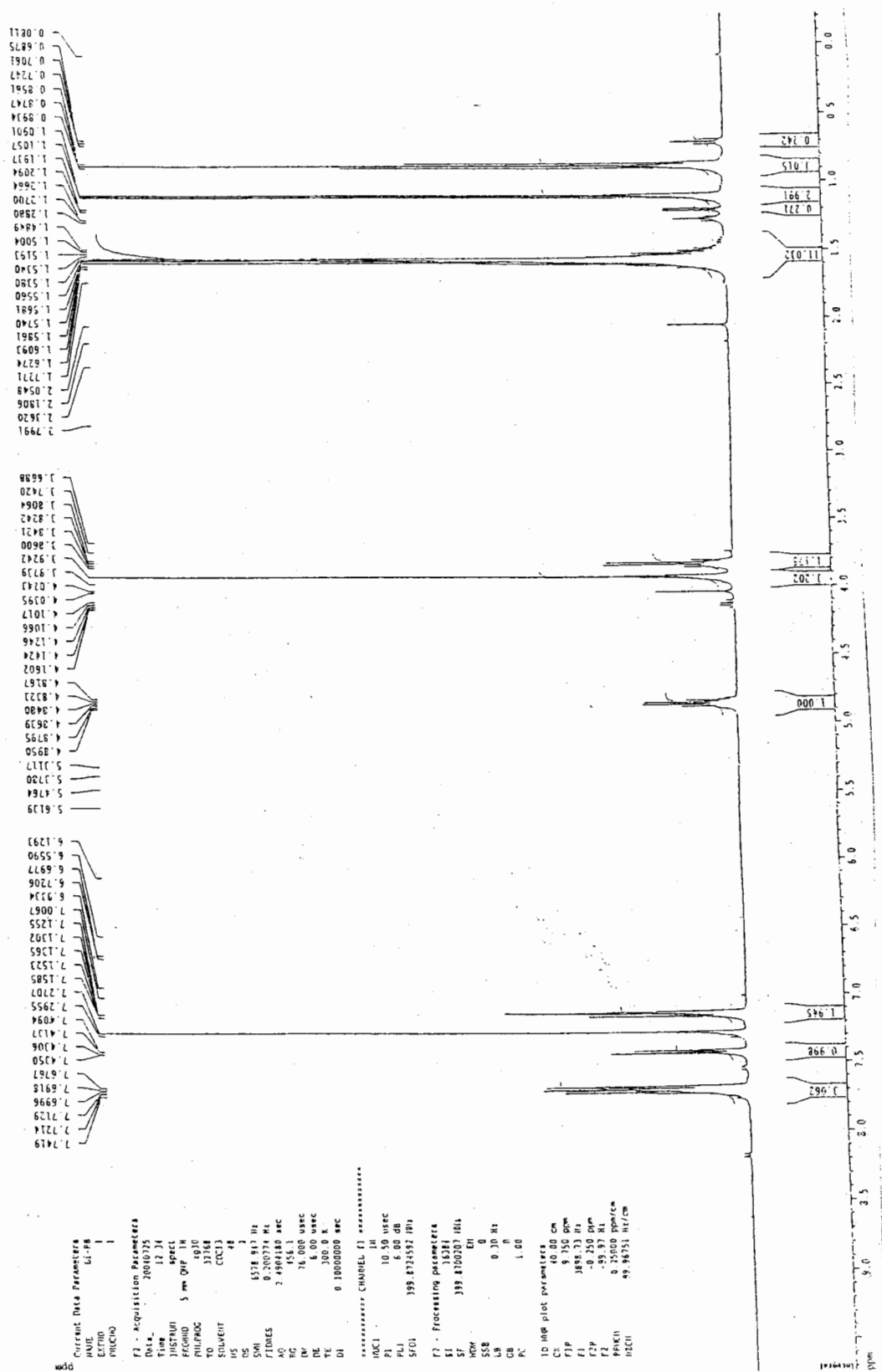
===== CHANNEL f1 =====
 NUC1 1H
 P1 10.50 usec
 PL1 6.00 dB
 SFO1 399.971582 MHz

F2 - Processing parameters
 SI 16384
 SF 399.970202 MHz
 INW 64
 EN 0
 SSF 0
 LB 0.30 Hz
 GB 0
 PC 1.00

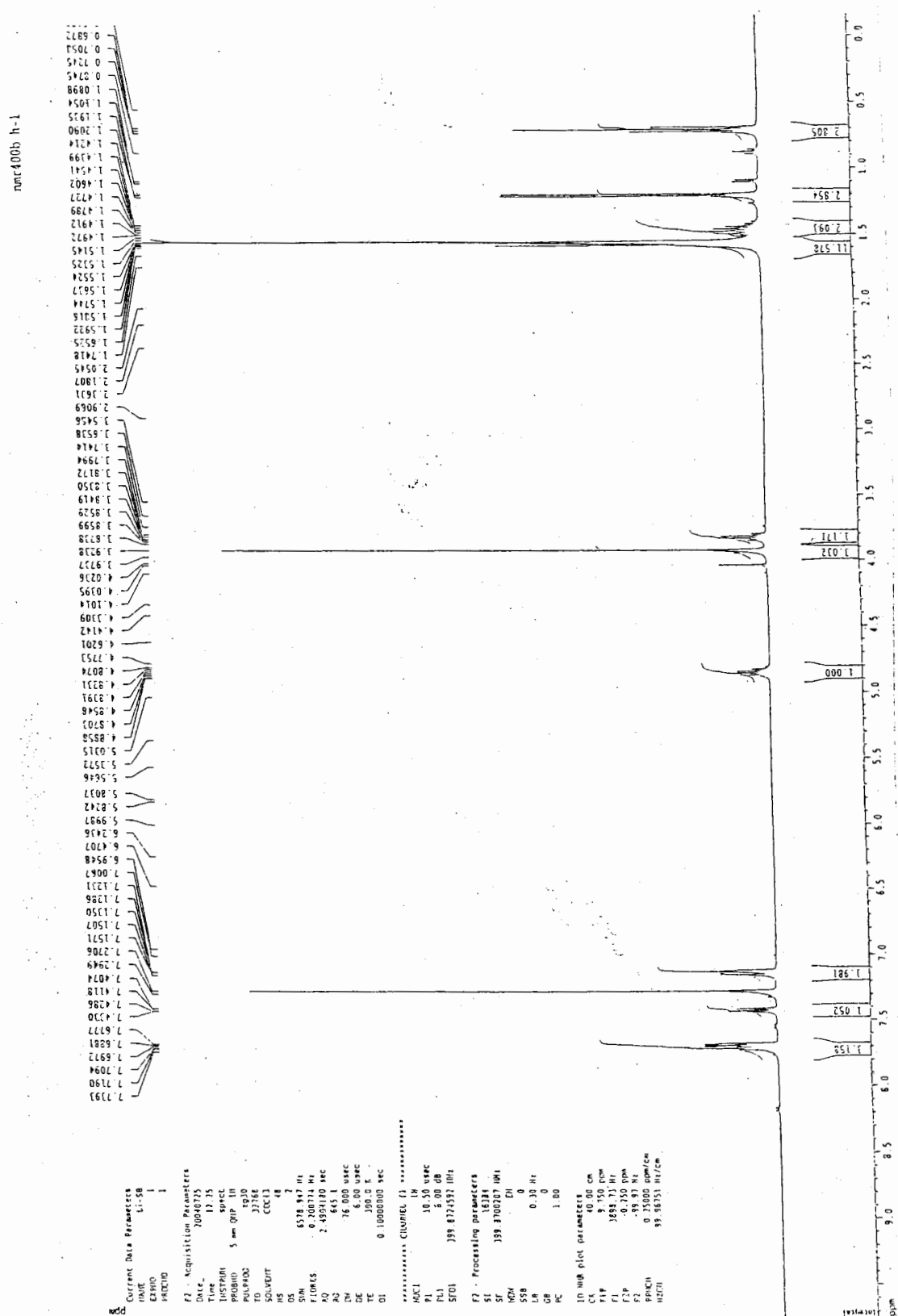
1D NMR plot parameters
 C1 40.00 cm
 F1 9.750 ppm
 F2 399.72 Hz
 F3 -0.250 ppm
 F4 -99.97 Hz
 PITCH 0.25000 ppm/cm
 REC1 99.95751 Hz/cm



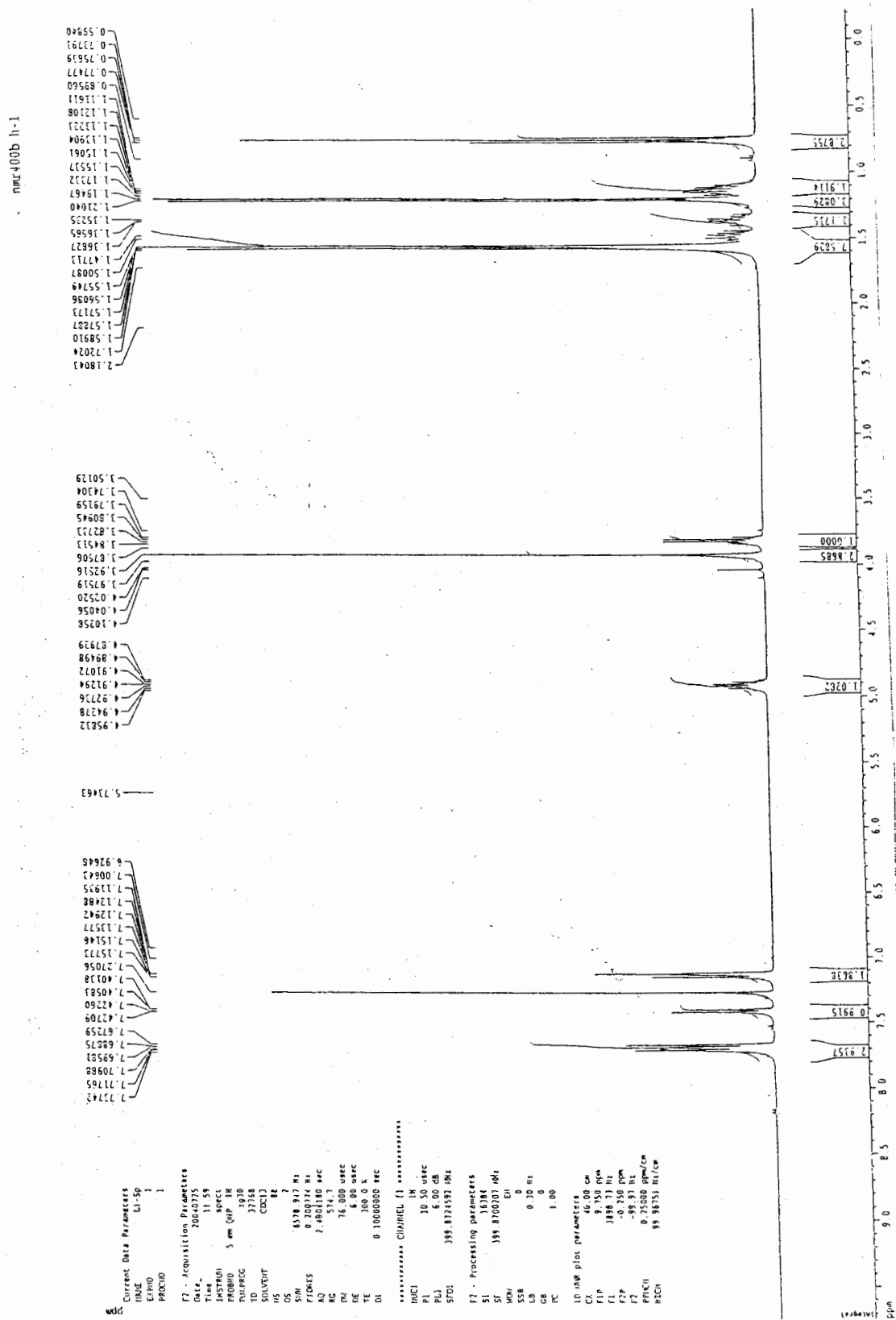
NMR Spectrum of 2-(R)-Butanol (S)-Naproxen Ester



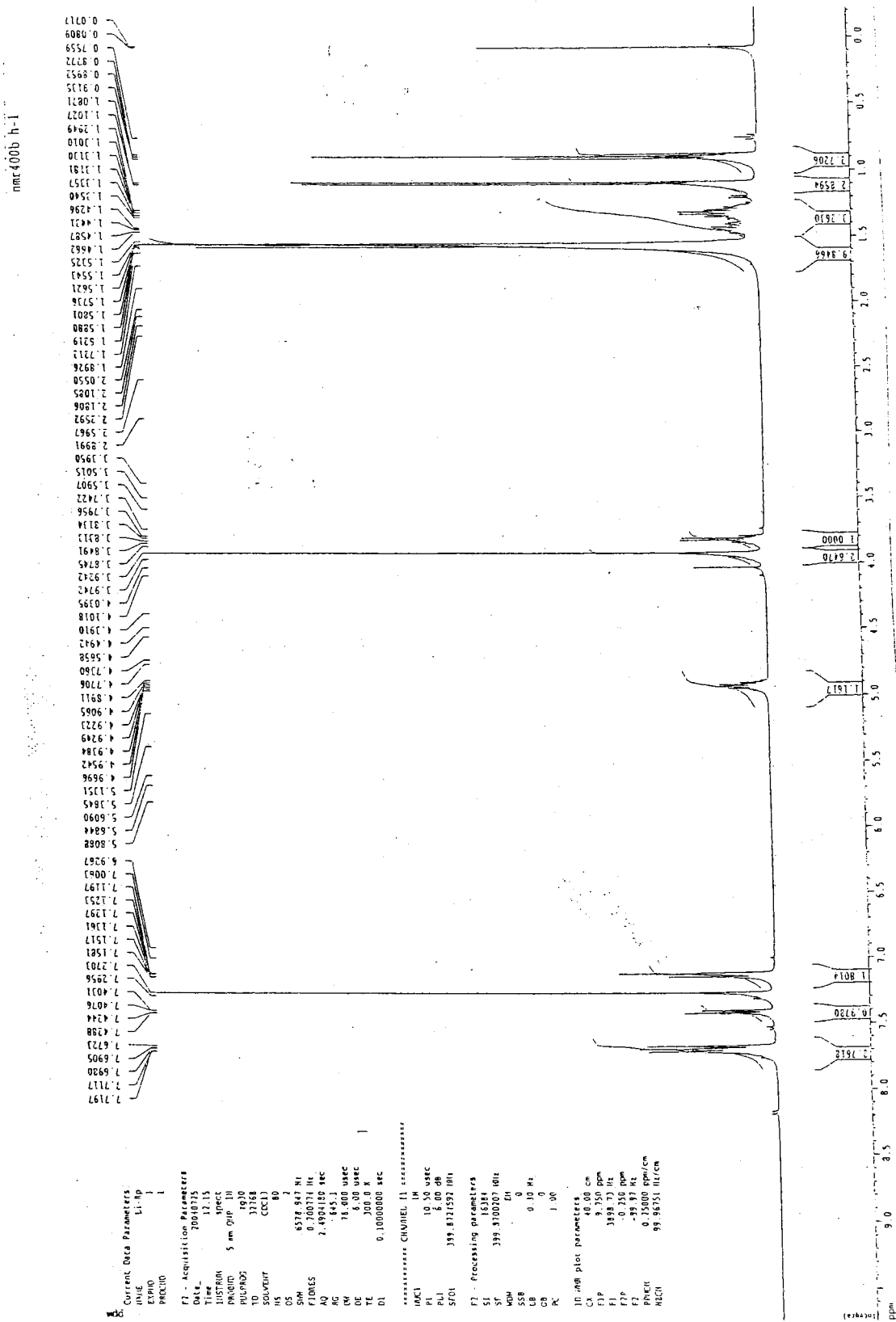
NMR Spectrum of 2-(S)-Butanol (S)-Naproxen Ester



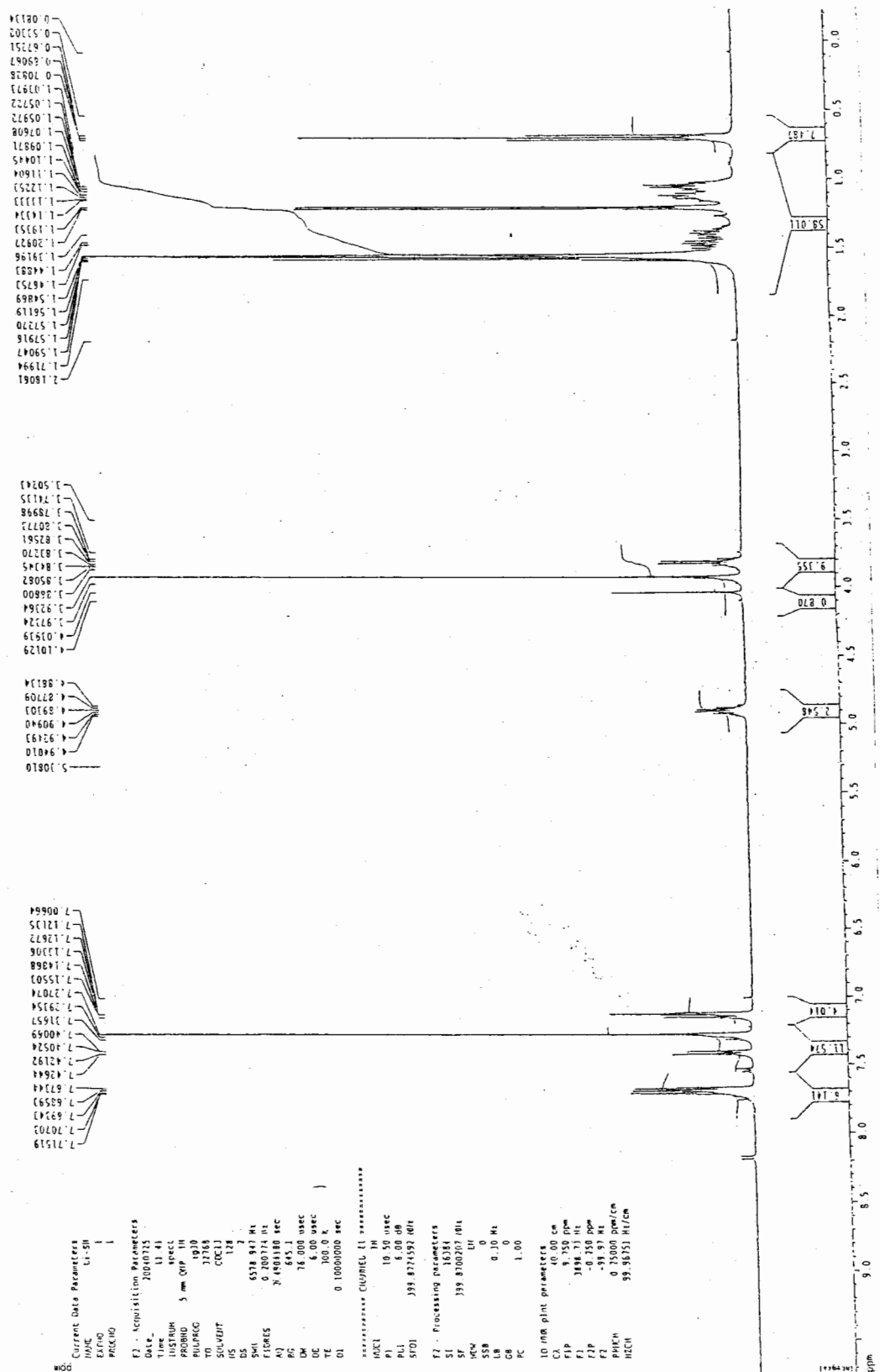
NMR Spectrum of 2-(S)-Pentanol (S)-Naproxen Ester



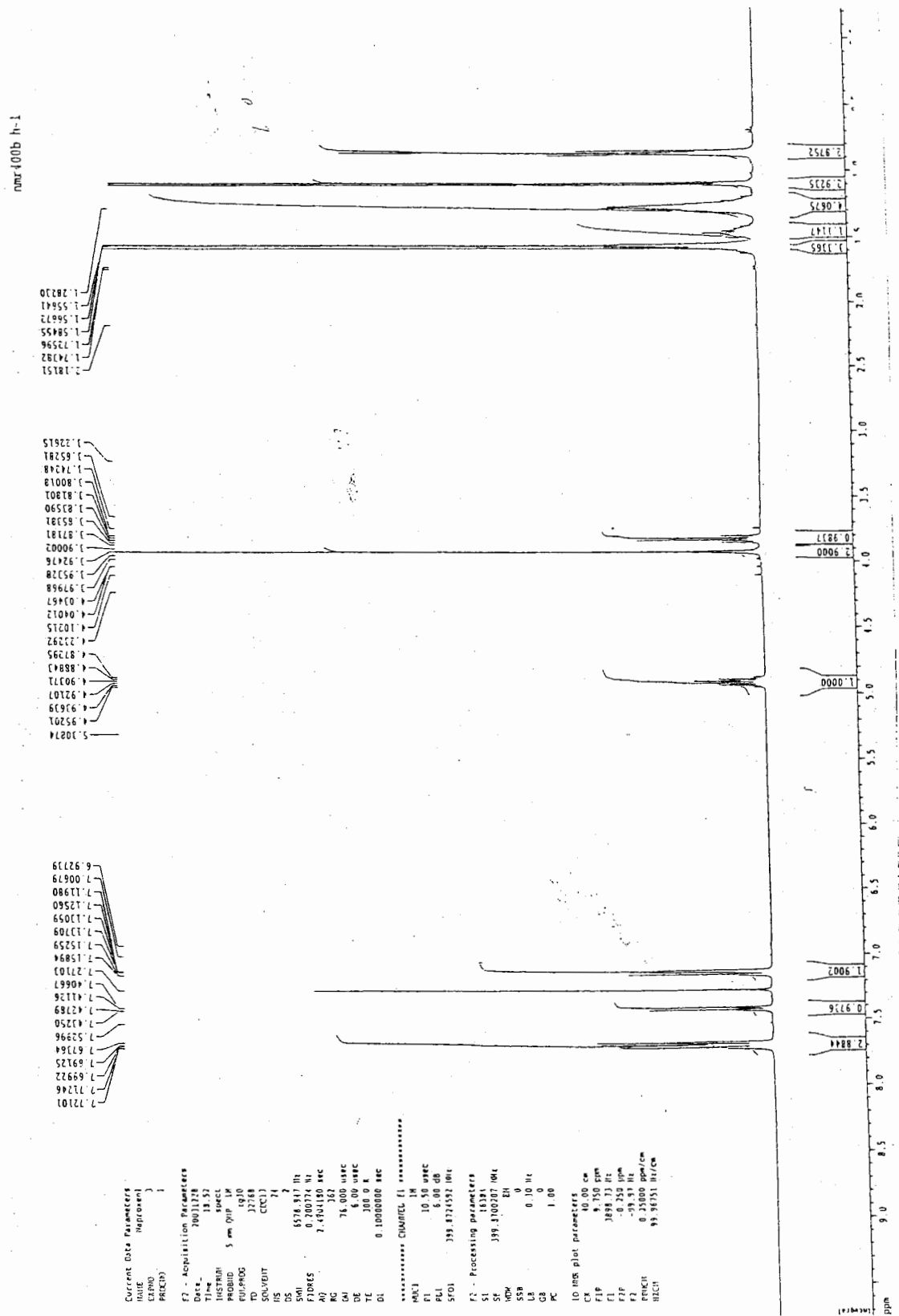
NMR Spectrum of 2-(R)-Pentanol (S)-Naproxen Ester



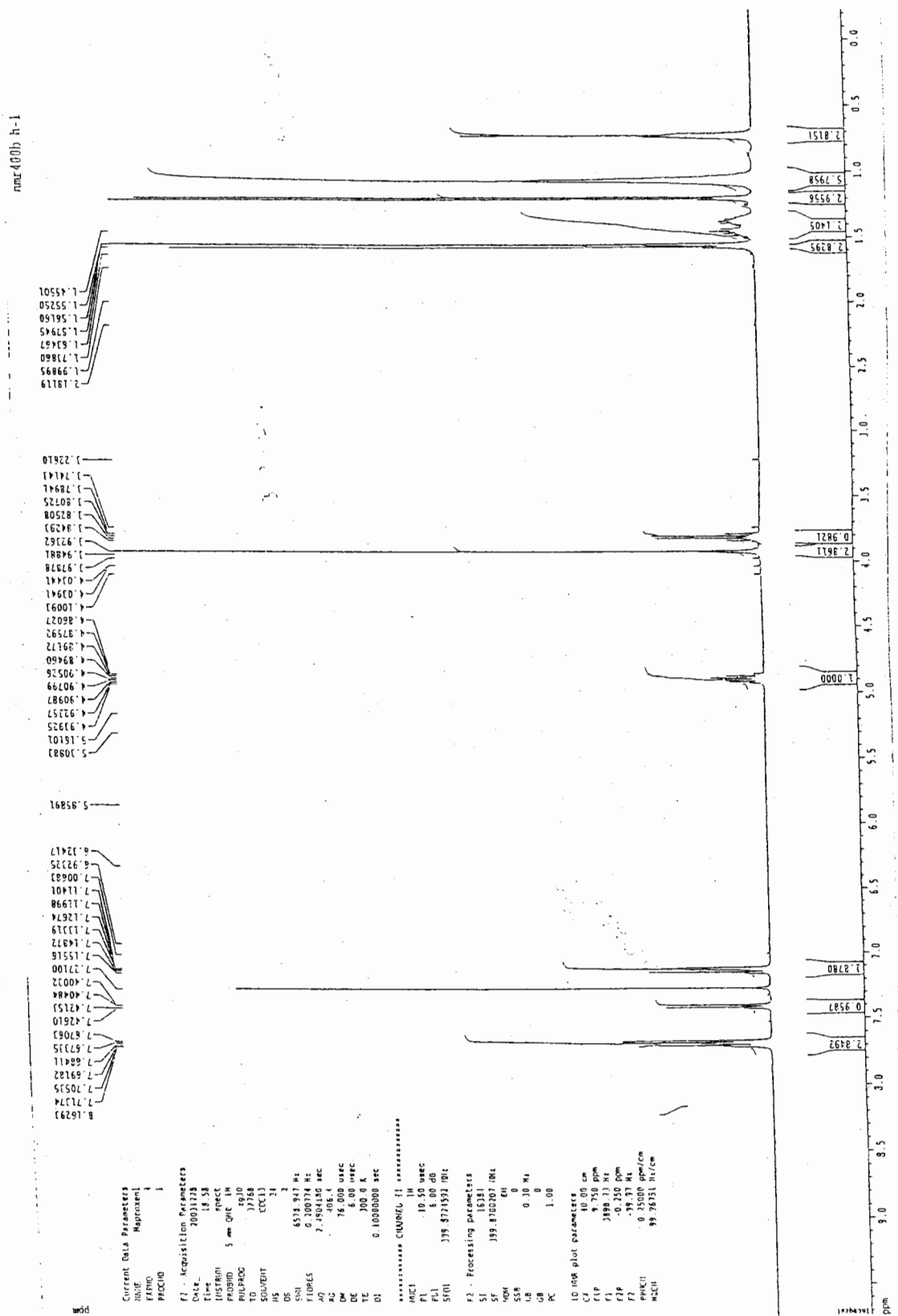
T-4 Q007.100L



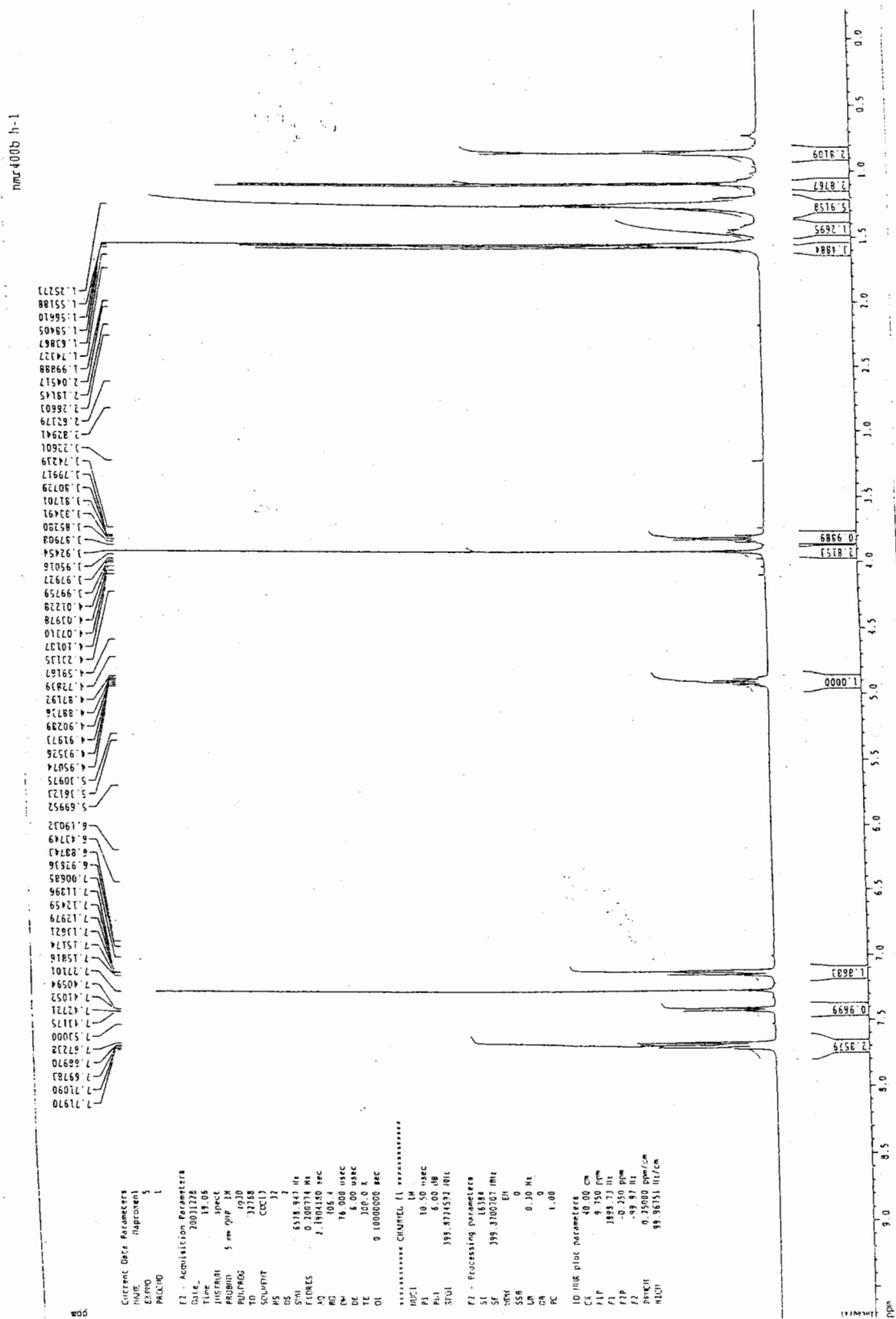
NMR Spectrum of 2-(R)-Hexanol (S)-Naproxen Ester



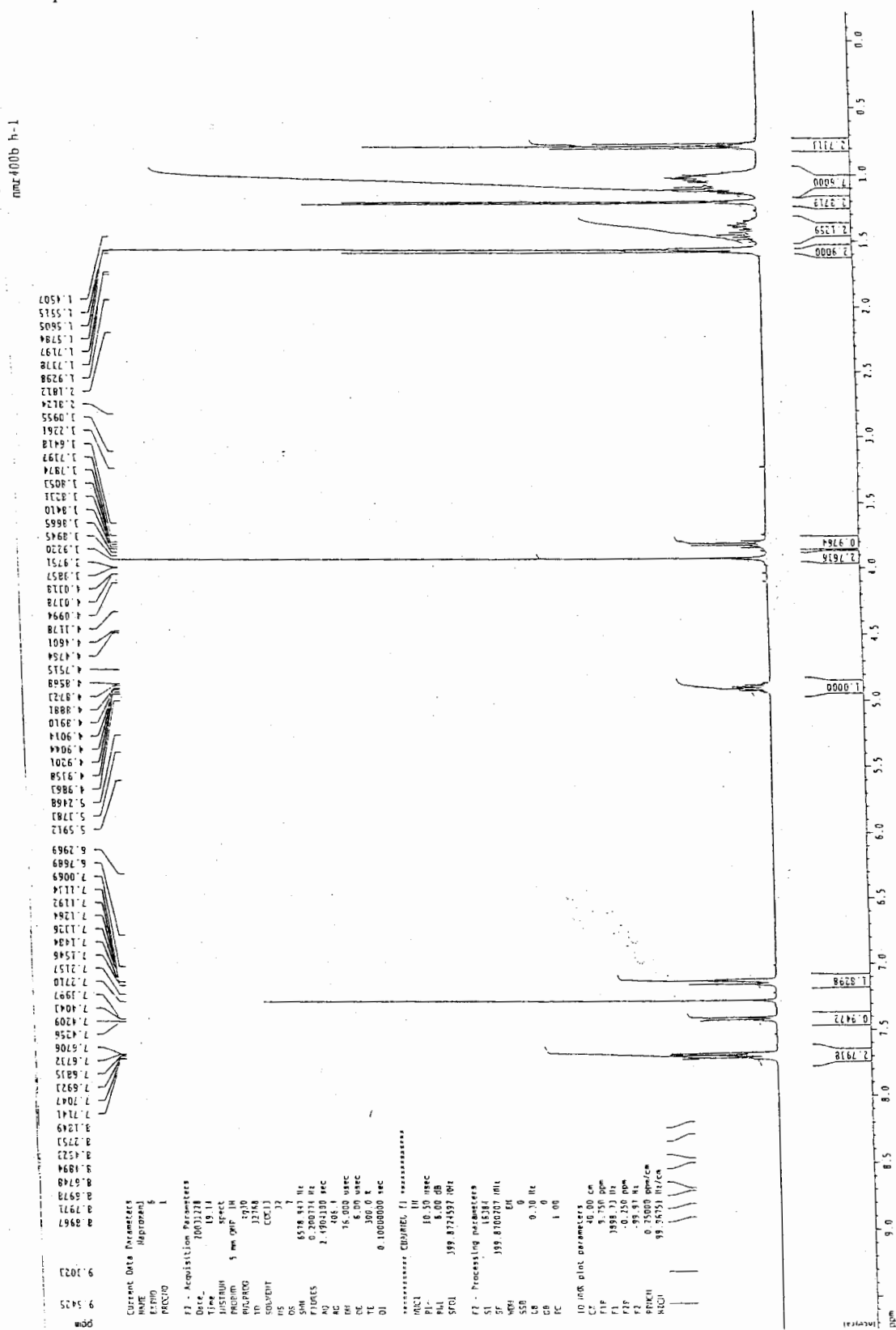
NMR Spectrum of 2-(S)-Heptanol (S)-Naproxen Ester



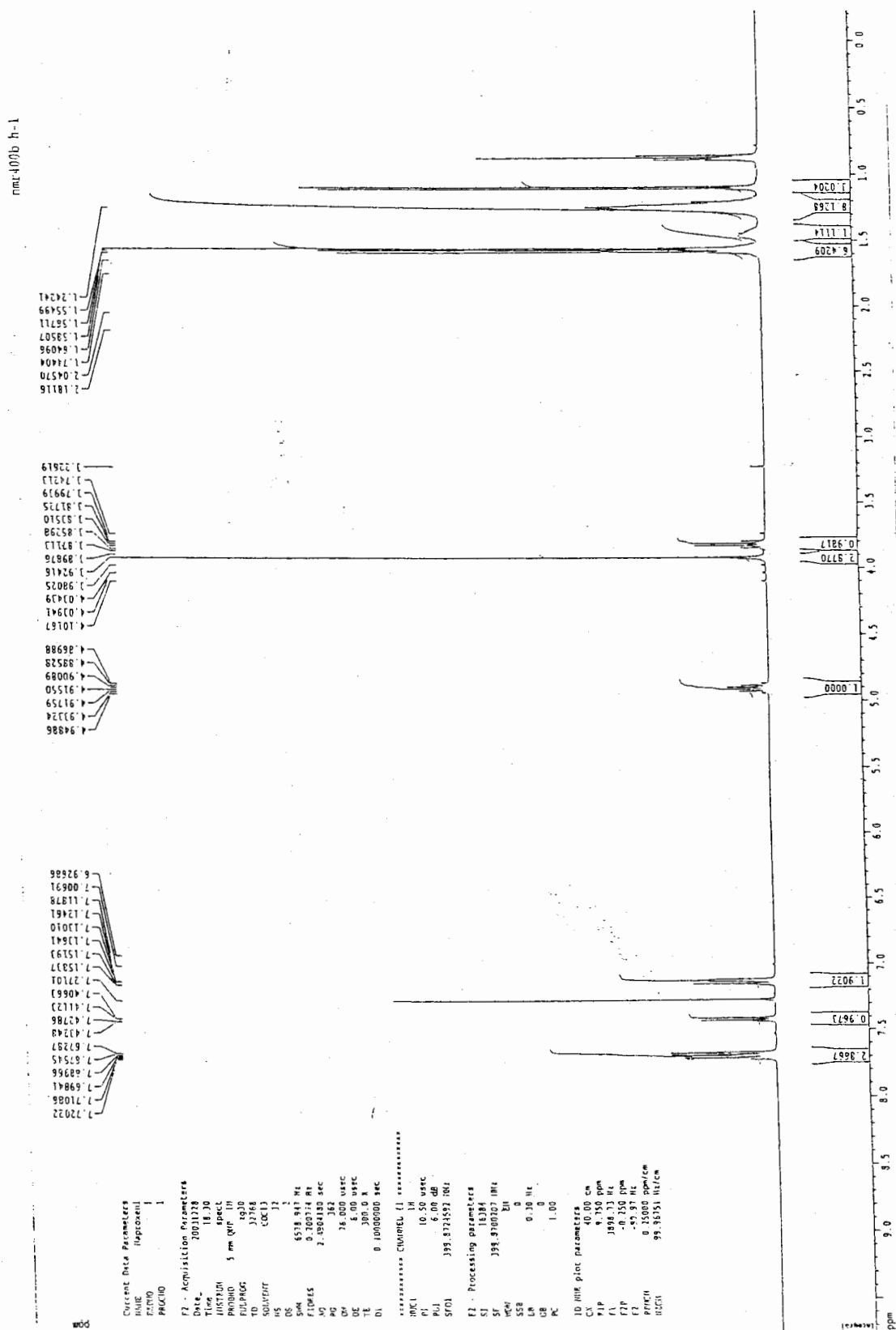
NMR Spectrum of 2-(R)-Heptanol (S)-Naproxen Ester



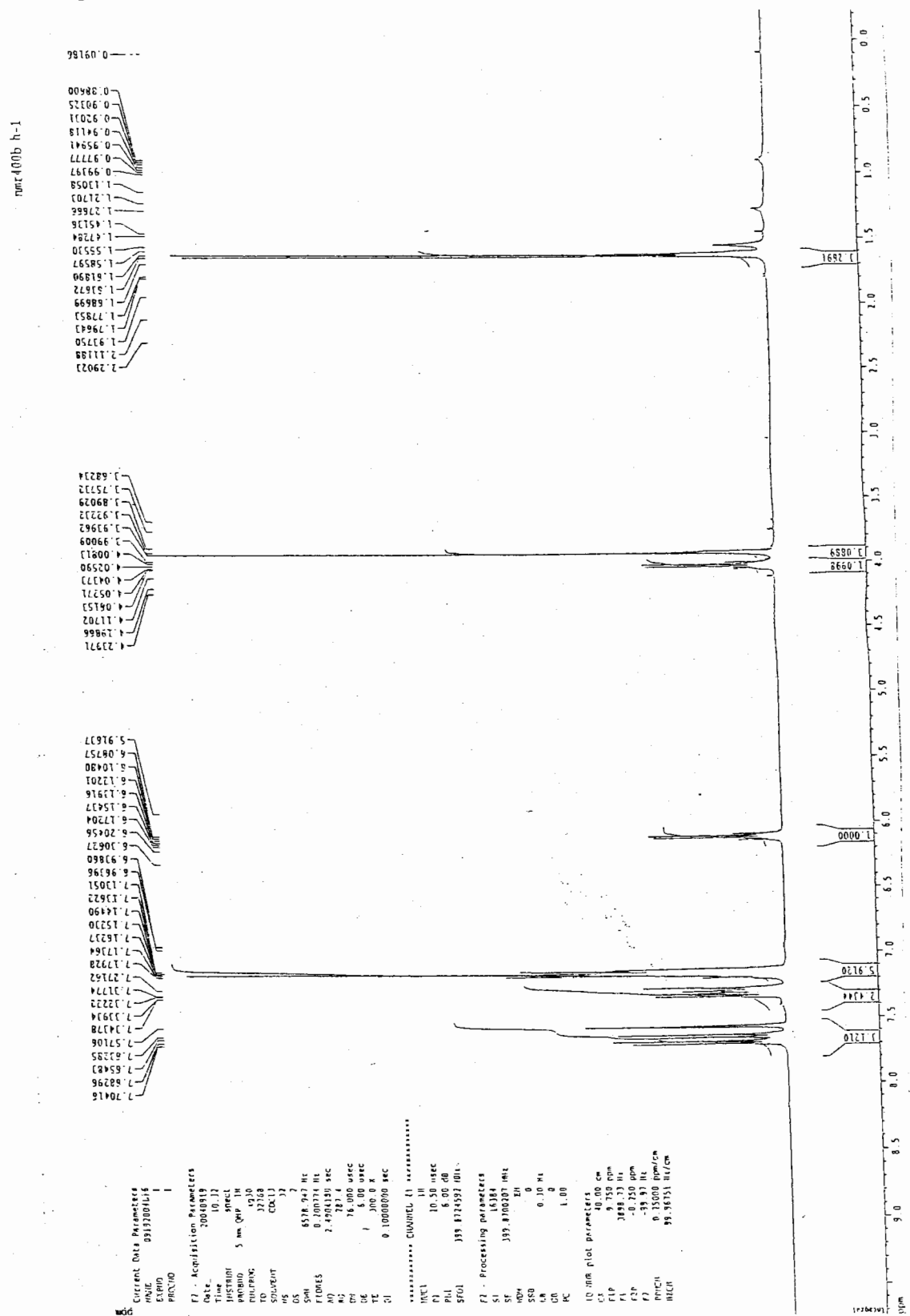
NMR Spectrum of 2-(S)-Octanol (S)-Naproxen Ester



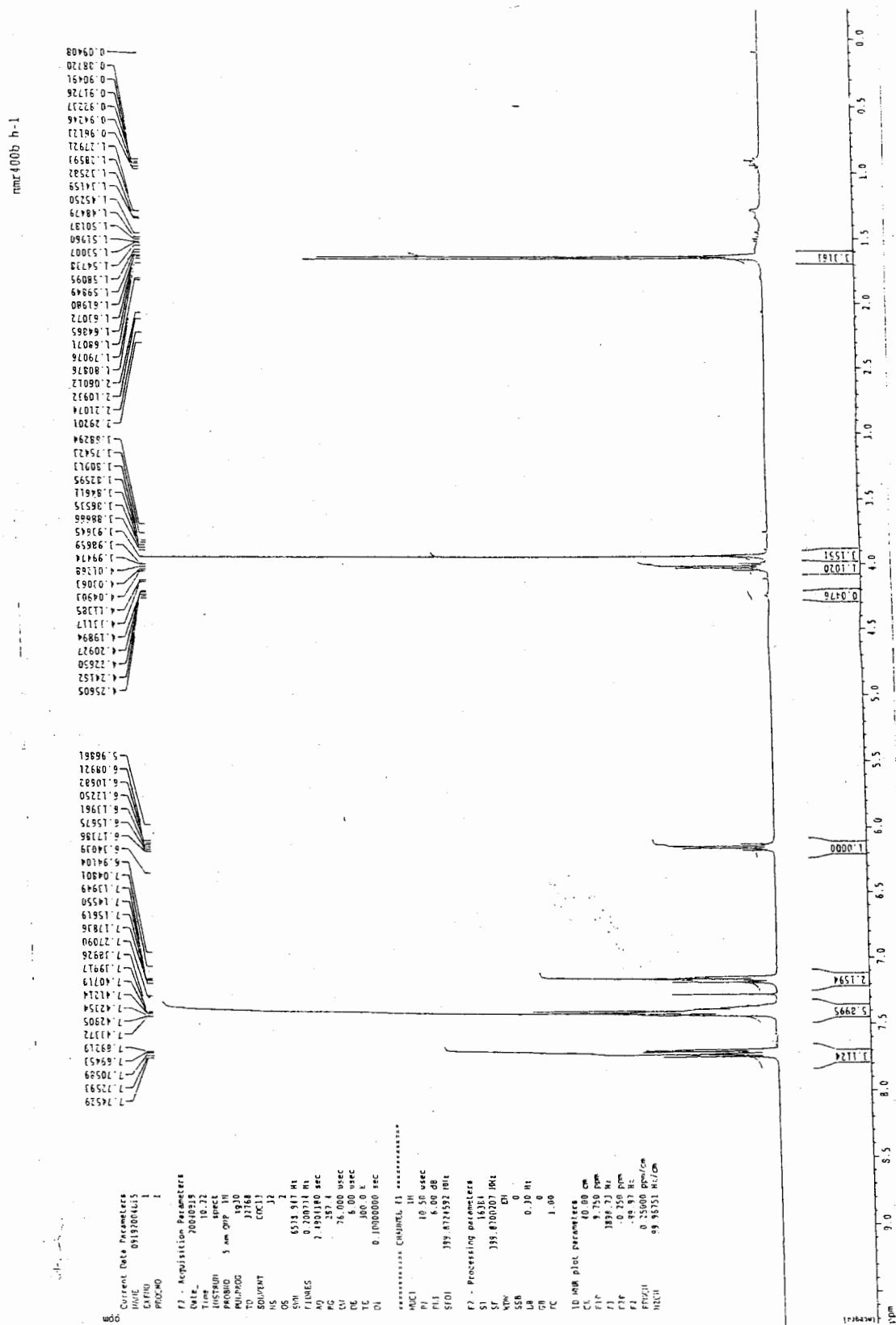
NMR Spectrum of 2-(R)-Octanol (S)-Naproxen Ester



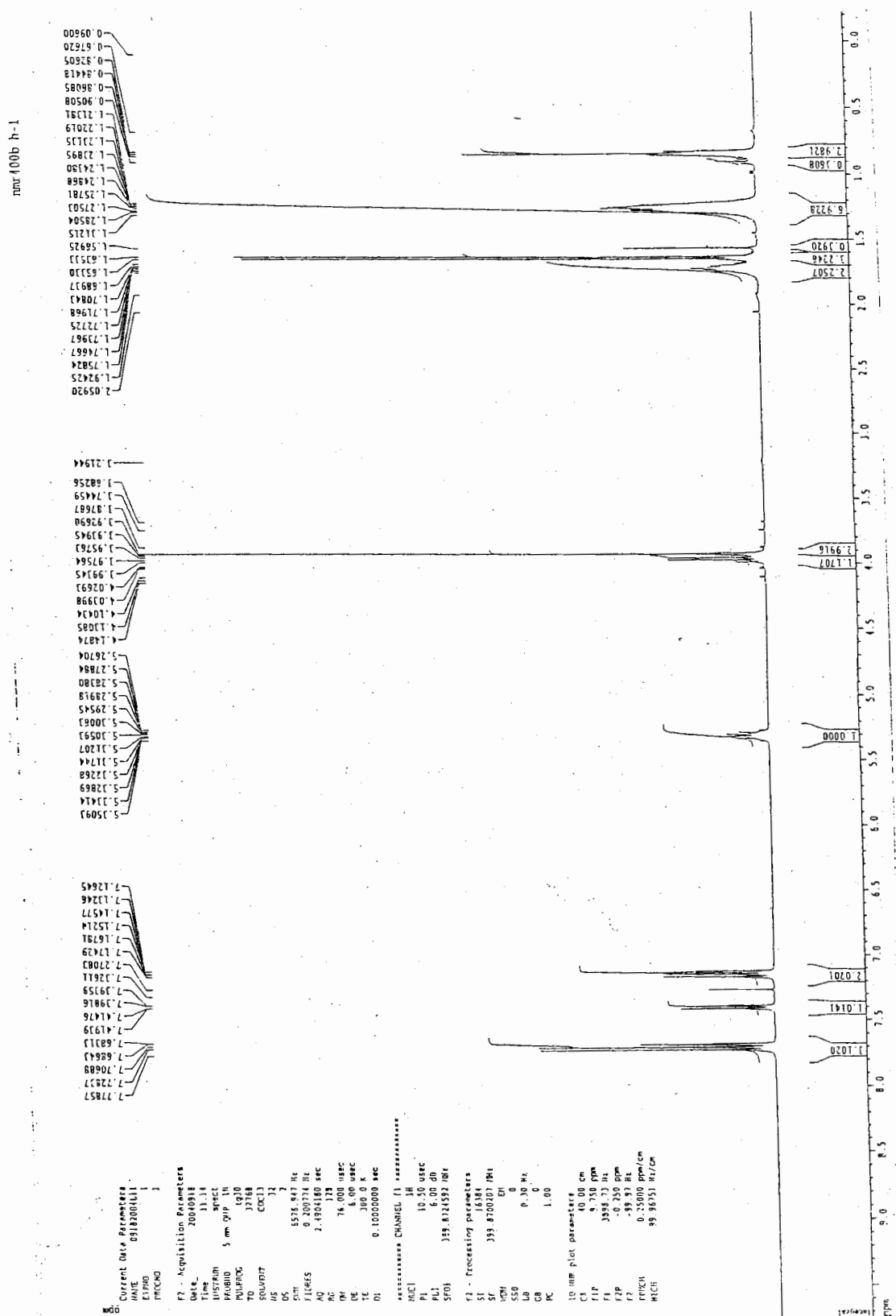
NMR Spectrum of (R)-(-)-(Trifluoromethyl) Benzyl Alcohol (S)-Naproxen Ester



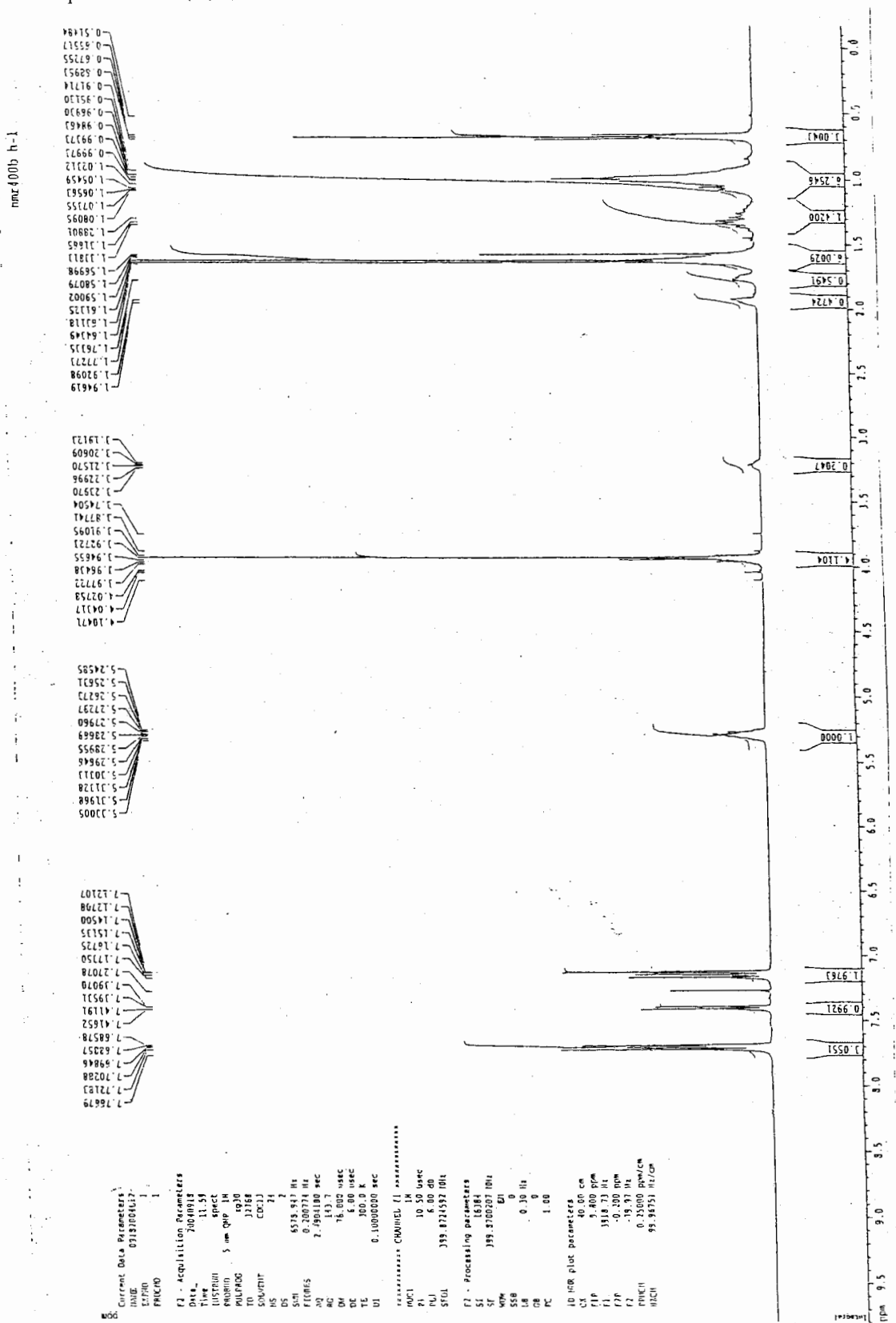
NMR Spectrum of (S)-(-)-(Trifluoromethyl) Benzyl Alcohol (S)-Naproxen Ester



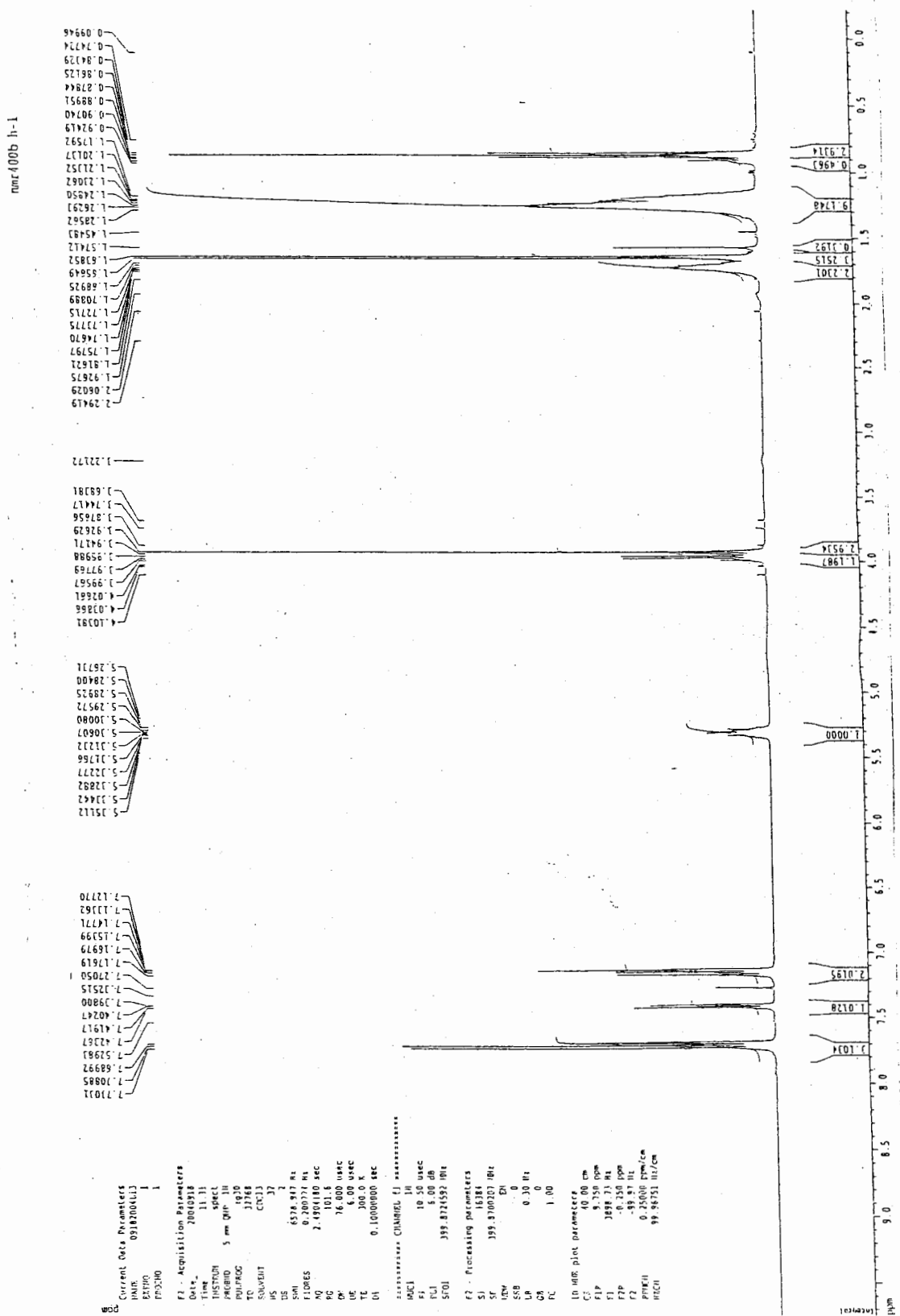
NMR Spectrum of (S)-(-)-1, 1, 1-Trifluoroheptan-2-ol (S)-Naproxen Ester



NMR Spectrum of (R)-(-)-1, 1, 1-Trifluoroheptan-2-ol (S)-Naproxen Ester



NMR Spectrum of (S)-(-)-1, 1, 1-Trifluorooctan-2-ol (S)-Naproxen Ester



NMR Spectrum of (R)-(-)-1, 1, 1-Trifluorooctan-2-ol (S)-Naproxen Ester



NMR Spectrum of 1-Phenyl-1-propanol (S)-Naproxen Ester (R : S / 10 : 90)

nmr400b h-1

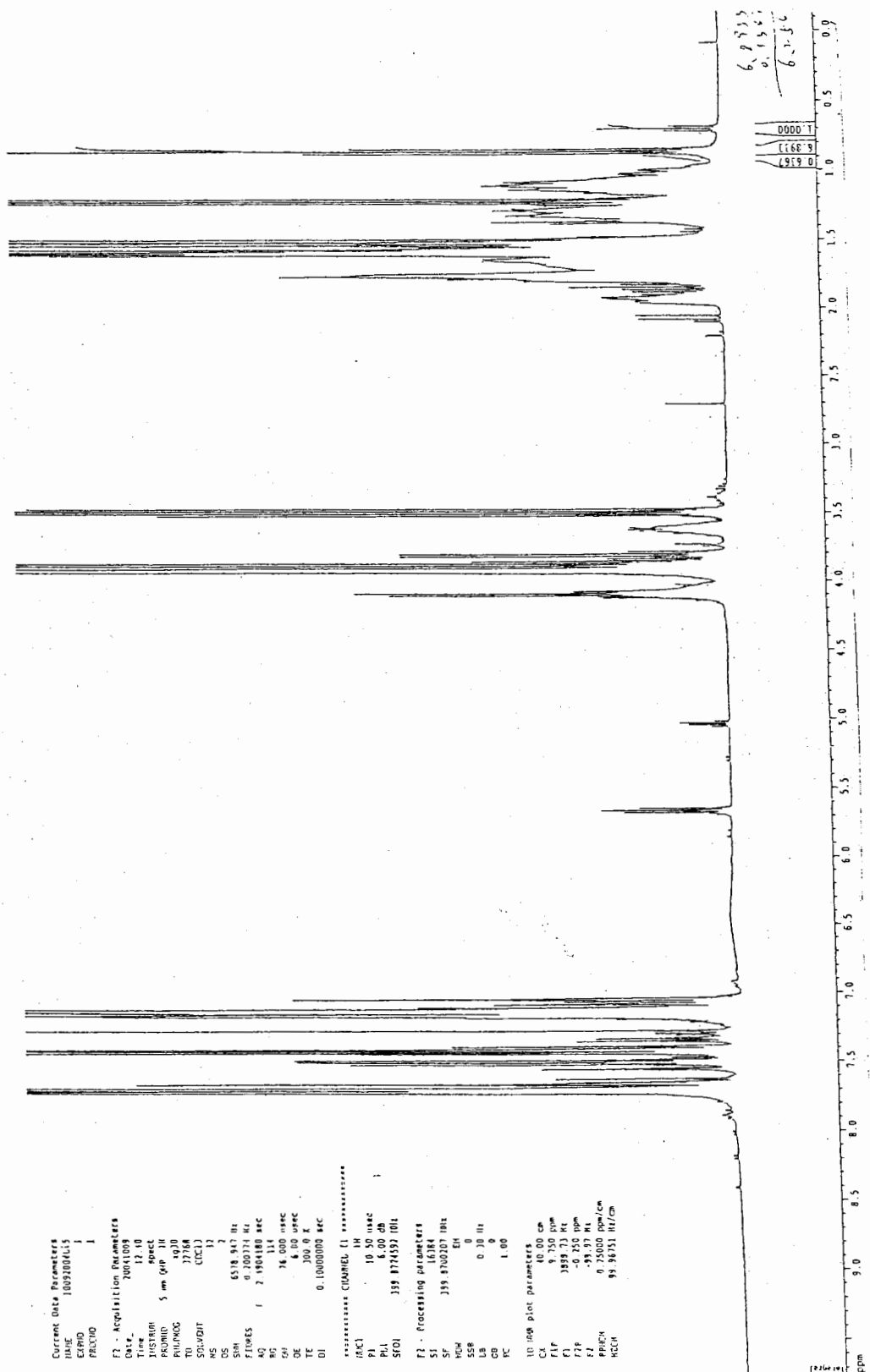
Current Data Parameters
NAME 10091001015
EXPNO 1
PROCNO 1

F2 - Acquisition Parameters
Date_ 20011009
Time 12.10
INSTRUM spect
PROBHD 5 mm QNP 1H
PULPROG zgpg30
TD 65536
SOLVENT H₂O
NS 12
DS 2
SWH 6518.947 Hz
SFO 300.135 MHz
AQ 0.200774 sec
RG 134
GB 34.000 usec
PC 1.00 usec
TE 300.2 K
DE 0.10000000 sec
DI 0.10000000 sec

***** CHANNEL f1 *****
NUC1 1H
P1 10.50 usec
PL1 6.00 dB
SFO1 399.874592 MHz

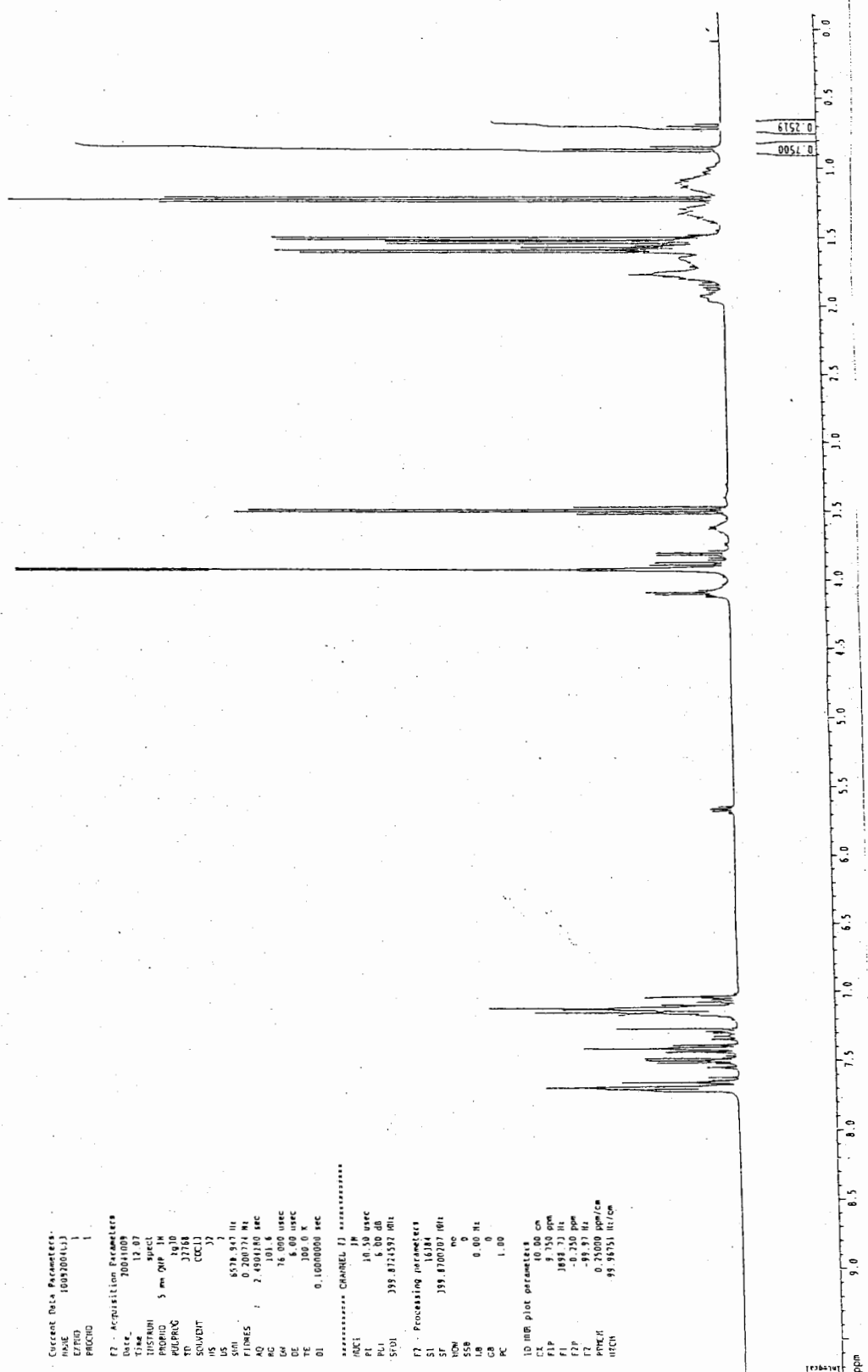
F2 - Processing parameters
SI 16384
SF 399.870207 MHz
WDW EM
SSB 0.30 Hz
GB 0
PC 1.00

1D IRG plot parameters
CA 40.00 cm
ZLP 9.750 ppm
F1 389.73 Hz
F2 9.750 ppm
ZL 99.87 Hz
RG 0.25000 ppm/cm
HSCN 99.86551 Hz/cm



NMR Spectrum of 1-Phenyl-1-propanol (S)-Naproxen Ester (R : S / 25 : 75)

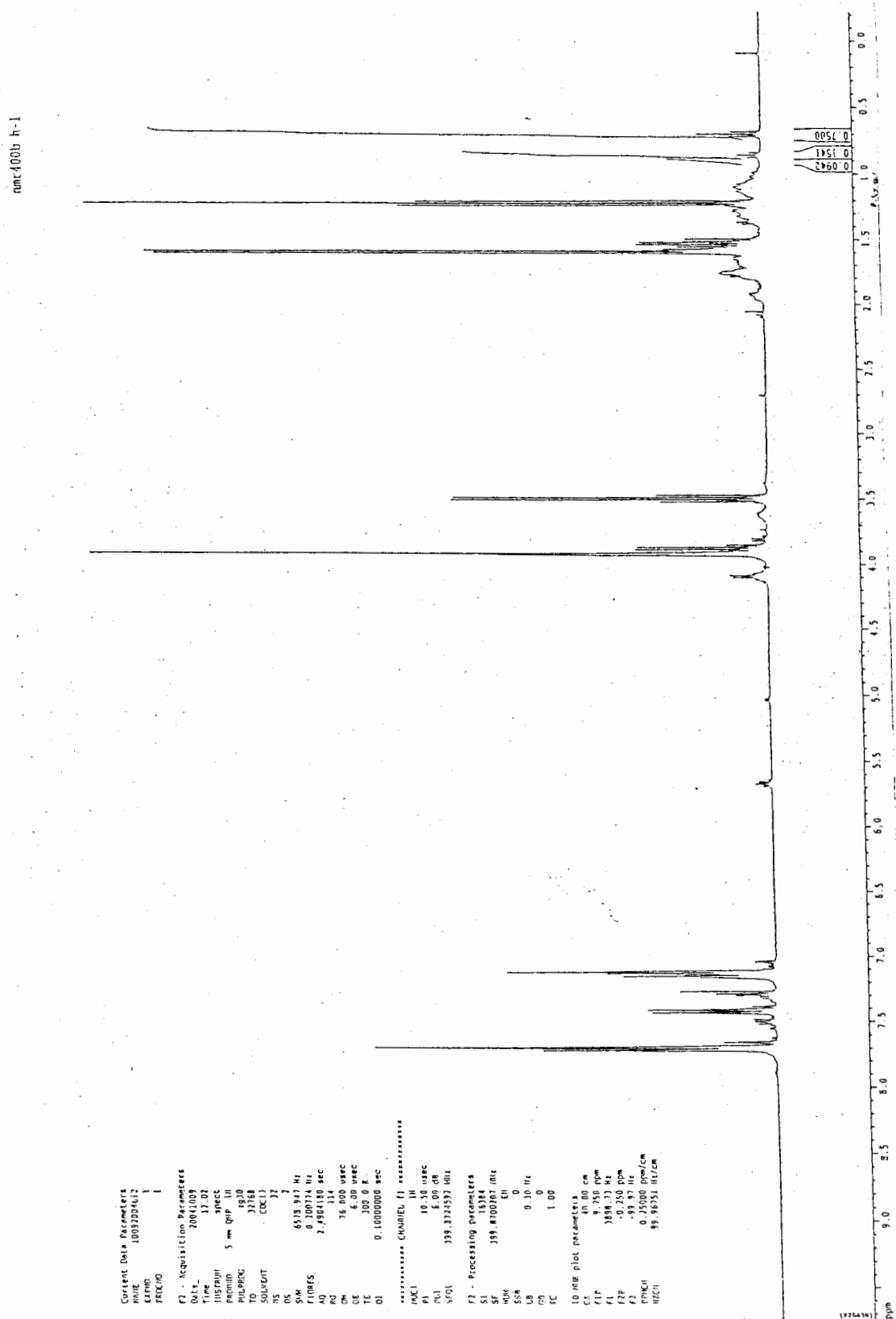
nmr400b h-1



nmr400b h-1



NMR Spectrum of 1-Phenyl-1-propanol (S)-Naproxen Ester (R : S / 75 : 25)



PMR 400b H-1

